J. Print Media Technol. Res. 9(2020)3
September 2020

3-2020

ISSN 2414-6250 (Online)
CODEN JPMTBI
UDC 665

Journal of Print and Media Technology Research

Scientific contributions

Professional communication

ISSN 2414-6250

Editor-in-Chief
Gorazd Golob (Ljubljana)

Published by iarigai
www.iarigai.org

The International Association of Research Organizations for the Information, Media and Graphic Arts Industries

J. Print Media Technol. Res. 9(2020)3
September 2020
ISSN 2414-6250 (Online)
A print version is available on-demand
ISSN 2223-8905 (Print)

Journal of Print and Media Technology Research

A PEER-REVIEWED QUARTERLY

PUBLISHED BY

The International Association of Research Organizations
for the Information, Media and Graphic Arts Industries
Magdalenenstrasse 2, D-64288 Darmstadt, Germany
http://www.iarigai.org
journal@iarigai.org

A mission statement

To meet the need for a high quality scientific publishing platform in its field, the International Association of Research Organizations for the Information, Media and Graphic Arts Industries is publishing a quarterly peer-reviewed research journal.

The journal is fostering multidisciplinary research and scholarly discussion on scientific and technical issues in the field of graphic arts and media communication, thereby advancing scientific research, knowledge creation, and industry development. Its aim is to be the leading international scientific journal in the field, offering publishing opportunities and serving as a forum for knowledge exchange between all those interested in contributing to or learning from research in this field.

By regularly publishing peer-reviewed, high quality research articles, position papers, surveys, and case studies as well as review articles and topical communications, the journal is promoting original research, international collaboration, and the exchange of ideas and know-how. It also provides a multidisciplinary discussion on research issues within the field and on the effects of new scientific and technical developments on society, industry, and the individual. Thus, it intends to serve the entire research community as well as the global graphic arts and media industry.

The journal is covering fundamental and applied aspects of at least, but not limited to, the following topics:

Printing technology and related processes

- Conventional and special printing
- Packaging
- Fuel cells and other printed functionality
- Printing on biomaterials
- Textile and fabric printing
- Printed decorations
- Materials science
- Process control

Premedia technology and processes

- Colour reproduction and colour management
- Image and reproduction quality
- Image carriers (physical and virtual)
- Workflow and management

Emerging media and future trends

- Media industry developments
- Developing media communications value systems
- Online and mobile media development
- Cross-media publishing

Social impact

- Media in a sustainable society
- Environmental issues and sustainability
- Consumer perception and media use
- Social trends and their impact on media

Submissions to the Journal

Submissions are invited at any time and, if meeting the criteria for publication, will be rapidly submitted to peer-review and carefully evaluated, selected and edited. Once accepted and edited, the papers will be published as soon as possible.

✉ Contact the Editorial office: journal@iarigai.org

Journal of Print and Media Technology Research

3-2020

September 2020

J. Print Media Technol. Res. 9(2020)3, 131–200

Journal of Print and Media Technology Research is listed in:

Emerging Sources Citation Index

Scopus

Index Copernicus International

PiraBase (by Smithers Pira)

Paperbase (by Innventia and Centre Technique du Papier)

NSD – Norwegian Register for Scientific Journals, Series and Publishers

Printed in Slovenia by Collegium Graphicum, d. o. o. Ljubljana

Contents

A letter from the Editor

Gorazd Golob
Editor-in-Chief
E-mail: gorazd.golob@jpmtr.org
journal@iarigai.org

The present issue is a step forward to the changes in design and rearrangement of the Journal, which are planned for the March 2021 issue due to the expressed need for better accessibility to the published papers for indexing purposes. The full pdf file of each issue including cover, scientific content, and Topicalities are and will remain available free of charge as before, however, now you can also access and download single papers.

The scientific content begins with an original scientific paper on irreversible hydrochromic inks for smart packaging, followed by the research paper on water-based ink formulation based on polyurethane dispersion, and a case study on the lateral web shifting during printing. The last paper in this issue is a professional communication on the influence of material properties on the bonding strength of multilayer packaging.

The Topicalities bring in News & more section an overview of changes in ISO standards under the responsibility of TC 130 – Graphic technology, together with an interesting analysis of trends in the publications on printing and an overview of research activities at RITs College of Art and Design. The analysis of trends in the publications, prepared by the member of editorial team Markéta Držková (marketa.drzkova@jpmtr.org) shows the huge amount of published papers somehow connected to the term »print« in the last two decades. Also, the numbers of citations of some papers are impressive, and the main goal of the Journal of Print and Media Technology Research is to become comparable to the journals, where authors are reaching a wide audience, and where the importance of their papers is recognized as worth for citation by other authors of papers in indexed journals. The following overview of the recently published books is covering a wide research area, from image processing to media history, design, information, and material science.

Three summaries of academic dissertations are also introduced. Nicholas Richard Fry successfully finished his doctoral studies with a thesis on robotic manufacturing system for printing at the University of Leeds, Arnau Oliva Puigdomènech defended his thesis on copper nanocrystals-based conductive ink at Ghent University, the third presented thesis on the development of a digital microfluidic toolkit was defended at the University of Hertfordshire by Eli Nadia Abdul Latip. All three theses are oriented into the future printing technology and development of new materials, mainly inks, for production of 3D printed objects, printed electronics, and alternative fabrication technologies for chemical and biological assay platforms. Their orientation to contemporary topics of interest for researchers and end-users is also a proof of the successful transition of conventional printing technologies into new interesting research and professional field of additive manufacturing technologies.

As usual, the Topicalities are bringing an overview of forthcoming conferences, exhibitions, and other events. Unfortunately, many of them were canceled or adapted due to pandemic. It is worth checking availability and new opportunities to attend some events online, to stay in touch with colleagues from the same research field, or to get new ideas, information, and contacts. The world is affected by the Covid-19, however, life is going on and many research groups are continuing with their activities, so you can also be a part of it.

After iarigai International Research Conference at Clemson University was canceled, we already received the first manuscripts for publication in the Journal. I hope you will also submit your full paper, and I would also appreciate it if your paper will be recognized by other researchers as an appropriate reference to their work. Join us, the Call for papers is open all the time.

Ljubljana, September 2020

JPMTR 136 | 2004
DOI 10.14622/JPMTR-2004
UDC 621.798:366.4-026.19-035.67

Original scientific paper
Received: 2020-04-03
Accepted: 2020-07-03

Development of an irreversible hydrochromic ink for smart packaging

Mustafa Bilgin and Johannes Backhaus

University of Wuppertal,
Rainer-Gruenter-Straße 21, 42119 Wuppertal, Germany

bilgin@uni-wuppertal.de
jbackhaus@uni-wuppertal.de

Abstract

Smart materials are based on chemical-physical processes that react to environmental factors or a specific stimulus. These factors or a predefined stimulus lead to structural changes. In this way, several smart materials can react to various influences such as temperature, UV light, or other. Smart materials of the type of hydrochromic inks change their colour under the influence of water or humidity. This stimulus-induced colour change process can occur in either reversible or irreversible form. Irreversible hydrochromic inks are preferable for a significant indication of the influence of water or moisture. Therefore, this research project focuses on the development and investigation of an irreversible hydrochromic ink for piezoelectric inkjet printing. For this purpose, the theoretical aspects of the chemical compound are discussed and the concept behind an irreversible hydrochromic ink is introduced. Several concentrations are evaluated and characteristic properties like viscosity, surface tension, particle size, and characteristic remission are analysed.

Keywords: smart materials, colour irreversibility, piezoelectric inkjet, spectrophotometry

1. Introduction and background

This research work is part of an overall concept of inkjet-printed multi-functional sensors and their use via smart devices. Smart materials of the type of hydrochromic inks change their structure under the influence of water or moisture in a way that they also change their colour. This stimulus-induced colour change process can occur in either reversible or irreversible form. This colour changing behaviour can be used to develop printable sensors (Bilgin and Backhaus, 2017). Therefore, the focus of this research is on irreversible hydrochromic inks, which change their colour under the influence of water and remain in their condition (Figure 1). The following irreversible hydrochromic ink was developed for piezoelectric inkjet printing based on a solvent-based matrix in which a hydrochromic dye is embedded. In the following, different experimental concentrations of a hydrochromic ink will be investigated. The viscosity, surface tension and particle size distribution of the concentrations and their suitability for inkjet printing will be analysed. Additionally, the colour change behaviour before and after contamination will be described. Various types of hydrochromic materials can be found in different ranges. Hydrochromic dyes or indicators can be combined with a desiccant such as silica gel to detect the moisture content of the desiccant (e.g. super absorber in nappies). Natural hydrochromic phenomena are also found in the environment, such as the skeleton flower (*Diphylleia grayi*). The flower has white petals but becomes translucent when it is in contact with water. After a drying period, the petals turn white again (Yong, et al., 2015). Some materials have hydrochromic properties, for example, the reversible copper(II) sulfate, which shows a white colour in a dry state and a blue colour in a humid state. Another example is the reversible cobalt(II) chloride, which shows blue colour in the dehydrated state and a red colour after hydration as hexahydrate.

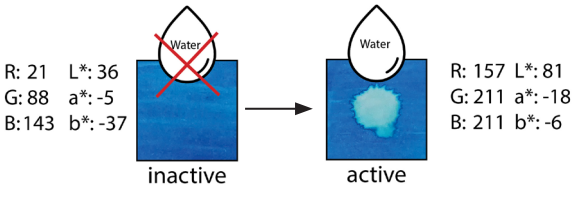

Figure 1: Hydrochromic ink (irreversible): left inactive (blue) and right active (transparent)

An alternative way of developing hydrochromic materials is microencapsulation. Microcapsule has an inner core, which often contains a dye or active ingredient, and a shell, which has functionality such as elasticity, a predefined breaking strength, or permeability (Ghosh, 2006). In this way, the permeability can release an active ingredient due to water or moisture (e.g. medication, coatings, etc.).

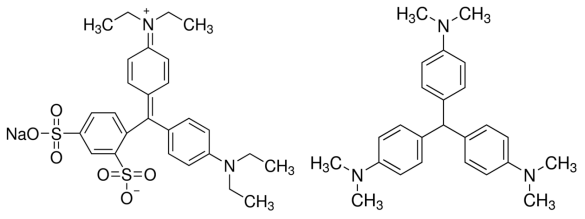

a) *b)*

Figure 2: Structural formula of (a) Patent blue V (2020), and (b) Crystal violet (2020) dyes

This research is based on a triphenylmethane dye, a leuco dye that is colourless in its triphenylmethane partial structure. Due to electron-supplying substituents (auxochromes), at least two aromatic rings in the ortho-position that are attached to a central unsaturated carbon atom can form a chromophore that can shift the absorption further into the long-wave range (invisible colour). Through adding a second auxochrome (CH3)2N group to the structure, the conjugative interaction, and delocalization of the π-electrons of the structure increases and forms, as a result, the dye malachite green. When a third auxochrome group is added, a hypsochromic shift occurs in the opposite direction and the dye crystal violet is formed (Figure 2). The application area of triphenylmethane dyes is in the production of printing inks, indicators, copy papers, smart coatings, etc. (Klöckl, 2015). Patent blue V (Figure 2) is also a triphenylmethane dye and is used in inks, food colouring (E 131) and colouring of papers. According to the regulation EU no. 231/2012 of the European commission, Patent blue V (E 131) consists essentially of calcium, sodium or potassium compounds. The structural formula of the compound is composed as follows (EFSA Panel on Food Additives and Nutrient Sources added to Food, 2013):

> N-(4-((4-(diethylamino)phenyl)(2,4-disulfophenyl) methylene)-2,5-cyclohexadien-1-ylidene) -N-ethylethanaminium, hydroxide, inner salt, sodium salt.

Patent blue V is manufactured through the "condensation and sulphonation of N,N-diethylaniline, and 3-hydroxybenzaldehyde in acidic conditions (sulphuric acid) to produce the substance under leuco form" (ibid.).

The ink eraser contains on one side a colourless felt impregnated with an oxidising agent for erasing, and on the other side a pen with an ink eraser resistant ink for correcting the previously erased area. Sodium hydrogen carbonate ($NaHCO_3$) is used as an oxidising agent to erase the triphenylmethane dye. Because of the sp^2-hybridisation of the central carbon atom, the triphenylmethane dye is coloured. This is attributable to the reason that the molecules are completely planar. The π-electrons of the double bonds and the non-binding electrons of the substituents are delocalized over the entire molecule. Consequently, the electrons are more easily excited and low-energy radiation from the visible spectrum can be absorbed more easily. The non-absorbed but reflected spectral component causes the perceptible colour impression. The invisible mechanism: anions negatively charged with water such as the hydroxide ion (OH^-) or the hydrogen sulphite ion (HSO_3^-) attack the central carbon atom and are added together. As a result, the geometry of the dye molecule is changed and the central carbon atom is sp^3-hybridised. Thus, the delocalising (resonance) of the electrons is consequently restricted, whereby visible light can no longer interact with the electrons. (Blume, 2003)

The Patent blue V now absorbs only UV radiation instead of visible light and is no longer in the visible wavelength range and therefore it appears colourless. When developing a hydrochromic inkjet ink, the chemical process of an ink eraser was used. Through the addition of the hydrogen sulphite ion ($HSO3^-$) from

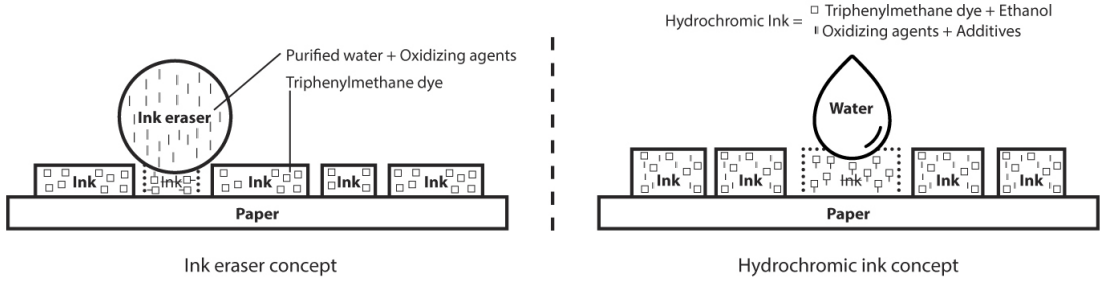

Figure 3: Concepts of (a) ink eraser and (b) hydrochromic ink

the hydrogen carbonate to the central carbon atom, the geometry of the triphenylmethane dye Patent blue V is modified. The result is that it loses its hybridised sp^2 planarity that is necessary for the colouration, changes its structure, and takes the tetrahedral arranged sp^3 form and becomes invisible. Figure 3 shows the concept behind the hydrochromic ink. The ink eraser concept (Figure 3a) is based on the principle that the ink has firstly to be applied to the paper. The ink eraser, which consists of purified water, oxidising agents, and other additives, changes the geometry of the ink and becomes invisible. The principle of the irreversible hydrochromic ink (Figure 3b) is based on a formulated ink that consists of a triphenylmethane dye Patent blue V, ethanol, oxidising agent (sodium hydrogen carbonate) and other additives that are necessary for the printability. After printing the hydrochromic ink, the ink is ready to react with water. On contact with water, the reaction of the oxidising agents with the triphenylmethane dye is stimulated and the colour becomes invisible. (Blume, 2003)

The irreversible hydrochromic ink is a part of the development of a smart code that can be applied with other smart materials in an inkjet process as printable sensors. For example, an irreversible photochromic ink was already presented in a previous publication (Bilgin and Backhaus, 2018). Possible technical solutions to read and analyse the smart code were also presented in a previous publication (Bilgin and Backhaus, 2019).

2. Materials and methods

The hydrochromic ink was developed for piezoelectric inkjet printing and is based on the solvent ethanol, to which the dye Patent blue V, a defined amount of sodium hydrogen carbonate, and additives were added. For the printing process of the hydrochromic ink, a piezo inkjet printer, commonly used in the non-professional printer segment, was used (Epson Stylus Photo 1500W / 1430W / Artisan 1430 / EP-4004). The printer showed the following technical parameters: print head IH710-9 (Part Code: F173090), MicroPiezo TFP® print head technology; thin film piezo element 1/1000 mm (PZT piezo crystal element based on lead zirconium titanate); droplet size 1.5 picolitres at 8 kHz up to 32.5 picolitres, the print head is adjustable to 5 ink droplet sizes per nozzle; nozzle configuration: 90 nozzles for black (K), 90 nozzles per colour (CMY and light variants of C and M); max. printing resolution 5760 dpi × 1440 dpi (horizontal × vertical).

The colour change process (decolourising process) of the hydrochromic ink was measured with a spectral densitometer (TECHKON SpektroDens). It is used to examine the colour values (RGB and CIE $L^*a^*b^*$) of the different colour change states (a process of decolourisation). Technical parameters: polarising filter off; type of light D50; 2° standard observer; diameter of measuring orifice 3 mm.

The hydrochromic samples were captured through a reflex camera from Nikon (D7100): image sensor size 23.5 mm × 15.6 mm; 24.71 million pixels; file format NEF (RAW), 12 or 14 bit, lossless compressed; objective AF-S 24/1,4G ED Nikkor.

The particle filtration process was performed through filtration equipment listed in Table 1 where also the materials used for the experiment are presented.

Table 1: Experimental materials and filtration equipment

Substrate	**Inapa tecno**, oxygen pure high-white recycled paper; format: 210 mm × 297 mm (A4), grammage: 80 g/m^2
Dye	**Hydrochromic blue** (Patent blue V), N-(4-((4-(diethylamino)phenyl) (5-hydroxy-2,4-disulfophenyl)methylene)-2,5-cyclohexadiene-1-ylidene)-N-ethylethanaminium, hydroxide, inner salt, sodium salt; CAS Number: 129-17-9; Chemical formula: $C_{27}H_{33}N_2O_7S_2Na$; Molar mass: 566.66 g·mol^{-1}
Oxidising agent	**Sodium hydrogen carbonate**; CAS Number: 497-19-8; Chemical formula: Na_2CO_3; Molar mass: 105.99 g·mol^{-1}
Ink base	**Ethanol**; CAS Number: 64-17-5; Chemical formula: C_2H_6O; Molar mass: 46.069 g·mol^{-1} **E24**, Octopus Fluids GmbH & Co KG; colourless, pH 7.86; Conductivity: <5 mS/cm; Viscosity: 3.00 mPa·s
Ink additive	**Urea** (humectant); Chemical formula: CH_4N_2O
Filtration equipment	**Millex-SV** (SLSV025LS); Pore size: 5.0 µm **Millex-HPF HV filter** (SLHVM25NS); Pore size: 0.45 µm **Membrane filter Express®** (PLUS PES); Pore size: 0.22 µm Filtration area: 3.9 cm^2; Material: hydrophilic polyvinylidene fluoride (PVDF)

Rheological properties (viscous flow behaviour) were analysed with the help of a rotational rheometer (Physica MCR 101) through a corresponding cone

and plate measurement system (CP50-1); diameter 49.966 mm; cone angle 1°. Surface tension was controlled by using of SITA pro line bubble pressure tensiometer. This measuring method was used for the dynamic qualification of the wetting properties and to determine the optimum bubble lifetime. A standardised paper Inapa tecno was used in experiment to ensure the comparability of the samples. A solvent ink based on ethanol was used for the inkjet process, as logically water-based ink cannot be used.

All investigations were performed under controlled laboratory conditions. An air-conditioning system was used to ensure the reproducibility of the experiments. All deviations were continuously observed and recorded in protocols. The temperature during the experiments was 20 °C (±1 °C) and the relative humidity was 55 % (±1 %).

3. Results and discussion

3.1 Experimental concentration of hydrochromic ink

Various experimental concentrations of a hydrochromic ink are described in detail below. In previous test series, suitable oxidising agents and solvents were identified for suitability to form a hydrochromic ink (Bilgin and Backhaus, 2020). Furthermore, the most suitable concentration of oxidising agents and dyestuff (Patent blue V) was identified. Therefore, the developed hydrochromic ink prototype version four was used, which is described as 4.1.1 to 4.5.1 (Table 2). With the different concentrations of the hydrochromic ink, the solvent quantities remain constant at 10 ml and only the concentration of the dye Patent blue V and the oxidising agent sodium bicarbonate differ. These concentrations are used in the following examinations.

Table 2: Different concentrations of the hydrochromic ink

Ink	Patent blue V [g]	Sodium bicarbonate [g]	Ethanol [ml]
4.1.1	0.10	0.10	10
4.2.1	0.08	0.08	10
4.3.1	0.06	0.06	10
4.4.1	0.04	0.04	10
4.5.1	0.02	0.02	10

3.2 Evaluation of an inkjet-compatible viscosity

In the following, the rheological properties, especially the viscous flow behaviour of the water-reactive hydrochromic ink, were analysed. Each of the five concentrations in Table 2 was examined to determine its viscous flow behaviour (Figure 4). All inks show pure Newtonian flow behaviour with a low viscosity that is suitable for inkjet printing. The viscosity of the base ink E24 is about 4.24 mPa·s, which also serves as a reference for an inkjet ink to which the viscosity should be adjusted (the function of E24 is described below). Ethanol, which serves as a base and solvent for the hydrochromic ink, has a viscosity of about 1.32 mPa·s. The solvent shows the lowest viscosity value of all materials. The various concentrations of the hydrochromic inks have the viscosity around 1.89 mPa·s, above that of ethanol. The viscosity increase is caused by an increase in the amount of sodium bicarbonate and Patent blue V that is dissolved in ethanol. When these components are dissolved, their molecular structure is destroyed and the molecules are dispersed in the solvent separately from each other.

Figure 5 summarizes the results of the rheological investigation. The aim was to examine the rheological properties of current hydrochromic inks and to adjust their properties for inkjet printing. Therefore,

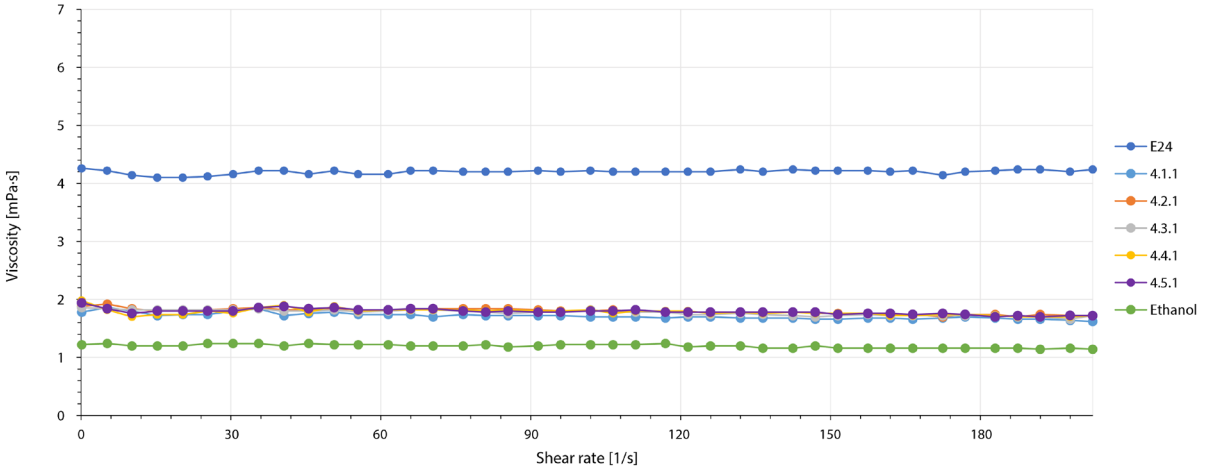

Figure 4: Viscosity analysis of all concentrations in comparison

a target process window with a minimum of 1 mPa·s (marked yellow) and a maximum of 25 mPa·s (marked grey) was defined that is in the recommended range from the literature (Magdassi, 2010). Furthermore, a water-based inkjet base ink called E24 (marked blue) specially developed for the Epson printer was used as a reference. As a result, the hydrochromic ink (actual state, marked orange) is below the range of E24 and above the minimum recommended range in the literature. Thus, the hydrochromic ink is located in the printable area. Besides, the viscosity is in the printable range also recommended by Zapka (2018) from 1 mPa·s to 50 mPa·s.

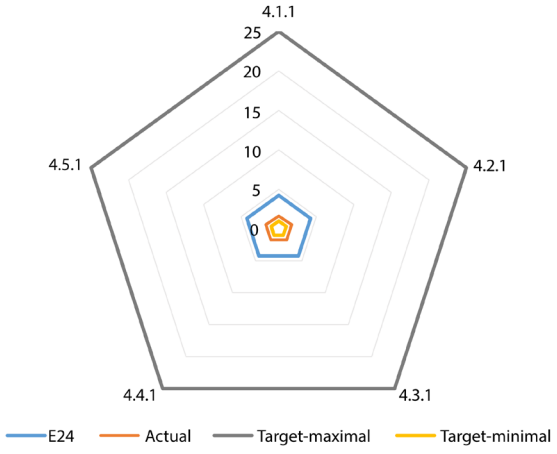

Figure 5: Viscosity analysis of the reference and prototype inks in the range up to 25 mPa·s

3.3 Evaluation of an inkjet-compatible surface tension

Subsequently, the surface tension was examined. Figure 6 describes the reference and prototype inks with different concentrations and their surface tension. The aim was to examine the surface tension of hydrochromic inks and to verify their properties and their suitability for inkjet printing. The mean temperature during the measurement of the surface tension was at around 21.6 °C. As shown in Figure 6, the surface tension of all concentrations is quite close to each other and therefore this concentration range has no significant influence on the change in surface tension. Figure 7 summarizes the results of the examination of the surface tension. As in rheology, a target process window was defined with a minimum of 20 mN/m (marked yellow) and a maximum of 50 mN/m (marked grey), which is within the recommended range from the literature (Hutchings and Martin, 2012). The Epson base ink E24 (marked blue) was also used as a reference. As a result, the hydrochromic ink (actual; marked orange) is below the range of the base ink E24 and above the minimum range recommended in the literature. Consequently, the surface tension of all hydrochromic inks is in the printable process area, above the recommended minimum requirements.

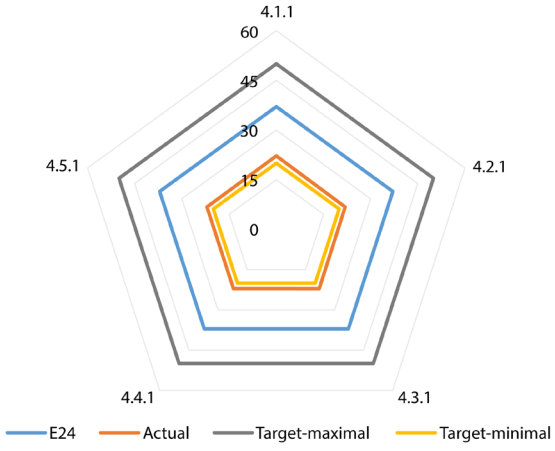

Figure 7: Surface tension analysis of the reference and prototype inks in the range up to 50 mN/m

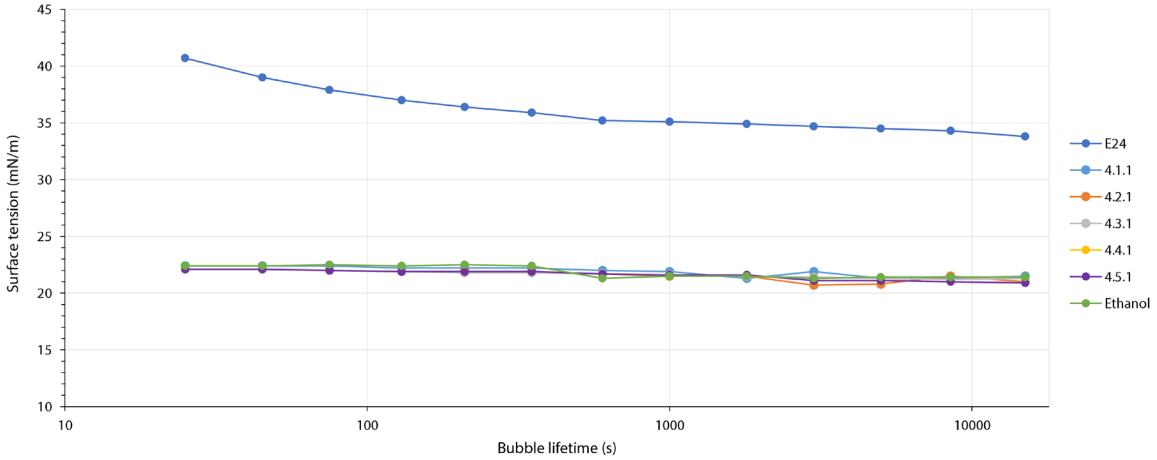

Figure 6: Surface tension of the reference and prototype inks with different concentrations

3.4 Evaluation of an inkjet-compatible particle size

Patent blue V has a solubility of 20 g/l at 20 °C and 100 g/l at 90 °C. According to Otterstätter (1999), it is recommended to work in a concentration range without the potential for crystallisation. Furthermore, the entire solution must be filtered to retain undissolved particles (Figure 8). For this purpose, a test has already been carried out to determine the undissolved particle components in the hydrochromic ink. In this context, the distribution of the undissolved particles in the solution was examined in detail (Bilgin and Backhaus, 2020).

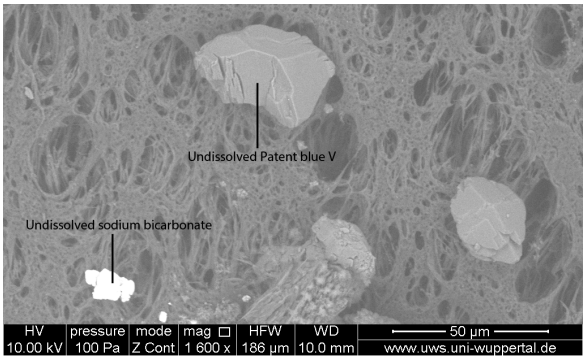

Figure 8: Microscopic examination of particles on a 220 nm filter

Before the inks were used for the printing process, the inks were filtered in three phases and then filled into an inkjet cartridge. Firstly, the particles were filtered with a Millex SV (SLSV025LS) filter membrane with a pore size of 5.0 µm, so that all particles larger than 5.0 µm were filtered out. Afterward, the remaining particles were filtered with a Millex HPF HV (SLHVM25NS) filter membrane with a pore size of 0.45 µm so that only particles smaller than 0.45 µm were present in the ink. Finally, the third filtration process using the Express® membrane filter was applied, in which all particle sizes above 0.22 µm were filtered out. Through the filtration process, the developed irreversible hydrochromic ink shows the recommended particle size range of less than 200–300 nm (Magdassi, 2010). This ensures that harmful residual particles that would otherwise lead to clogging of the inkjet pipes and the nozzles have been eliminated.

3.5 Spectrophotometric analysis

Figure 9 shows the remission curves in a reacted (transparent, marked turquoise) and unreacted state (blue, marked blue). The characteristic of the unreacted hydrochromic ink is visible in the wavelength range from 425 nm to approx. 560 nm, with a peak of the hydrochromic ink in the range of 470 nm. In the reacted state (after the influence of water), the peak extends into the region of 400 nm to 640 nm. This colour change process can also be seen in the CIE $L^*a^*b^*$ values, where a difference in lightness from $L^* = 52$ to $L^* = 87$ can be observed. Thus, statements about the influence of contamination with water/moisture can be determined by colorimetric detection (Bilgin and Backhaus, 2019).

4. Conclusions

This research was demonstrating a hydrochromic ink that changes its colour irreversibly under the influence of water and remains in that state. The theoretical background, colour-change functionality, and the concept of a hydrochromic ink was discussed. Furthermore, this work aimed to investigate the characteristic proper-

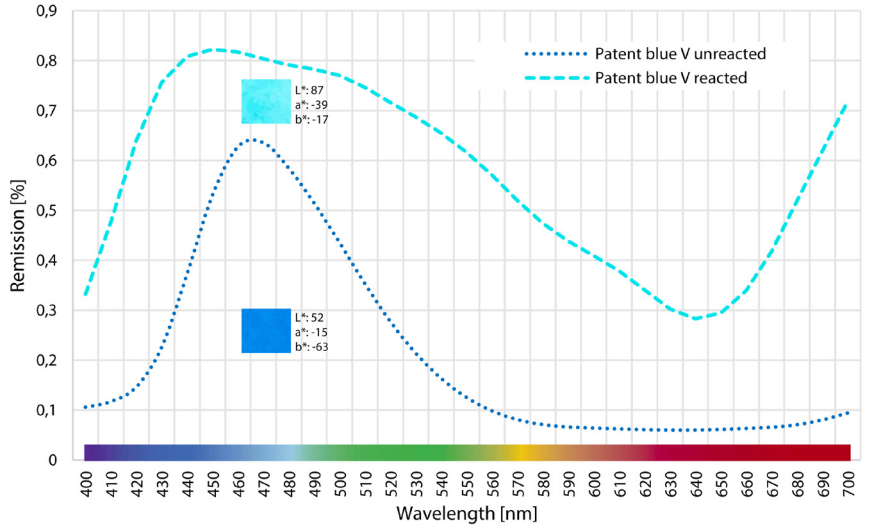

Figure 9: Spectrophotometric analysis of the hydrochromic ink

ties such as viscosity behaviour, surface tension and describe the filtration process to prevent harmful particles to adapt the hydrochromic ink for the piezoelectric inkjet printing. For this purpose, five different concentrations were selected to investigate the characteristic properties of the ink with reference to its suitability as an inkjet ink. Recommended limit values from the literature were used, which served as a guideline for the development of a hydrochromic ink. Besides, a base ink was used as a reference, which was already designed for piezoelectric inkjet printing. The next step in the development of a smart code, which can be applied with other smart materials in an inkjet process as printable sensors was taken.

Acknowledgments

Many thanks to my assistants Jacqueline Schrank and Nicole Paulke for their technical support in the laboratory. Furthermore, many thanks to Dr.-Ing. Qian Zhang for his advice on particle measurement.

References

Bilgin, M., and Backhaus, J., 2017. Smart packages by means of intelligent codes. In: P. Gane, ed. *Advances in Printing and Media Technology: Proceedings of the 44th International Research Conference of iarigai*. Fribourg, Switzerland, September 2017. Darmstadt, Germany: iarigai, pp. 89–96.

Bilgin, M. and Backhaus, J., 2018. Development of a unidirectional switchable photochromic ink for smart packaging. In: P. Gane, ed. *Advances in Printing and Media Technology: Proceedings of the 45th International Research Conference of iarigai*. Warsaw, Poland, October 2018. Darmstadt, Germany: iarigai, pp. 55–63.

Bilgin, M. and Backhaus, J., 2019. Smart materials detection using computer vision. In: C. Ridgway, ed. *Advances in Printing and Media Technology: Proceedings of the 46th International Research Conference of iarigai.* Stuttgart, Germany, September 2019. Darmstadt, Germany: iarigai, pp. 75–83.

Bilgin, M. and Backhaus, J., 2020. Hydrochromic ink as a security feature for piezoelectric inkjet printing. *International Circular of Graphic Education and Research*, 12, pp. 17–28.

Blume, R., 2003. *Chemie des Tintenkillers*. [online] Chemie und Didaktik der Chemie, University of Bielefeld. Available at: <www.chemieunterricht.de/dc2/tip/09_03.htm> [Accessed 27 January 2020].

Crystal violet, 2020. *Leucocrystal violet*. [online] Available at: <https://www.sigmaaldrich.com/catalog/product/aldrich/219215> [Accessed September 2020].

EFSA Panel on Food Additives and Nutrient Sources added to Food, 2013. Scientific opinion on the re-evaluation of Patent Blue V (E 131) as a food additive. *EFSA Journal*, 11(3): 2818. https://doi.org/10.2903/j.efsa.2013.2818.

Ghosh, S.K. ed., 2006. *Functional coatings: by polymer microencapsulation*. Weinheim, Germany: Wiley-VCH, p. 13.

Hutchings, I. and Martin, G. eds., 2012. *Inkjet technology for digital fabrication*. Chichester, UK: John Wiley & Sons, p. 91.

Klöckl, I., 2015. *Chemie der Farbmittel: in der Malerei*. Berlin, Germany: Walter de Gruyter, p. 384.

Magdassi, S. ed., 2010. *The chemistry of inkjet inks*. Singapore: World Scientific Publishing, p. 21, 34.

Otterstätter, G., 1999. *Coloring of food, drugs, and cosmetics*. New York, USA: Marcel Dekker, p. 51.

Patent blue V, 2020. *Patent blue V calcium salt*. [online] Available at: <https://www.sigmaaldrich.com/catalog/product/sial/74748> [Accessed September 2020].

Yong, J., Chen, F., Yang, Q., Du, G., Shan, C., Bian, H., Farooq, U. and Hou, X., 2015. Bioinspired transparent underwater superoleophobic and anti-oil surfaces. *Journal of Materials Chemistry A*, 3(18), pp. 9379–9384. https://doi.org/10.1039/C5TA01104C.

Zapka, W. ed., 2018. *Handbook of industrial inkjet printing: a full system approach*. Weinheim, Germany: Wiley-VCH Verlag, p. 12.

JPMTR 137 | 2005
DOI 10.14622/JPMTR-2005
UDC 544.77-035.67:546.212

Research paper
Received: 2020-06-22
Accepted: 2020-07-07

Optimization of water-based ink formulation based on different NCO : OH ratios of polyurethane dispersion

Shilpa Anchawale, M P Raghav Rao and Yogesh Nerkar

Department of Printing Engineering,
PVG's College of Engineering and Technology,
Savitribai Phule Pune University, Pune 411009

anchawale.shilpa@gmail.com

Abstract

Due to environmental concerns presently water-based inks are in demand in packaging and label printing, when the application is on paper and paperboard. But these inks are found to be incompatible while printing on a non-porous substrate like the films of polyethylene and polypropylene which are majorly used in the packaging industry for printing. Adhesion as well as optical properties (gloss) of water-based ink deposited onto the polymer film substrate are critical in flexible packaging. Hence the objective is to optimize water-based ink formulation for specific type of binder, its percentage, and percentage of other ingredients such as surfactant and polymer emulsion to achieve the complete adhesion and maximum gloss, which is utmost important for the growth of the water-based ink market in flexible packaging. The design of experiments (mixture model) was conducted to formulate water-based inks by varying the percentages of pigment–binder ratio (resin percentage), surface wetting agent, and polyethylene-based polymer emulsion. Scotch tape qualitative test method was used to measure the adhesion of ink. Adhesion percentage was calculated by analysing the area of ink which remained intact on the substrate. Data was analysed by using the multivariate data analysis method. This model was used to optimize the formulation for complete adhesion of water-based ink on the film substrate. The model explains that complete adhesion of water-based ink on polyethylene substrate takes place at 35.24 % of resin (1 : 1.5 pigment–binder ratio), 1 % of polymer emulsion, and 0.3 % of surfactant. Complete adhesion is observed for 1.35 and 1.4 NCO : OH ratios of polyurethane dispersion. Response surface design was used to find out the effect of binder and surfactant on the gloss of ink. The response surface model explains that surface tension is the dominant parameter for improving the gloss of ink on the substrate. Maximum 80.5 % gloss was observed for higher means at 1.4 NCO : OH ratio of binder and when 0.3 % of substrate wetting agent was used.

Keywords: adhesion, gloss, surface tension, flexography, statistical analysis

1. Introduction

Solvent-based inks have been successfully used in flexography for printing on both absorbent (paper and paper board) and non-absorbent (plastic film) substrates. Environmentally friendly water-based ink (Verspoor, 2005; Saad, 2007; Gu, Li and Zhang, 2013) is an inspiring substitute for the solvent-based inks used in packaging applications. Eco-efficiency analysis of printing inks for flexible packaging has reported that the water-based ink system has a lower overall environmental impact and lower life cycle costs compare to the UV and solvent-based ink system. It also reduces the carbon footprint (Piluso, et al., 2009; BASF Group, 2017). Due to strict environmental rules and regulations industries have started using water-based ink in the packaging field. The water-based ink has been successfully implemented on paper or paperboard substrate which is used in different printing and packaging applications, but these inks are found to be incompatible while printing on a non-porous substrate like the films of polyethylene and polypropylene which are majorly used for packaging printing (Saad, 2007; Gu, Li and Zhang, 2013). High surface tension water-based inks spread poorly on the non-absorbent substrate as they have low surface energy. Poor wetting promotes the adhesion problem of water-based ink on the non-absorbent substrate (Ramirez and Tumolva, 2018). Nowadays, the atmospheric plasma is used to treat the polymer surface to increase the surface energy and hence wettability. Interaction of plasma species with the polymer surface produces chemical groups on the surface for crosslinking and activation (Wolf and

Sparavigna, 2010). Corona treatment is another method used to enhance the surface energy of substrate like polyethylene and hence the adhesion. This can be achieved by grafting appropriate functional groups on the polymer surface, however, corona treatment can damage the physical properties (Izdebska and Thomas, 2015; Ramirez and Tumolva, 2018). Along with these surface treatments up to a certain level, to form good bonding with the ink, modification in ink formulation as well as modification in ink chemistry is a considerable approach in the industry (Chashmejahanbin, et al., 2014; Ramirez and Tumolva, 2018).

Ink adhesion and gloss properties play an important role in flexible packaging as well as in label printing applications. Gloss is also strongly influenced by the surface properties of the substrate and the physical and chemical properties of the ink ingredients which strongly affect the smoothness of ink film (Bohlin, 2013; Ramirez and Tumolva, 2018). The gloss of water-based ink when printed on non-absorbent substrate is majorly influenced by pigment wetting, degree of dispersion, pigment particle size distribution, and the surface tension of water-based system, as these are the influencing parameters for the smoothness of water-based ink film on the non-absorbent surface (Olsson, Yang and Lestelius, 2007).

Experiments were conducted to improve the performance properties of water-based ink. Few of them focused on optimization of ingredients percentage to improve the performance of ink (Rentzhog, 2006; Ramirez and Tumolva, 2018). In some studies, binders were synthesized to improve the performance of ink in terms of gloss, water-resistance, and stability (Yu, Huang and Wei, 2011; Liang and Zhou, 2012; Fang, et al., 2014; Wang, et al., 2016). Few studies focused on the reduction of pigment particle size during the dispersion process which is also one of the influencing parameters for the gloss and performance properties of the ink (Fang, et al., 2010; Tai, et al., 2012; Liang and Zhou, 2012).

To get complete benefit of a pigment both visually and economically, reduction of pigment agglomerates up to the primary pigment particle size is recommended. Visual benefit in terms of color strength depends on the exposed surface area of pigment. Smaller the pigment size, the higher the surface area gets exposed and provides a stronger color (Klein, 2006). Thus, smaller pigment particle size reduces the pigment loading of the formulation (Herbst and Hunger, 2006; Klein, 2006). This reduced amount of pigment loading helps for improving gloss on the non-absorbent substrate.

Studies on pigment dispersion process parameters, their effect on the particle size distribution of pigment, and final performance properties of ink have been in focus from many researchers (Inam, 2010; Inam, Ouattara and Frances, 2011; Abrahão, 2013; Ohenoja, Illikainen, and Niinimäki, 2013; Ohenoja, 2014; Senthilkumar and Akilamudhan, 2014; Simpson, et al., 2015). Studies from Fang, et al. (2010), Ramirez and Tumolva (2018). Inam (2010), Schmidt, et al. (2012) and Hamey (2005) concluded that dispersion process parameters, binders, and surfactants, influence particle size distribution, surface smoothness and the gloss of ink.

Hence optimization of dispersion process parameters as well as optimization of ink formulation needs to be done to improve the performance properties of water-based ink.

Binders, substrate wetting agents and polymer emulsion are the key influencing ingredients for surface tension, adhesion, and gloss of ink. Binder used in ink formulation has a major effect on ink performance properties. Strong demand for the use of eco-friendly products in the packaging industry has increased the demand for use of aqueous polyurethane (PU) binder which has the potential to significantly reduce volatile organic compounds (VOCs) and environmental hazards. NCO : OH ratio of polyurethane dispersion (PUD) alters the urea-urethane groups present in the PU structure (Athawale and Kulkarni, 2010). It also affects the ionic groups and isocyanate groups present in the formulation which are taking part during the reaction (Nanda, et al., 2005; Negim, et al., 2011). Negim, et al. (2011) reported that for increasing NCO : OH ratio, particle size of PUD increases and viscosity decreases. Lei, et al. (2014) also reported that an increase in ionic percentage increases the surface tension of PUD. Thus NCO : OH ratio influences various mechanical, physical, and optical properties of PUD.

There was a little focus on the effect of structural modification such as hard : soft segment ratio, ionic content of PUDs, and their interaction with other ingredients of water-based ink on the printability of ink while printing on non-absorbent substrate. Also, the effect of PUD synthesized from polyester polyol on the performance of water-based ink while printing on non-absorbent substrate is relatively unexplored.

Hence in this research PUD which is synthesized from polyester polyol and for different NCO : OH ratio has been used as one of the parameters during the design of the experiment (DOE).

The objective of this study is to optimize the formulation of water-based ink for specific NCO : OH ratio of polyester-based PUD, pigment–binder ratio, percentage of surfactant and polymer emulsion to get the complete adhesion and maximum gloss of ink on a film substrate.

2. Experimental procedure

Optimized mill base having 28 % pigment loading and 7 % dispersing agent, which provides 128 nm average particle size distribution width was used as a pigment pre-mixture during formulation. The PUDs based on four different NCO : OH ratios, 1.15, 1.27, 1.35, and 1.40, were used in the formulation. The DOE was developed for each NCO : OH ratio of binder and other ingredients of ink. The first part of the experiment consists of optimization of water-based ink in terms of pigment–binder ratio (resin percentage), percentage of wetting agent, and polymer emulsion for four types of resins to get the complete adhesion of ink on the substrate. The multivariate data analysis was conducted to optimize the formulation for each specified resin. Response optimizer was used to fix the pigment–binder ratio (resin percentage) and percentage of polymer emulsion in ink formulation for the adhesion of ink on the non-absorbent substrate.

The second part of the optimization of the formulation is carried out to achieve maximum gloss. Four resins based on different NCO : OH ratio and percentage of the wetting agents were considered as a variable for the DOE. Response surface analysis was carried out to find out the effect of NCO : OH ratios of binder and the effect of substrate wetting agent on the gloss of ink.

2.1 Materials

Stable, homogeneously distributed pigment concentrate consists of rubine red pigment (Sudacolor Red 604 PR 57:1) supplied by Sudarshan Chemical Industry, copolymer with pigment affinic group for improved attachment to the surface of polar pigments as dispersing agent (DISPERBYK-2015) provided by BYK Additives and solution of a polyether-modified polydimethyl siloxane as antifoaming agent (BYK-019) supplied by BYK Additives. The width of the particle size distribution (D90) of pigment paste was 128 nm and total solid loading of 35 % was kept constant throughout the DOE. Thus a constant percentage of pigment, dispersing agent, and antifoaming agent were used in the let-down formulation. Silicon surfactant (BYK-349) supplied by BYK Additives was used as a substrate wetting agent (WA) and deionized (DI) water as a solvent.

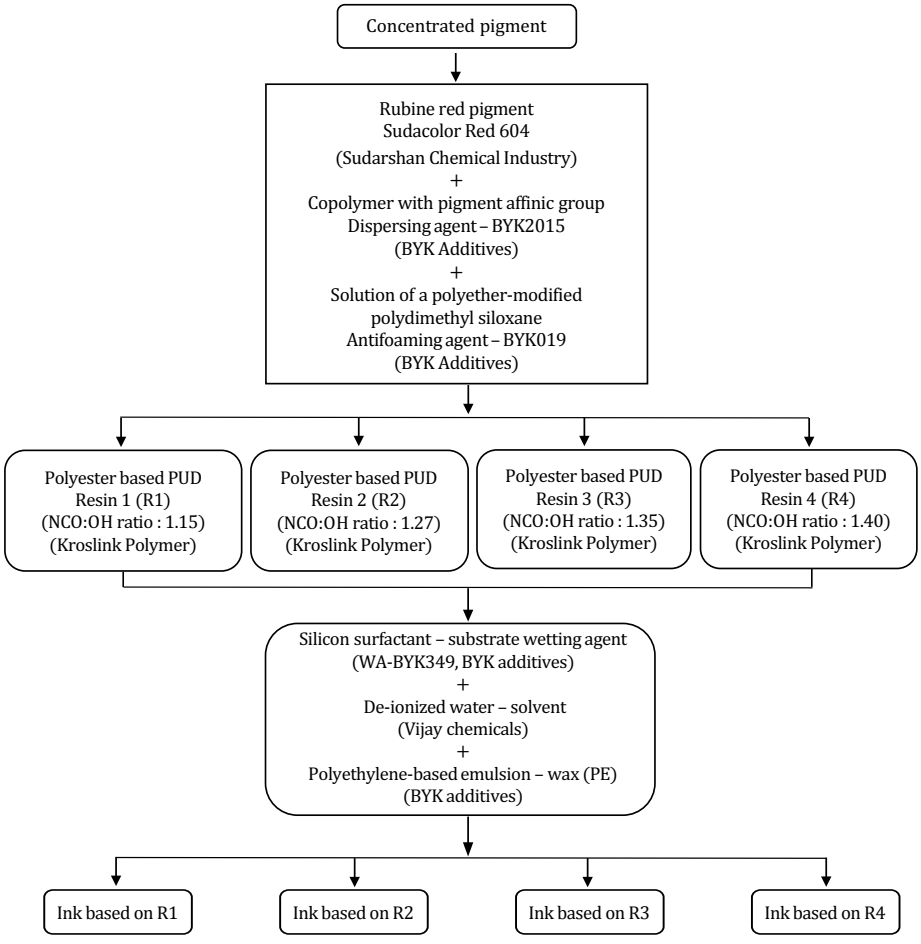

Figure 1: Flowchart for ink ingredients and stepwise addition

In order to improve the scratch resistance, polyethylene-based emulsion (Aquacer 532) provided by BYK Additives was used as a wax. Polyester-based PUD was synthesized by using isophorone diisocyanate, polyethylene-based polyol, and dimethyl propionic acid (DMPA) by the pre-polymerization method. Polyurethane dispersions were provided by Kroslink polymer. Four PUDs based on different NCO : OH ratios, 1.15 (R1), 1.27 (R2), 1.35 (R3), and 1.40 (R4), were used as one of the variables of DOE. The flexible substrate chosen was low density polyethylene (LDPE, thickness: 40 μm) provided by the Parakh Agro company. Figure 1 shows the flowchart for ink ingredients and their stepwise addition which is self-explanatory.

2.2 Characterization

Fourier transform infrared (FTIR) spectra of samples were recorded by using SHIMADZU IR spectrometer in the wavenumber range of 400–4 000 $cm^{-1.}$ Particle size distribution (PSD) measurements of PUD and ink samples were carried out using Malvern Particle Size Analyser, Zetasizer Nano-S90 model. The viscosity of PUD was measured with a rotational viscometer Anton Paar Physica MCR101. The glass transition temperatures (T_g) were determined on Pyris controlled PerkinElmer DSC 4000 Thermogravimetric Analyzer under the continuous purge of nitrogen at 20 ml/min. The measurements were carried out in the temperature range of –100 °C to 100 °C. Field emission scanning electron microscope (SEM) Nova NanoSEM 450 equipped with energy dispersive X-ray spectrometer (EDS) BRUKER, XFlash 6130 was used to investigate the microstructure and elemental composition of materials. Solid content of PUD and pigment dispersion paste was determined as per ISO 124:1997 standard procedure by using hot air oven (International Organization for Standardization, 1997). Viscosity measurements of the ink were performed using Brookfield DV-I viscometer, at a shear rate of 100 s^{-1} at 25 °C. The pH of ink was measured by Hanna pH meter HI991001P with 0.01 pH resolution and an accuracy of ±0.05 pH. A quantitative standard test method for specular gloss defined by ASTM (ASTM International, 2018a) was used in the second part of experiment. Gloss was measured by Rhopoint Novo-Gloss meter. The standard measurement geometry of the gloss meter is 20°, 60°, or 85° depending on the test sample. In this experiment, the medium gloss range (60° angle) was used to determine the gloss values.

2.3 Design of experiment

A mixture experiment model of a DOE is a special class of response surface experiments in which the product is made up of several components or ingredients. In mixture design, the product was formed by the mixture of product ingredients in different proportions. Product quality or performance of the product (response) is dependent on the relative proportions of the components. In this experiment performance of ink depends upon the relative proportion of ingredients such as pigment–binder ratio (resin percentage), wetting agent, and polymer emulsion. If we increase the percentage of one ingredient it reduces the percentage of other ingredients, which means the final performance properties of inks such as adhesion, surface tension, gloss and stability depend upon the relative proportion of each ingredient. Mixture design model provides the interaction of each ingredient and optimizes the percentage of ingredients by considering their interaction with each other.

The Minitab 17 statistical software was used to statistically analyze the data and for the prediction of response.

Table 1: Variables and levels for DOE

Variables	Level-1	Level-2
P : B ratio	1 : 1.3	1 : 1.5
WA (%)	0.2	0.3
PE (%)	0.5	1.0

Table 2: Design of experiment for analysis of adhesion for 24 formulations

Formul. no.	Resin (%)	WA (%)	PE (%)	Water (%)
1	30.56	0.2	0.5	36.87
2	30.56	0.2	0.5	36.87
3	30.56	0.2	0.5	36.87
4	30.56	0.3	0.5	36.77
5	30.56	0.3	0.5	36.77
6	30.56	0.3	0.5	36.77
7	30.56	0.2	1.0	36.37
8	30.56	0.2	1.0	36.37
9	30.56	0.2	1.0	36.37
10	30.56	0.3	1.0	36.27
11	30.56	0.3	1.0	36.27
12	30.56	0.3	1.0	36.27
13	35.24	0.2	0.5	32.19
14	35.24	0.2	0.5	32.19
15	35.24	0.2	0.5	32.19
16	35.24	0.3	0.5	32.09
17	35.24	0.3	0.5	32.09
18	35.24	0.3	0.5	32.09
19	35.24	0.2	1.0	31.69
20	35.24	0.2	1.0	31.69
21	35.24	0.2	1.0	31.69
22	35.24	0.3	1.0	31.59
23	35.24	0.3	1.0	31.59
24	35.24	0.3	1.0	31.59

The DOE for ink formulation involves two levels of each: pigment to binder ratio (P : B) expressed also as resin percentage, wetting agent (WA), and polymer emulsion (PE) as shown in Table 1. The DOE was repeated for four resins to determine the performance of different properties of a resin with other ink ingredients. The DOE is as shown in Table 2, which considers the total of 24 formulations for one resin. These 24 formulations were repeated for four resins, thus a total of 96 formulations were evaluated for adhesion of ink.

In this experiment, pigment paste was used as 31.87 % to get 9 ± 0.5 % pigment loading in let-down formulation, which maintains the constant pigment loading, constant percentage of a dispersing agent, and an antifoaming agent in the let-down formulation designed by the mixture model of the DOE.

The second part of the experiment considers four PUD resins based on different NCO : OH ratios and two percentages of the wetting agent as a variable to find out their effect on gloss and optimize the formulation for highest gloss. The values for both variables are as shown in Table 3.

Table 3: Design of experiment for gloss

Variables	Level-1	Level-2	Level-3	Level-4
PUD with different NCO : OH ratio	1.16	1.27	1.35	1.40
WA (%)	0.5	0.3	–	–

2.4 Surface energy

The surface energy of the LDPE substrates was determined from the contact angle measurements. Three liquids (purified deionized water supplied by Vijay Chemicals, formamide, and glycerol both supplied by Thermo Fisher Scientific) of known surface tension i.e. surface energy γ, with dispersive component γ_d and polar component γ_p of the liquids (Table 4) were used, and the contact angle of these liquids on LDPE films was measured by using the Holmarc contact angle meter.

Table 4: Surface energy, polar and dispersive component of test liquids

Sample	γ (mJ/m^2)	γ_d (mJ/m^2)	γ_p (mJ/m^2)
Water	72.8	21.8	51.0
Formamide	58.2	39.6	18.6
Glycerol	63.4	37.0	26.4

Surface energy, dispersive components, and polar components of LDPE substrates were calculated by using Fowke's model. The theoretical basis of this is the Young–Dupre equation. In this model, as shown in Equation [1], the work of adhesion (adhesion energy) W_a is expressed in terms of the dispersive and polar components of the surface energy (Carré, 2007; Izdebska and Thomas, 2015).

$$\gamma_l (1 + \cos\theta) = 2[(\gamma_{ld} \cdot \gamma_{sd})^{1/2} + (\gamma_{lp} \cdot \gamma_{sp})^{1/2}] \quad [1]$$

where γ_l is the surface tension of the ink, θ is the angle made by ink with the surface of the substrate, γ_{ld} and γ_{sd} are dispersive components of the ink and solid substrate, and the γ_{lp} and γ_{sp} are polar components of the ink and solid substrate, respectively.

The interfacial tension γ_{sl}, work of adhesion W_a, and spreading coefficient S have been calculated using Equations [2] to [4]:

$$\gamma_{sl} = \gamma_s - \gamma_l (\cos\theta) \quad [2]$$

$$W_a = \gamma_s + \gamma_l - \gamma_{sl} \quad [3]$$

$$S = \gamma_s - \gamma_l - \gamma_{sl} \quad [4]$$

where γ_s is the surface energy of the substrate.

Surface tension of the ink was measured by using a ring tensiometer. The interfacial surface tension between ink formulated from PUD which was based on different NCO : OH ratio and LDPE substrate were calculated by the Young equation.

A stirrer with a maximum speed of 2 600 rpm was used for mixing of all the ink ingredients. Each let-down mixture was stirred for 30 minutes. Automatic film applicator LLOYD model SM 102 and barcoater (number: 0, thickness: 4 µm) was used for a drawdown of each formulation onto the substrate. Drawdowns were taken at 65 mm/s speed.

2.5 Adhesion of ink

Adhesion of water-based ink was measured by using the ASTM adhesion method (ASTM International, 2017). Adhesion test method F2252 / F2252M (ASTM International, 2018b) was performed using a standard 3M #610 Scotch tape, 25–38 mm (1–1.5 inch) wide, and manually pulling off the tape to determine the degree of ink adhesion or ink removal from the substrate.

For evaluation the glass slab which is marked with a one-inch square area (25.4 mm × 25.4 mm) divided into 16 squares was used. As the grid was applied on the glass slab it did not affect the printed ink layer of the sample. The peeling off the Scotch tape from the ink coated substrate was done as per the standard method. The peeled tape was pasted on the non-printed area of the substrate. The marked grid of glass slab was

kept on the peeled tape and each area of the grid was examined to investigate the removal of ink through an optical microscope. The number of squares which remain intact provides the total adhesion of ink on the substrate. The percentage of adhesion was calculated by using Equation [5].

$$\text{Adhesion of ink} = \frac{\text{Number of intact squares}}{\text{Number of total squares}} \cdot 100 \ (\%) \quad [5]$$

Grading A to E was used based on an intact percentage. Reference for intact percentage and grading is as follows:

A – 100 % adhesion and 0 % removal of an ink,
B – 75 % adhesion and 25 % removal of an ink,
C – 50 % adhesion and 50 % removal of an ink,
D – 25 % adhesion and 75 % removal of an ink,
E – 0 % adhesion and 100 % removal of an ink.

2.6 Printed samples preparation

The formulated water-based inks were printed on a LDPE substrate by the drawdown method. After printing, samples were dried using air blower for 5–10 s, and then allowed to dry for 24 h to cure the ink. Ten drawdowns for each condition were printed. Thus, a total of 1080 samples were printed. The density value D of each sample was measured at 6 different places and the sample which has minimum deviation ($D = 0.85 \pm 0.5$) was selected for sampling. Three samples having minimum deviation were selected as a sample size for each condition of the mixture model. A total of 288 samples were selected for all four types of resin models.

3. Results and discussion

3.1 Fourier transform infrared spectroscopy

Fourier transform infrared spectroscopy was used to analyse the functional group of PUD. Figure 2 shows the FTIR of PUD used during formulation.

The FTIR spectra of all the PUDs showed characteristic absorption band between 3457 cm^{-1} to 3352 cm^{-1} indicating N-H stretching vibrations. The absorption bands observed at 2952 cm^{-1} and 2950 cm^{-1} are associated with C-H stretching of the CH_2 group. The band at 1718 cm^{-1} to 1709 cm^{-1} corresponds to C=O stretching from ester and urethane groups. According to the characteristic peaks, C=O (1718 cm^{-1} to 1709 cm^{-1}) and N=H (1532 cm^{-1} to 1530 cm^{-1}), the formation of the urethane group (-NHCOO-) was confirmed. Slight transmittance at 2270 cm^{-1} shows the presence of a slight percentage of NCO. The presence of the NCO band at 2355 cm^{-1} confirms the presence of free urethane as a higher percentage of NCO : OH ratio is used.

3.2 Characterization of PUDs

Table 5 shows the characteristics of the PUDs (binders) prepared by using different NCO : OH ratios, marked from R1 to R4, used for the DOE.

Table 5: Physical properties of PUDs for different NCO : OH ratio and constant molar ratio of PEG and DMPA

Variables	R1	R2	R3	R4
NCO : OH ratio	1 : 1.15	1 : 1.27	1 : 1.35	1 : 1.40
Avg. particle size (nm)	29.02	47.88	64.98	65.63
Width of PSD (nm)	57.30	59.50	71.90	80.00
Viscosity at 30 °C (mPa·s)	734	665	520	494
Solids (mass fraction, %)	36.04	35.95	36.95	36.16

3.3 Effect of NCO : OH ratio on T_g of PUD

The result of differential scanning calorimetry (DSC) measurement of PUD with NCO : OH ratio of 1.4 is shown in Figure 3. The results of retrieved T_g of PUDs for different NCO : OH ratios are shown in Table 6. It was observed that T_g of PUD increases from −16.40 °C to −8.35 °C as NCO : OH ratio increases from 1.16 to 1.40. The results are in line with previous research (Negim, et al., 2011).

The higher percentage of NCO contributes to the formation of urea groups. The T_g value is slightly higher for 1.4 NCO : OH ratio due to an increased percentage of hard segments. Increased hard segment provides stronger physical crosslinking through hydrogen bonding and improve the adhesion of water-based ink on the non-absorbent substrate such as LDPE.

Table 6: Glass transition temperature of PUDs for different NCO : OH ratios

NCO : OH ratio	T_g (°C)
1.15	−16.40
1.27	−11.58
1.35	−9.40
1.40	−8.35

3.4 Scanning electron microscope and energy-dispersive X-ray results

Figure 4 shows SEM and EDS results of the LDPE surface. The EDS analysis shows the presence of nitrogen and oxygen groups on the surface of LDPE material. Strong bond formation observed with these groups may be explained with the urea and urethane group present in the PUD. Free NCO present in the dispersion will help to form a stronger bond with the substrate.

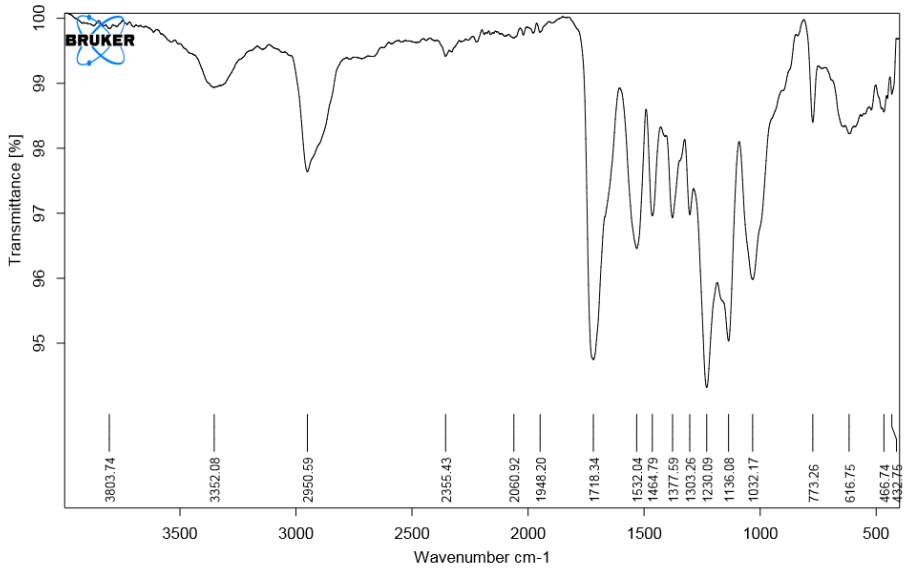

Figure 2: The FTIR spectrum of PUD

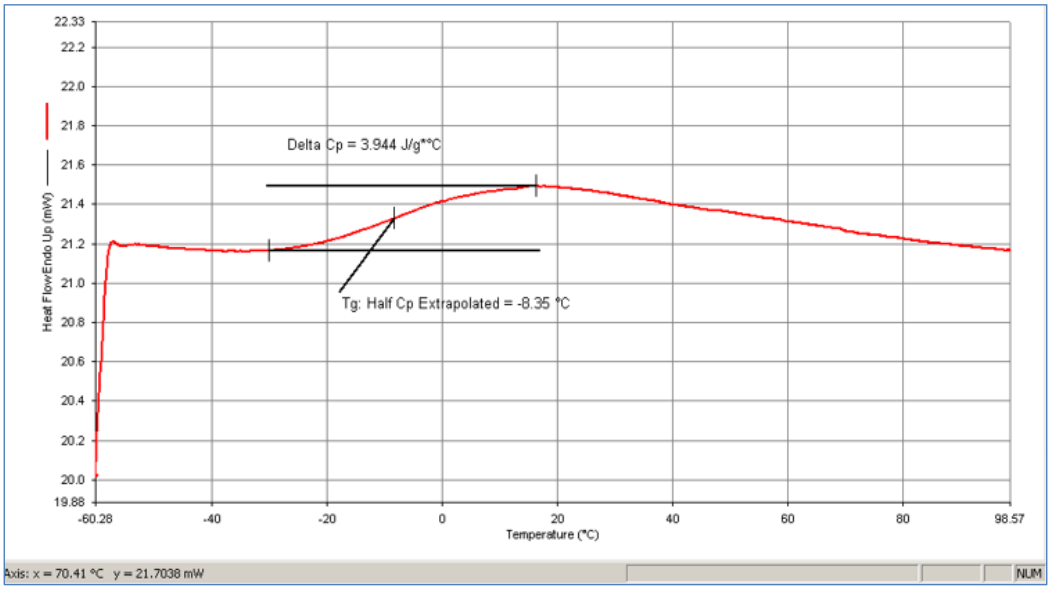

Figure 3: The DSC curve of PUD at 1.4 NCO : OH ratio

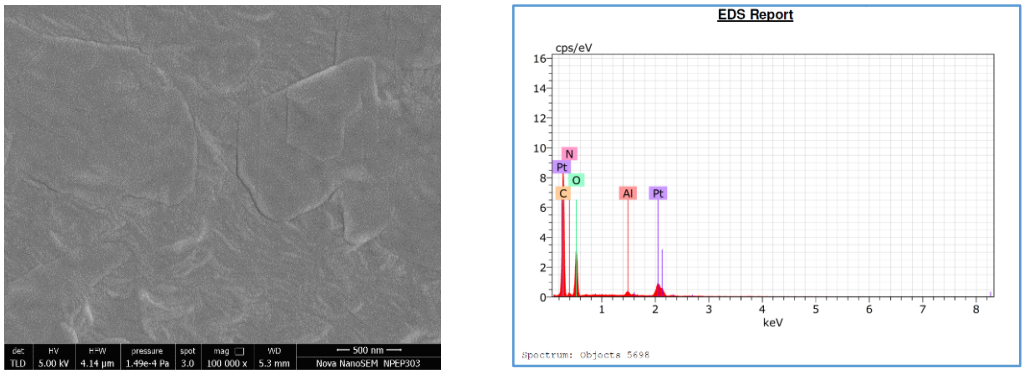

a) *b)*

Figure 4: The LDPE surface: (a) SEM picture, and (b) EDS analysis results

3.5 Surface energy of LDPE film

Table 7 shows the average value of the polar component, disperse component, and surface energy of LDPE film calculated by using three liquids.

Table 7: Surface energy, dispersive and polar components of LDPE non-absorbent film

Sample	γ_s (mJ/m^2)	γ_{sd} (mJ/m^2)	γ_{sp} (mJ/m^2)
LDPE	39.63	36.44	3.19

4. Statistical analysis

4.1 Simplex design plot

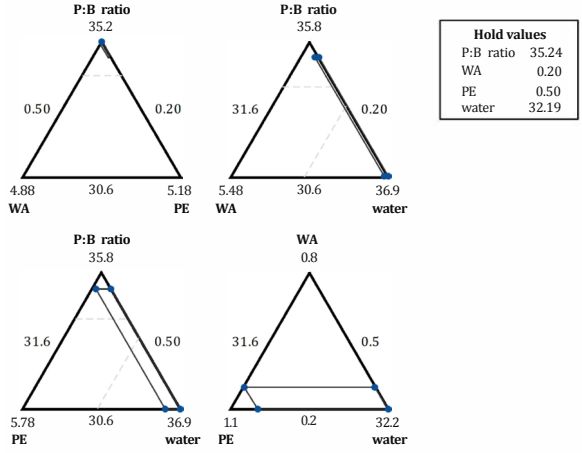

Figure 5: Simplex design plots in amounts for P : B ratio, PE, WA and water

A simplex design plot is used to visualize the mixture design space or a slice of the design space for more than three components. Minitab software plots the design points on the triangular axes as shown in Figure 5. The vertices of the triangle show the three pure mixtures for each component (PE, P : B ratio, WA, and water). Three binary blends are found at the midpoint of each edge of the triangle. Inside the triangle, blends are for three components but not in equal proportion. The blend at one centre point (or centroid) represents the proportions of all three components.

4.2 Statistical analysis for adhesion of water-based ink

Table 8 presents the analysis of variance (ANOVA) for the adhesion test and regression mixture model for PUD resin based on 1.16 NCO : OH ratio, marked as WB_AD_R1.

The ANOVA Table 8 helps to understand the significance of a ratio of ink ingredients for the adhesion of ink on the non-absorbent substrate. For mixture design the main terms that represent the three factors are P : B ratio, WA, and PE, among that the magnitude of the coefficient indicates that for P : B ratio (44) provides adhesion with higher acceptance levels. The individual responses of WA (–11350) and PE (–1751) have no impact on the adhesion. Positive coefficients for two blend mixtures such as P : B ratio with WA, P : B ratio with PE, and PE with WA indicate that two components of each blend act synergistically with each other.

The significance of the ratio of elements is defined by the nearness of the *p*-values of a parameter to the defined significance level. If *p*-value is lower than 0.05, the ratio is significant for the adhesion of ink. From the ANOVA Table 8, it is observed that P : B ratio with the WA and P : B ratio with PE both have *p*-value less than 0.05, which means these ratios are significant for the adhesion of ink on the non-absorbent substrate. Significance of P : B ratio with PE is higher than that of P : B ratio with WA ratio. Ratio of WA and PE has a *p*-value above 0.05 which indicates that ratio is having less influence for the adhesion. Also, the model has an *R*-squared value of 97.96 %, which indicates a good data fit without excluding insignificant terms.

Table 9 shows ANOVA and the magnitude of coefficients for resin, PE, and WA for the ink formulated from 1.4 NCO : OH ratio, marked as WB_AD_R4. For higher NCO : OH ratio even though the NCO terminated polymer chain is dispersed in water, free NCO is available in the dispersion. This free NCO tends to crosslink with the surface as well as with another ingredient in the presence of water and this will promote the adhesion of ink on a non-absorbent surface. Thus water-based inks which are formulated from PU resin which have higher NCO : OH ratio i.e. 1.4 in this experiment provide better interaction with other ingredients of ink and thus complete adhesion of ink on LDPE substrate.

4.3 Histogram and plot of residual

Figure 6a shows the normal probability plot for the adhesion response obtained from the DOE conducted for binder R1. Normal probability plot determines how well data follow a specific distribution. The degree of fit is indicated by the degree to which the data points follow the fitted line.

Figure 6b shows the histogram of the adhesion response. This is the distribution of the residuals for all observations. The histogram helps to understand the spread, variation, and shape of the distribution and if any unusual values are present in data. Data follows the normal distribution plot with a mean value of the adhesion response of 76.93 % and a standard deviation of 4.04 %.

Table 8: Statistical analysis for WB_AD_R1 (resin based on 1.15 NCO : OH ratio)
Regression for mixtures: WB_AD_R1 versus P : B ratio, WA, PE, water

Estimated regression for WB_AD_R1 (component proportions)

Term	Coef.	SE coef.	*t*-test	*p*-value	VIF
P : B ratio	44	14.7	*	*	1 920.3
WA	−11 350	3 183.1	*	*	5 360.1
PE	−1 751	655.9	*	*	2 188.5
Water	84	13.8	*	*	1 820.7
P : B ratio * WA	26 548	6 454.6	4.11	0.001	5 165.6
P : B ratio * PE	5 356	1 290.9	4.15	0.001	1 986.8
WA * PE	28 779	60 414.6	0.48	0.640	260.0

S = 0.80 PRESS = 21.52

R-sq = 98.43 % *R*-sq(pred.) = 96.87 % *R*-sq(adj.) = 97.88 %

Analysis of variance for WB_AD_R1 (component proportions)

Source	DF	Seq. SS	Adj. SS	Adj. MS	*F*-value	*p*-value
Regression	6	676.90	676.90	112.82	177.90	0.000
Linear	3	655.07	41.43	13.81	21.74	0.000
Quadratic	3	21.83	21.83	7.27	11.45	0.001
P : B ratio * WA	1	10.75	10.75	10.75	16.92	0.001
P : B ratio * PE	1	10.93	10.93	10.93	17.21	0.001
WA * PE	1	0.14	0.14	0.14	0.23	0.640
Residual error	17	10.80	11.00	0.63		
Lack-of-fit	1	2.73	2.73	2.73	5.42	0.033
Pure error	16	8.07	8.07	0.50		
Total	23	687.70				

Table 9: Statistical analysis for WB_AD_R4 (resin based on 1.40 NCO : OH ratio)
Regression for mixtures: WB_AD_R4 versus P : B ratio, WA, PE, water

Estimated regression for WB_AD_R4 (component proportions)

Term	Coef.	SE coef.	*t*-test	*p*-value	VIF
P : B ratio	63	6.5	*	*	1 920.3
WA	−2 404	1 410.3	*	*	5 360.1
PE	−3 036	290.6	*	*	2 188.5
Water	95	6.1	*	*	1 820.7
P : B ratio * WA	8 678	2 859.8	3.03	0.007	5 165.6
P : B ratio * PE	7 720	572.0	13.50	0.000	1 986.8
WA * PE	8 510	26 768.8	0.32	0.754	260.0

S = 0.35 PRESS = 4.23

R-sq = 99.47 % *R*-sq(pred.) = 98.94 % *R*-sq(adj.) = 99.28 %

Analysis of variance for WB_AD_R4 (component proportions)

Source	DF	Seq. SS	Adj. SS	Adj. MS	*F*-value	*p*-value
Regression	6	394.900	394.970	65.810	527.7100	0.000
Linear	3	371.000	23.700	7.900	63.6500	0.000
Quadratic	3	23.900	23.880	7.960	63.8200	0.000
P : B ratio * WA	1	1.100	1.148	1.150	9.2100	0.007
P : B ratio * PE	1	22.700	22.720	22.720	182.1600	0.000
WA * PE	1	0.013	0.013	0.013	0.1000	0.754
Residual error	17	17.000	2.120	2.120	0.1247	
Lack-of-fit	1	0.600	0.550	0.550	5.6800	0.030
Pure error	16	1.600	1.560	0.098		
Total	23	397.000				

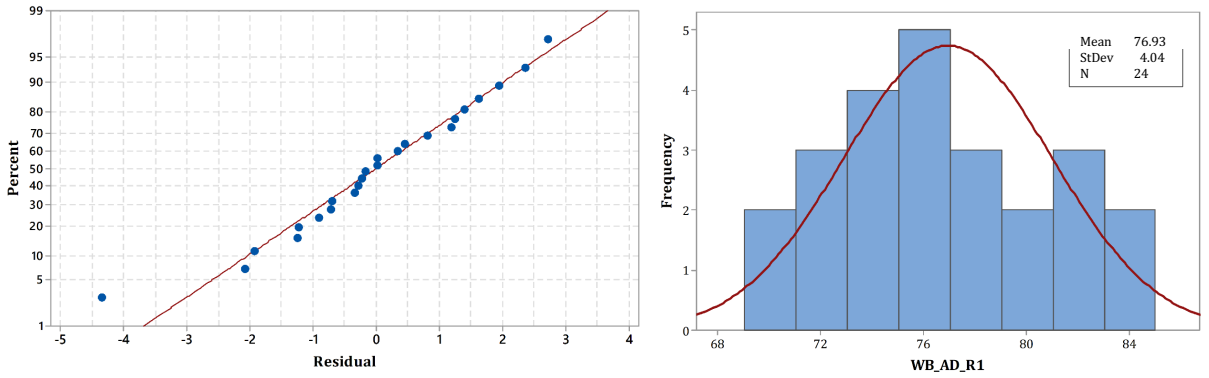

a) *b)*

Figure 6: Response of WB_AD_R1 formulation: (a) normal probability plot, and (b) histogram of the adhesion

4.4 Main effect plot and interaction plot

The main effect plot (Figure 7a) shows the effect of ingredients on the adhesion of water-based ink. This plot considers the data means at the various levels of each factor, with a reference line drawn at the grand mean of the response data. Main effect plot shows that the adhesion of water-based ink on the non-absorbent substrate is obtained for a higher level of P : B ratio (resin percentage), WA, and PE.

Figure 7b shows the interaction plot for all three ingredients. An interaction plot is a plot of means for each level of a factor with the level of a second factor held constant. Interaction plots are useful for judging the presence of interaction. Interaction is present when the response at a factor level depends upon the level(s) of other factors. Parallel lines in an interaction plot indicate no interaction. The greater the departure of the lines from the parallel state, the higher the degree of interaction. Figure 7b shows that interaction takes place between P : B ratio with WA, P : B ratio with PE, and WE with PE as lines are not parallel. Interaction between resins with WA is more acceptable than the interaction between resin and PE for the adhesion of ink.

Overall, all regression mixture model explains the significance of P : B ratio (resin percentage), a blend of resin with WA, resin with PE for the adhesion of ink on the non-absorbent surface. From the estimated regression coefficient of all four models, it is observed that the magnitude of resin and magnitude of a blend of resin with PE increase for increasing NCO : OH ratio of resin. For the increasing value of NCO : OH ratio, more interaction is observed between resin and polymer emulsion which is observed from the magnitude of these coefficients.

4.5 Mixture contour plot

Figure 8a shows the contour plot for the mixture model for R4 resin. A contour plot provides a two-dimensional view where all points that have the same response are connected to produce contour lines of constant response.

The response optimizer uses the model equation to optimize the result. Response optimizer shown in Figure 8b predicts that complete adhesion of water-based ink on LDPE substrate will be observed when NCO : OH ratio of the PU resin is 1.4. At this NCO : OH

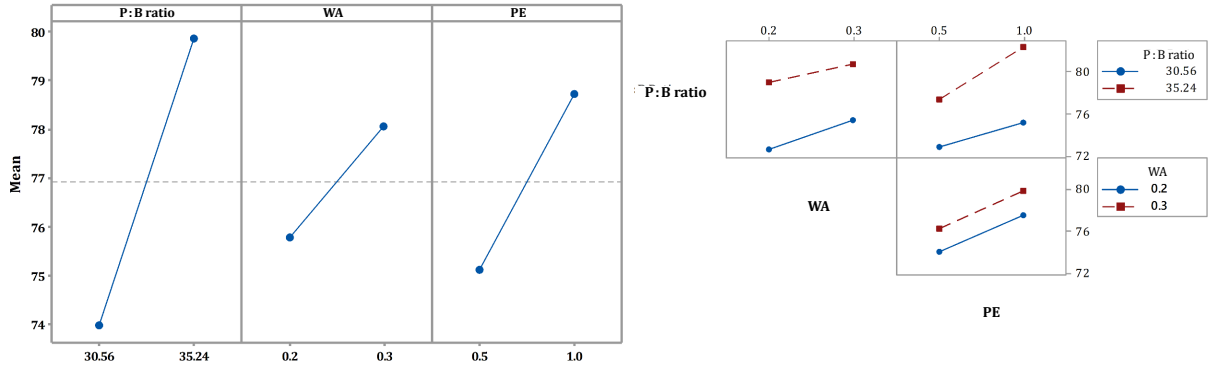

a) *b)*

Figure 7: The effect of ingredients in WB_AD_R1: (a) main effect plot, and (b) interaction plot

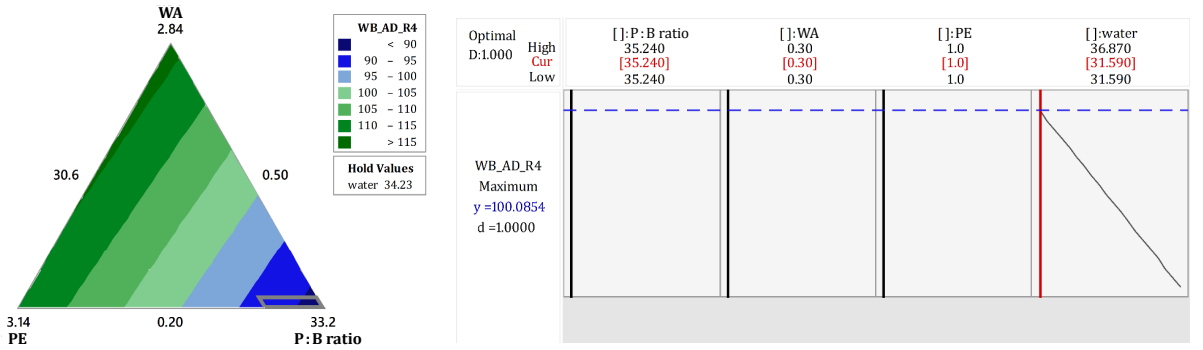

a) *b)*

Figure 8: Component amounts in WB_AD_R4: (a) mixture contour plot, and (b) response optimizer

ratio, 35.24 % of resin, 1 % of polymer emulsion, and 0.3 % of surfactant provides the complete adhesion of water-based ink on LDPE substrate. Table 10 shows the values obtained from the response optimizer.

Table 10: Statistical analysis for WB_AD_R4 response optimization

Goal	Lower	Target	Upper	Weight	Import
Maximum	80	100	100	1	1

Predicted responses

Components	
P:B ratio	35.24
WA	0.30
PE	1.00
Water	31.59

WB_AD_R4 = 100.00

5. Effect of NCO:OH ratio on the surface tension of water-based ink

The surface tension of four water-based ink formulated based on R1, R2, R3, and R4 resin with a constant percentage of WA as 0.3 % and PE as 1 % were measured by using a ring tensiometer. Figure 9 shows the effect of NCO:OH ratio of PUD on the surface tension of the ink.

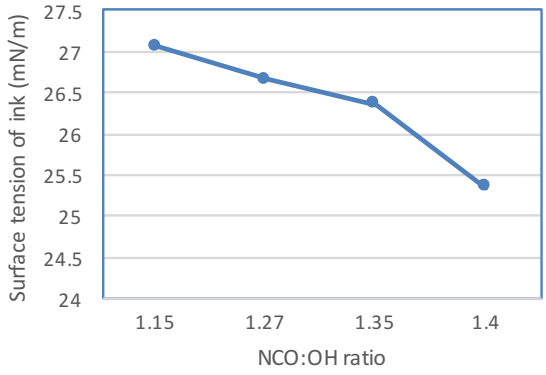

Figure 9: Surface tension of ink for different NCO:OH ratios

The surface tension values of ink formulated from different NCO:OH ratios were analyzed. Four PUDs based on four NCO:OH ratio, 1.15, 1.27, 1.35, and 1.4, have a constant molar ratio of polyester glycol and DMPA. When NCO:OH ratio is higher, the percentage of NCO increases while the amount of hydrophilic carboxyl group contents reduces. Reduced amount in ionic groups reduces polar group element of PUD; ultimately surface tension of ink gets reduced for higher NCO:OH molar ratio.

The interfacial tension between water-based ink and substrate plays a significant role in the wetting of the substrate. The higher interfacial tension produces uneven surface performance. Table 11 shows the values for the interfacial surface tension of ink and LDPE

Table 11: Interfacial surface tension, work of adhesion and coefficient of spreading for inks made from four binders

Substrate	Ink based on PUD	Θ (°)	Cos Θ	γ_s (mN/m)	γ_l (mN/m)	γ_{sl} (mN/m)	W_a (mJ/m^2)	S (mJ/m^2)
LDPE	R1	44.12	0.72	39.63	27.06	20.20	46.49	−7.63
	R2	41.00	0.75	39.63	26.65	19.59	46.69	−6.61
	R3	38.25	0.78	39.63	26.35	18.98	47.00	−5.70
	R4	30.37	0.86	39.63	25.35	17.76	47.22	−3.48

film. It was observed that when NCO : OH is higher, the hydroxyl group percentage is less, which reduces the interfacial surface tension between ink and film and allows the ink to wet the LDPE substrate easily and provide a uniform surface of ink on LDPE film.

The interaction between the ink and the substrate plays a major role in print quality. During the transfer of ink from anilox cylinder to image carrier and from the image carrier to the substrate, how the ink behaves, is a significant aspect for printability. The spreading/wetting of ink over the substrate leads to a reduction in voids, which also helps to improve the adhesion of ink over the substrate. Poor wetting causes uneven spreading of ink over the substrate which provides uneven reflectance from the printed surface. This also leads to poor adhesion and hence less scratch resistance and abrasion resistance. The γ_{sl}, W_a, and S have been calculated using the Equations [2] to [4].

The W_a is the work required to separate the interface between ink and substrates. The greater adhesion energy is a decisive parameter to get good adhesion between liquid and substrate.

Table 11 shows the lower contact angle is achieved by water-based ink on LDPE substrate when NCO : OH ratio is high i.e. 1.4. The lower value of the contact angle provides a higher spreading of ink for the substrate. The high surface energy of the LDPE substrates increases the wettability as spreading or wettability is directly proportional to the difference in the surface energy of the substrate and water-based ink. Improved wettability improves the ability of the substrate to bind with the water-based ink. The higher W_a on the LDPE substrate from the ink which is formulated from PUD of NCO : OH ratio 1.4, indicates a higher adhesion between the ink and the substrate. Negative value S shows that the spreading does not occur impulsively. The higher is the negative magnitude of S, the lower is the spreading for the corresponding combination of ink and substrate. The water-based ink formulated from PUD of 1.4 NCO : OH ratio provides a very small negative coefficient which is close to zero, hence provides spreading but not spontaneously. Also, work done at this NCO : OH ratio is also high to get the adhesion between ink and substrate.

6. Statistical analysis for gloss of water-based ink

6.1 Gloss of water-based ink on LDPE substrate

Table 12 shows the formulation of water-based ink for the different DOE, measured at 60° angles of light reflection in the second part of experiment.

Table 12: Ink formulation for design of experiment for gloss

Sample	NCO : OH ratio	WA (%)
1	1.15	0.2
4	1.15	0.3
7	1.27	0.2
10	1.27	0.3
13	1.35	0.2
16	1.35	0.3
19	1.40	0.2
22	1.40	0.3

Table 13 shows the output from two way ANOVA table summarizing the linear term, the squared term, and the interaction for gloss. The small p-value for the linear term of NCO : OH ratio and WA shows that they are linearly affecting gloss of ink. The small p-values for the square term of NCO : OH ratio and the interaction of NCO : OH ratio and WA suggest that there is the curvature in the response surface. The F-values from the model indicate that their linear significance for NCO : OH ratio and WA is higher than the quadratic significance of the interaction between both factors. The model has an R-squared value of 91.28 %, which indicates almost perfect data fit of the model.

6.2 Histogram and residual plot

Figure 10 shows the normal distribution plot and histogram of data with mean of 73.3 and standard deviation of 4.7.

6.3 Main effect and interaction plot for gloss

Figure 11 shows the main effect plot and interaction plot for different NCO : OH ratios and wetting agent percentage. The percentage of wetting agent provides linear relation for the gloss of ink. NCO : OH ratio is affecting by the different rates on the response gloss. Different rates of response interpreted that different surface tension of ink due to NCO : OH ratio and particle size distribution of binder for different NCO : OH ratios are simultaneously affecting with substrate wetting agent. This leads to the uneven response rate for the gloss of ink.

A gloss of ink is majorly dependent upon the uniform and smoothness of the ink layer on the substrate. Reduced surface tension provides the spreading of ink on substrate uniformly while a narrow particle size distribution helps to provide a smoother surface on film.

From interaction plot (Figure 11b) it is observed that NCO : OH ratio of 1.35 and 0.3 % of wetting agent provide slightly higher gloss means (higher by 0.63 %).

Table 13: Response surface regression for gloss

Response surface regression: gloss versus NCO : OH and WA

Stepwise selection of terms α to enter = 0.15, α to remove = 0.15

Analysis of variance for gloss

Source	DF	Adj. SS	Adj. MS	*F*-value	*p*-value
Model	4	454.6	113.6	49.7	0.000
Linear	2	410.7	205.3	89.8	0.000
NCO : OH	1	228.8	228.8	100.0	0.000
WA	1	181.9	181.9	79.6	0.000
Square	1	7.8	7.8	3.4	0.080
NCO : OH * NCO : OH	1	7.8	7.8	3.4	0.080
2-way interaction	1	17.1	17.1	7.5	0.013
NCO : OH * WA	1	17.1	17.1	7.5	0.013
Error	19	43 429.0	2 286.0		
Lack-of-fit	3	30 965.0	10.3	13.2	0.000
Pure error	16	12.5	0.8		
Total	23	498.0			

Model summary

S = 151186

R-sq = 91.3 % R-sq(pred.) = 87.2 % R-sq(adj.) = 89.4 %

Coefficients

Term	Effect	Coef.	SE coef.	*T*-value	*p*-value	VIF
Constant		712.0	0.5	136.2	0.000	
NCO : OH	8.2	4.1	4.1	10.0	0.000	1.01
WA	5.6	2.8	0.3	8.9	0.000	1.01
NCO : OH * NCO : OH	2.7	1.3	0.7	1.8	0.080	1.01
NCO : OH * WA	2.2	1.1	0.4	2.7	0.013	1.03

Regression equation in uncoded units

Gloss = 227.2 – 252 NCO : OH – 183.9 WA + 93.4 NCO : OH * NCO : OH + 187.2 NCO : OH * WA

This is because resin R3 has smaller average particle size than resin R4, so even though the surface tension of resin R3 is slightly higher than that of resin R4, when it interacts with a surfactant, it helps to reduce the surface tension of ink up to the level which is sufficient to get a uniform layer of ink on LDPE surface. This condition highlights that the resin particle size also contributes to the gloss of ink.

The contour plot (Figure 12a) shows the lines for the same gloss percentage for different combinations of ink. Maximum gloss is observed at 0.3 % of the wetting agent and for the binder of 1.4 NCO : OH ratio. A surface plot displays the three-dimensional relationship in two dimensions, with the variables WA on the *x*-axis, NCO : OH on the *y*-axis, and the gloss response on the *z*-axis, represented by a smooth surface.

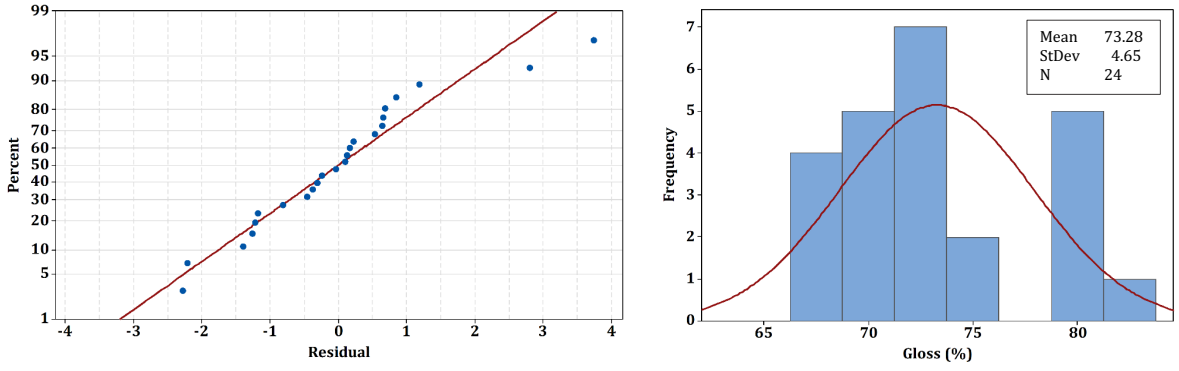

a) *b)*

Figure 10: Response of gloss: (a) normal probability plot, and (b) histogram

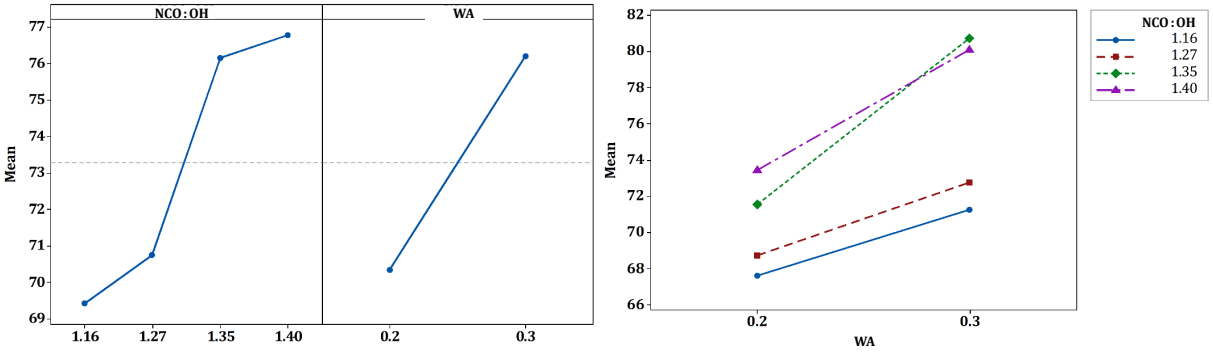

a) *b)*

Figure 11: Gloss values: (a) main effect plot, and (b) interaction plot for diffrenet NCO : OH ratios

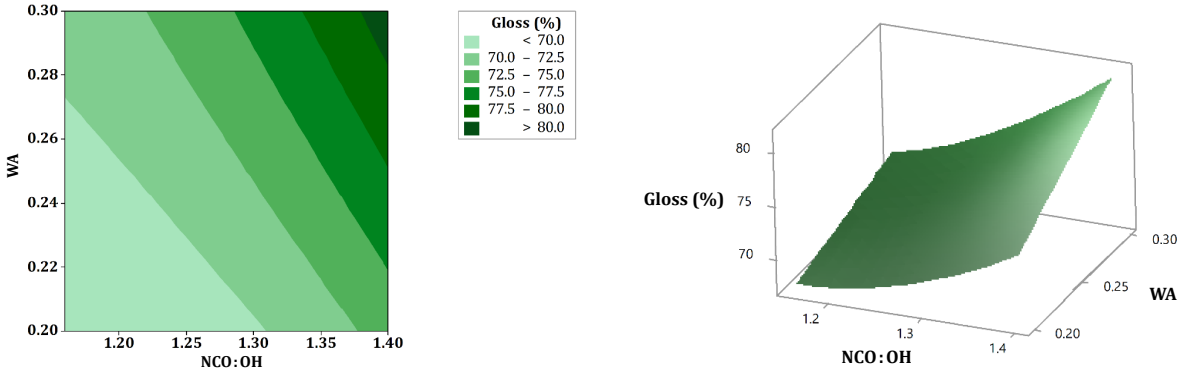

a) *b)*

Figure 12: Gloss values vs WA content and NCO : OH ratios: (a) contour plot, and (b) surface plot

6.4 Validation trial

A validation trial was conducted for the optimized setting of ink ingredients (Table 14) for complete adhesion and maximum gloss. Results of validation trial are shown in Table 15.

Table 14: Ink formulation for validation trial

Ink ingredients	Amount (%)
Premixture	31.87
Binder	35.24
Wetting Agent	0.30
Polymer Emulsion	1.00
Water	31.59

Table 15: Characteristics of validation trial

Ink characteristic	Value
Gloss (%)	80.5
Adhesion (%)	100.0
Surface Tension (mN/m)	26.0
pH	8.7
Solids (%)	34.0
Viscosity (mPa·s)	220.0

6.5 Response optimizer

The response optimizer shown in Figure 13 uses the model equation to optimize the result. Response optimizer predicts that a maximum 81.3 % gloss of water-based ink on LDPE substrate will be observed when NCO : OH ratio of the PU resin is 1.4 and 0.3 % of WA is used in the formulation. Table 16 shows the values obtained from the response optimizer.

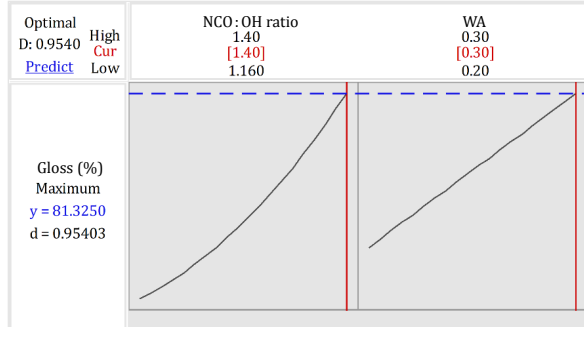

Figure 13: Response optimizer for gloss

Table 16: Response optimization for gloss of water-based ink

Response optimization: gloss

Parameters

Response	Goal	Lower	Target	Upper	Weight	Importance
Gloss	Maximum	67.1	82.0		1	1

Solution

Solution	NCO : OH ratio	WA	Gloss fit	Composite desirability
1	1.4	0.3	813 252	954 044

Multiple response prediction

Variable	Setting
NCO : OH ratio	1.4
WA	0.3

Response	Fit	SE Fit	95 % CI	95 % PI
Gloss	81.3	0.7	(79.8, 82.9)	(77.8, 84.8)

7. Conclusion

Mixture design model for all resins based on different NCO : OH ratio shows that interaction of resin with polymer emulsion and resin with a wetting agent are significant parameters for enhancing the adhesion of ink on the non-absorbent substrate. It was observed that adhesion values checked by the tape test are gradually increased from 1.16 to 1.4 NCO : OH ratio. Complete adhesion was observed for a binder which is based on 1.4 NCO : OH ratio.

For the lower NCO : OH ratio surface tension of the ink is higher due to higher number of hydroxyl value, which decreases the wetting of ink on LDPE film. Higher NCO : OH ratio reduces the surface tension of the ink, and increases the wetting of ink on LDPE film.

While formulating, the surface tension of ink and particle size distribution of resin interacts with the substrate wetting agent which significantly affects the gloss of the ink layer formed on the surface of the LDPE surface.

Regression model and response optimizer, optimize the complete adhesion and maximum gloss up to 80.5 % on LDPE substrate for 31.87 % dispersed pigment, 35.24 % of PU resin synthesized for 1.4 ratio of NCO : OH, 1 % of polymer emulsion, 0.3 % of surfactant and 31.59 % of deionized water.

Acknowledgment

Authors thank to M/s BYK India for providing additives and instrumentation facility. Thank to M/s Sudarshan Chemical Industries for providing pigment and instrumentation facility. Authors thank to M/s Kroslink polymer for providing polyurethane dispersions of specific properties. Corresponding author thanks to HoD, Mrs. Madhura Mahajan, and Principal of the college Dr. Y. P. Nerkar for the encouragement and extending the facilities for the completion of the research.

References

Abrahão, R.T., 2013. *Study on the dispersion of titanium dioxide pigment particles in water*. Doctoral thesis. Universidade de São Paulo.

ASTM International, 2017. *ASTM D3359 – 17 Standard test methods for rating adhesion by tape test.* West Conshohocken, PA, USA: ASTM International.

ASTM International, 2018a. *ASTM D523 – 14(2018) Standard test method for specular gloss*. West Conshohocken, PA, USA: ASTM International.

ASTM International, 2018b. *ASTM F2252 / F2252M – 13(2018) Standard practice for evaluating ink or coating adhesion to flexible packaging materials using tape.* West Conshohocken, PA, USA: ASTM International.

Athawale, V.D. and Kulkarni, M.A., 2010. Effect of dicarboxylic acids on the performance properties of polyurethane dispersions. *Journal of Applied Polymer Science*, 117(1), pp. 572–580. https://doi.org/10.1002/app.31267.

BASF Group, 2017. *Lighten your carbon footprint! Water-based technologies for flexible packaging: Eco-Efficiency Analysis for printing inks and adhesives for flexible packaging*. [pdf] BASF Group. Available at: <http://www2.basf.de/basf2/html/e/resins-additives/newsletter/content/1-printing-packaging/20170427-eco-efficiency-analysis/basf-resins-and-additives_water-based-technologies_factsheet.pdf> [Accessed June 2020].

Bohlin, E., 2013. *Surface and porous structure of pigment coatings: interactions with flexographic ink and effects on print quality*. Doctoral thesis. Karlstad University.

Carré, A., 2007. Polar interactions at liquid/polymer interfaces. *Journal of Adhesion Science and Technology*, 21(10), pp. 961–981. https://doi.org/10.1163/156856107781393875.

Chashmejahanbin, M.R., Daemi, H., Barikani, M. and Salimi, A., 2014. Noteworthy impacts of polyurethane-urea ionomers as the efficient polar coatings on adhesion strength of plasma treated polypropylene. *Applied Surface Science*, 317, pp. 688–695. https://doi.org/10.1016/j.apsusc.2014.08.094.

Fang, C., Zhou, X., Yu, Q., Liu, S., Guo, D., Yu, R. and Hu, J., 2014. Synthesis and characterization of low crystalline waterborne polyurethane for potential application in water-based ink binder. *Progress in Organic Coatings*, 77(1), pp. 61–71. https://doi.org/10.1016/j.porgcoat.2013.08.004.

Fang, C.Q., Zhang, M.R., Li, T.H. and Zhou, S.S., 2010. Study on polyurethane/polyurethane emulsion water-based ink. *Key Engineering Materials*, 428–429, pp. 524–527. https://doi.org/10.4028/www.scientific.net/KEM.428-429.524.

Gu, W.J., Li, Y. and Zhang, X.H., 2013. Printing Industry and the environment. *Advanced Materials Research*, 663, pp. 759–762. https://doi.org/10.4028/www.scientific.net/AMR.663.759.

Hamey, R.G., 2005. *Production of organic pigment nanoparticles by stirred media milling*. Master thesis. University of Florida.

Herbst, W. and Hunger, 2006. *Industrial organic pigments: production, properties, applications*. 3rd ed. Weinheim, Germany: WILEY-VCH Verlag.

Inam, M.A., 2010. *Particle sizing and product quality in production of fine and nano particles by means of wet grinding process*. PhD thesis. Université de Toulouse.

Inam, M.A., Ouattara, S. and Frances, C., 2011. Effects of concentration of dispersions on particle sizing during production of fine particles in wet grinding process. *Powder Technology*, 208(2), pp. 329–336. https://doi.org/10.1016/j.powtec.2010.08.025.

International Organization for Standardization, 1997. *ISO 124:1997 Latex, rubber — Determination of total solids content*. Geneva Switzerland: ISO.

Izdebska, J. and Thomas, S., eds. 2015. *Printing on polymers: fundamentals and applications*. Oxford, UK: Elsevier.

Klein, L.C., 2006. Solgel coatings. In. A.A. Tracton, ed. *Coatings materials and surface coatings*. Boca Raton, FL, USA: CRC Press. https://doi.org/10.1201/9781420044058.

Lei, L., Xia, Z, Cao, G. and Zhong, L., 2014. Synthesis and adhesion property of waterborne polyurethanes with different ionic group contents. *Colloid and Polymer Science*, 292, pp. 527–532. https://doi.org/10.1007/s00396-013-3129-0.

Liang, F. and Zhou, J.F., 2012. Synthesis and properties of waterborne polyurethane emulsions using in printing ink. *Advanced Materials Research*, 554–556, pp. 115–121. https://doi.org/10.4028/www.scientific.net/AMR.554-556.115.

Nanda, A.K., Wicks, D.A., Madbouly, S.A. and Otaigbe, J.U., 2005. Effect of ionic content, solid content, degree of neutralization, and chain extension on aqueous polyurethane dispersions prepared by prepolymer method. *Journal of Applied Polymer Science*, 98(6), pp. 2514–2520. https://doi.org/10.1002/app.22141.

Negim, E.-S., Bekbayeva, L., Mun, G.A., Abilov, Z.A., Saleh, M.I., 2011. Effect of NCO/OH ratios on physico-mechanical properties of polyurthane dispersion. *World Applied Sciences Journal*, 14(3), pp. 402–407.

Ohenoja, K., 2014. Particle size distribution and suspension stability in aqueous submicron grinding of $CaCO_3$ and TiO_2. Doctoral thesis. University of Oulu. https://doi.org/10.13140/RG.2.1.4321.5525.

Ohenoja, K., Illikainen, M. and Niinimäki, J., 2013. Effect of operational parameters and stress energies on the particle size distribution of TiO_2 pigment in stirred media milling. *Powder Technology*, 234, pp. 91–96. https://doi.org/10.1016/j.powtec.2012.09.038.

Olsson, R., Yang, L. and Lestelius, M., 2007. Water retention of flexographic inks and its influence on final print gloss. *Nordic Pulp and Paper Research Journal*, 22(3), pp. 287–292. https://doi.org/10.3183/npprj-2007-22-03-p287-292.

Piluso, C., Serafano, J., Kloock, L.M., Grandke, R. and Bradlee, C.A., 2009. Eco-efficiency analysis demonstrates the environmental and economic benefits of flexographic printing inks in film applications. *Ink World*, 15(6), pp. 66–73.

Ramirez, J.C.C. and Tumolva, T.P., 2018. Analysis and optimization of water-based printing ink formulations for polyethylene films. *Applied Adhesion Science*. Springer International Publishing, 6: 1. https://doi.org/10.1186/s40563-017-0102-z.

Rentzhog, M., 2006. *Water-based flexographic printing on polymer-coated board*. Doctoral thesis. Royal Institute of Technology Stockholm.

Saad, A.A.E.-R.E., 2007. *Environmental pollution reduction by using VOC-free water-based gravure inks and drying them with a new drying system based on dielectric heating*. Dr.-Ing. Dissertation. Bergische Universität Wuppertal.

Schmidt, J., Plata, M., Tröger, S. and Peukert, W., 2012. Production of polymer particles below 5 µm by wet grinding. *Powder Technology*, 228, pp. 84–90. https://doi.org/10.1016/j.powtec.2012.04.064.

Senthilkumar, K. and Akilamudhan, P., 2014. Experimental studies on effect of grinding additives in size reduction process. *International Journal of ChemTech Research*, 6(9), pp. 4428–4433.

Simpson, A.B.G., Byrne, J.A., McLaughlin, J.A.D. and Strawhorne, M., 2015. Effect of solids concentration on particle size distribution of deagglomerated barium titanate in stirred media mills. *Chemical Engineering Research and Design*, 93, pp. 287–292. https://doi.org/10.1016/j.cherd.2014.04.006.

Tai, J.L., Chen, G.X., Chen, Q.F. and Tang, B.L., 2012. Study on polyurethane-acrylic hybrid emulsion applying to water-based ink. *Applied Mechanics and Materials*, 182–183, pp. 3–7. https://doi.org/10.4028/www.scientific.net/AMM.182-183.3.

Verspoor, P.W., 2005. *Solvent based or water borne inks in flexography: a cost comparison – a study for Johnson Polymer*. [pdf] Johnson Polymer / Sitmae Consultancy bv. Available at: <http://ec.europa.eu/environment/archives/air/stationary/solvents/activities/pdf/d039_ink_cost_comparison_report_sitmae.pdf> [Accessed June 2020].

Wang, X., Li, J., Yu, Y., Wang, H. and Gao, X., 2016. Study on the performance of adherence of plastic water-based flexographic ink. In: Y. Ouyang, M. Xu, L. Yang and Y. Ouyang, eds. *Advanced Graphic Communications, Packaging Technology and Materials: Lecture Notes in Electrical Engineering, vol 369.* Hanzhou, China, 22–24 October 2015. Singapore: Springer Science+Business Media, pp. 1019–1024. https://doi.org/10.1007/978-981-10-0072-0_125.

Wolf, R. and Sparavigna, A.C., 2010. Role of plasma surface treatments on wetting and adhesion. *Engineering*, 2(6), pp. 397–402. https://doi.org/10.4236/eng.2010.26052.

Yu, M.J., Huang, B.Q. and Wei, X.F., 2011. Influence of resin on the performance of water-based plastic gravure ink. *Advanced Materials Research*, 287–290, pp. 1680–1684. https://doi.org/10.4028/www.scientific.net/AMR.287-290.1680.

JPMTR 138 | 2010
DOI 10.14622/JPMTR-2010
UDC 676.22:774.56-023.881:024.524|62-56

Case study
Received: 2020-07-07
Accepted: 2020-09-22

Lateral paper web shifting during commercial heat set web offset printing

George Shields[1], Alexandra Pekarovicova[2], Paul D. Fleming[2] and Jan Pekarovic[2]

[1] UPM Kymmene Co.
[2] Center for Printing and Coating Research,
College of Engineering and Applied Science,
Western Michigan 4601 Campus Drive,
A-217 Parkview, Kalamazoo, MI 49008-5462

a.pekarovicova@wmich.edu

Abstract

Paper properties and their role in preventing lateral web movement from cross machine air flows in the drying section during normal heat set web offset litho printing operations were examined. Tensile properties of sheets were measured at various moisture contents and then used to determine the equilibrium stress–strain relationship for papers at moisture contents typical of heat set web offset printing. Air permeability, creep, hygroexpansion, and ultrasonic measurement of tensile stiffness orientation module were evaluated against lateral web movement on heat set web offset litho press. It was found that the only item of interest from these results with respect to the lateral movement performance is the ratio between tensile stiffness orientation modules in the machine direction and cross machine direction, indicating orientation of the fibers in the paper web, and showing that more oriented fibers are less likely to shift on heat set web offset litho printing press. Understanding the effect of water absorption and absorption rate on the stress–strain relationship of paper may yield further understanding of web break tendency during heat set web offset printing.

Keywords: fiber orientation, tensile stiffness index, water absorption, stress–strain in paper, creep, hydroexpansion

1. Introduction and background

The effect of water and heat on the behavior of paper sheets has been studied frequently over many years. Two effects of water, either in liquid or vapor form, on paper sheets are hydro/hygro-expansion (Kajonto and Niskanen, 1998), and softening of the fiber matrix through plasticization (Niskanen and Kärenlampi, 1998). In both cases it appears that water molecules interact with fiber material through a hydrogen bonding mechanism. Swelling of the fiber wall and translation of the swelling to the paper sheet dimensions results in hydro/hygro-expansion. Creep, or at least the increased rate of creep, is the result of fiber plasticization and the corresponding loosening of the fiber matrix (Brezinski, 1956). This occurs because water acts as a softener preferentially bonding with hydroxyl sites in the amorphous cellulose in or between the microfibrils that make up fibers. In commercial printing using the heat set web offset (HSWO) process, water is the largest component of dampening solution, which is applied to the paper surface in conjunction with oil based inks. Part of the water prints and sorbs into the paper (non-image areas), part of the water emulsifies with the ink and prints (image areas) and part of the water evaporates. Hot air floatation dryers are used to evaporate the printed water and a portion of the oils from the ink (Kipphan, 2001).

The purpose of this work is to determine the paper-making reasons for lateral shift of the moving paper web, made on a particular paper machine, on a specific printing press during HSWO litho printing. The lateral movement is seen as a steady state shift to the gear side of the printing press, which can be measured at the exit of the chill section. In upset conditions, such as start up or blanket wash, the web may move so far that it shifts off the paper guiding rollers and/or jams the folder section of the printing press. The lateral shift has been observed on several HSWO printing presses

running the subject paper, and attempts to correct the problem have met with little success. The propensity of the web to shift in the extreme during upset conditions has been linked to how the web shifts under steady state printing conditions. For the paper in question made under specific conditions, the amount of water applied during printing appears to govern the magnitude of the lateral shift during steady state conditions.

The hypothesis for why the lateral web shift occurs is related to the air currents within the floatation dryers of HSWO printing presses. The air currents have a machine direction component and a cross machine direction, or, lateral component. Low web tension allows the lateral component of the air flow to move the paper web sideways. Papers with higher web tension will be less impacted by the lateral air flows and therefore will be more centered on the printing press. Moisture addition from printing will reduce the tensile stiffness of the paper and swell the fibers giving rise to hydroexpansion and provide the conditions for increased creep. All of these effects of moisture addition will have the result of reducing web tension. Drying of the paper and ink will cause the fibers to contract and increase tensile stiffness, both of which will increase web tension. The time from water application to drying during HSWO printing is short and it is possible that the rate of tension loss is more important than residual steady state tension.

Some of the results of this study were published elsewhere (Shields, 2017; 2018). The work is divided into field and laboratory portions. The field work involved making paper on the target paper machine, using various papermaking treatments to manufacture 11 specific paper rolls. The trial rolls were printed on the target printing press and the lateral position of the web at the exit of the chill section was recorded. The rolls of the paper were ranked by deviation from the center position at the chill section exit. In this way, papermaking factors that impact lateral position were identified. The hygroexpansion and creep of paper under load were tested for an estimate of hygroexpansion and creep potential during printing. Hygroexpansion rather than hydroexpansion is studied due to the ease of conditioning paper to a known moisture content by controlling the relative humidity of the testing environment. Understanding the methods to reduce the lateral web movement may lead to further understanding about the impacts of water on sheet properties during HSWO printing and methods to reduce web break rates for papers made with mechanical pulps.

2. Materials and methods

The paper in question is a grade 4 coated mechanical paper made on a Fourdrinier paper machine in the northern United States, using pressurized groundwood (PGW) mechanical pulp and softwood bleached kraft (SBK) pulp. The paper is coated with a blend of kaolin and ground calcium carbonate pigments, along with starch and latex binders, supercalendered to 64 % gloss and wound into customer rolls on a single drum winder. The subject printing press is a side by side design of two HSWO presses operating at a nominal speed of 8.1 m/s. Each web is fitted with a reel, pre-tensioning section and guiding section prior to four printing units, a 3-zone hot air floatation dryer and a chill section. One of the two presses (left hand press, LHP) follows with a short web lead, displacement guide, silicone emulsion applicator, and slitter section. The second web press (right hand press, RHP) is identical to the LHP through the chill section but differs further along the web path in that the web passes through a long open span, which crosses two 45° air turns before meeting the displacement web guide and slitter section. Both webs come together in the common folder section where the webs are folded and cut into books. A key factor in the design of the target press is the extra distance the web travels between the chill section and web guide on the RHP. The additional distance is 17.4 m. Assuming a nominal press speed of 8.1 m/s the extra travel time before the web guide is 2.15 s. The RHP web behavior is the subject of this work. Lateral shift happening on RHP is schematically illustrated in the Figure 1.

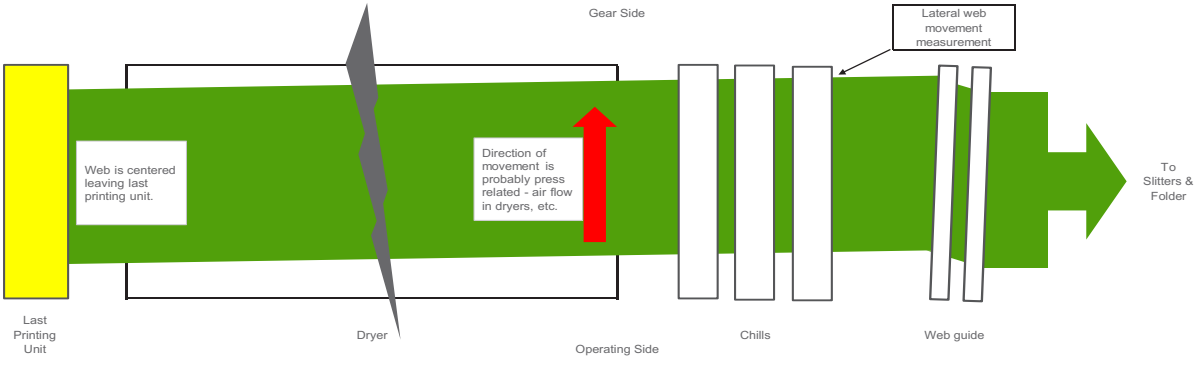

Figure 1: Mechanism of lateral web shift on HSWO printing press (Shields, 2017)

2.1 Laboratory testing

A total of 25 paper samples, including the 11 target paper machine (PM) rolls manufactured for the printing trials (Table 1), and 14 other paper samples, 11 of which are known to not suffer from lateral web movement, were tested in the laboratory conditions. Not all samples were tested for each activity, however all samples that were tested are from this lot of 25 papers.

Table 1: Papers manufactured for the printing trials

1	Standard front edge roll
2	Standard center roll, increased fiber orientation
3	Edge flow closed, increased fiber orientation
4	Increased strain at 20 % solids
5	Reduced ratio of headbox jet velocity to forming fabric velocity (J/W), decreased fiber orientation
6	Softwood bleached kraft (SBK) pulp refining increased
7	The SBK refining decreased
8	Zero pressurized groundwood (PGW) refining
9	Lower wet end starch
10	Higher wet end starch
11	Reduced strain at 90 % solids

The air permeability of all 25 papers was measured using a Technidyne Profile Plus set up for Gurley permeability. Units for the test results are s per 100 ml. Higher Gurley porosity results indicate lower permeability. The procedures, according to TAPPI test method T 460 om-11, section 5.2.1, were followed the standard (TAPPI, 2011). Each paper sample was tested 10 times, 5 on each side. The results reported were the average and standard deviation.

Ultrasonic measurement method was used for determination of tensile stiffness. For the 11 sample papers plus sheets that are uncoated or have the base paper of the coated sheets available, a 340 mm wide strip of paper spanning the full width of the paper machine was measured every 180 mm. The testing device was a Kajaani Tensile Stiffness Orientation module mounted in a Metso Paperlab paper testing station, where definitions are taken from (Lindblad and Furst, 2001). The following measurements were reported:

- MD Angle – the angle between the machine direction of the paper and the maximum tensile stiffness index,
- TSI MD – the tensile stiffness index (TSI) in the machine direction (MD),
- TSI CD – the tensile stiffness in the cross machine (CD) direction,
- TSI Ratio – the ratio between TSI MD and TSI CD.

An experimental test was attempted with the potential outcome of being able to measure the effects of hygroexpansion and creep. The test device used is shown in Figure 2 and Figure 3. A 25 mm wide strip of paper approximately 350 mm long was clamped at one end to a stationary horizontal bar while the free end passed horizontally over a roller that was free to rotate. The free end of the paper strip was clamped to a free hanging 1 kg weight. The 1 kg weight plus the weight of the clamp represents a load of 0.41 kN/m, quite similar to the web tension on a printing press prior to the print units. In a 50 % relative humidity (RH), and temperature of 23 °C environment, according to TAPPI (2013) conditions, the weight was attached to the strip and a mark placed on the sample at 250 mm from the stationary bar. The sample remained under tension for 30 s when the position of the mark was recorded relative to the initial length. A hand held hot air dryer was used to heat and dry the sample to approximately 125 °C, similar to web temperatures used in HSWO printing. The position of the mark relative to the original position

a) *b)*

Figure 2: Creep and hygroexpansion test set up: (a) view of apparatus from above, (b) side-view of apparatus from end with 1 kg weights suspended from samples (Shields, 2017)

was recorded. The sample was allowed to cool and condition for 30 s back to TAPPI (2013) conditions and the mark was recorded again. The samples and test set up were relocated to a 90 % RH, 23 °C atmosphere and allowed to acclimatize for 4 h. In the 90 % RH environment, the paper samples were re-clamped to the horizontal bar and the 1 kg weight clamped to the free end. The initial position of the mark was recorded relative to the original position in the 50 % RH environment. The testing procedure followed the protocol from the 50 % RH environment of straining for 30 s, heating to approximately 125 °C, and acclimatizing to the 90 % RH environment. At each step, the position of the mark relative to its original 50 % RH environment was recorded. The test was performed on 3 sample conditions with two tests per condition and the average result was reported. The measurement was done with a steel ruler divided into 0.794 mm (1/32") increments. For results not measuring exactly to 0.794 mm (1/32"), an estimate to the nearest 0.198 mm (1/128") was made. The samples included paper made on the target PM, paper made on a competitive PM with similar basis weight, and a super calandered (SC) grade paper of 45 g/m^2. A schematic of the test set up is shown in Figure 3.

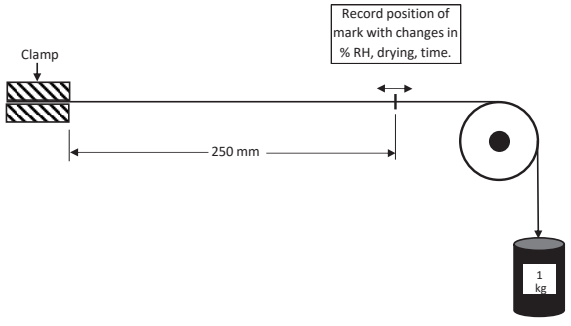

Figure 3: Humidity and creep measurement schematic (Shields, 2017)

3. Results and discussion

3.1 Lateral web shift

During printing, disturbances exist that act in the cross (lateral) direction of the web. Figure 4 illustrates the effect of a cross direction disturbance on the lateral web position as influenced by machine direction web tension.

As web tension increases, the effect of the lateral disturbances decreases, that is, the resulting angle between the machine direction and the path taken by the web is reduced. Examples of lateral disturbances include non-uniform paper properties, machine elements out of alignment, or lateral air flow in the dryer hoods. Therefore, a paper that has more web tension reduction, due to moisture increase during printing, will be more affected by the lateral forces existing in the paper/printing system.

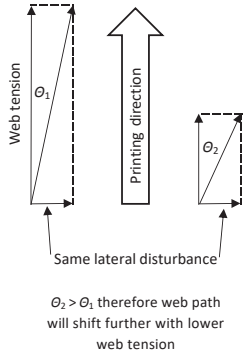

Figure 4: Lateral disturbance on web (Shields, 2017)

Variation in apparent density in the cross direction was considered as a possible contributor to lateral web movement. A variation across the web could conceivably contribute to lateral movement due to: variable water absorption rates, variable permeability, variable in plane tensile properties, etc. Apparent density was calculated as the apparent thickness (caliper) multiplied by the basis weight. In Figure 5a, the CD caliper profile and CD basis weight profile of the target PM is illustrated. The horizontal lines depict the location of individual customer rolls. The blacked out area indicates a roll that was not sent to the target pressroom. The same information was gathered for a competitive sheet that does not experience lateral web movement. A visual inspection of the caliper and basis weight profiles indicates the competitive PM has higher variability across the web than the target PM. The average caliper and basis weight of the paper from target PM and competitive PM are shown in Figures 5a and 5b.

The variation in paper density was calculated as the paper density for a particular roll divided by the average paper density of all customer rolls displayed for the paper machine, and it is illustrated on the Figure 6. The average paper density for the target PM is slightly higher than the competitive PM, likely due to higher coat weight. From previous work (Shield, 2017), it has been determined that the coat weight on the target paper machine sheet has no effect on the lateral web movement.

Figure 6 shows the paper density variation by roll position across the paper machine width. The competitive PM has higher paper density variability than the target PM, however it does not experience lateral web movement. It can be concluded that variation in apparent density does not correspond to increased lateral web movement on the target printing press.

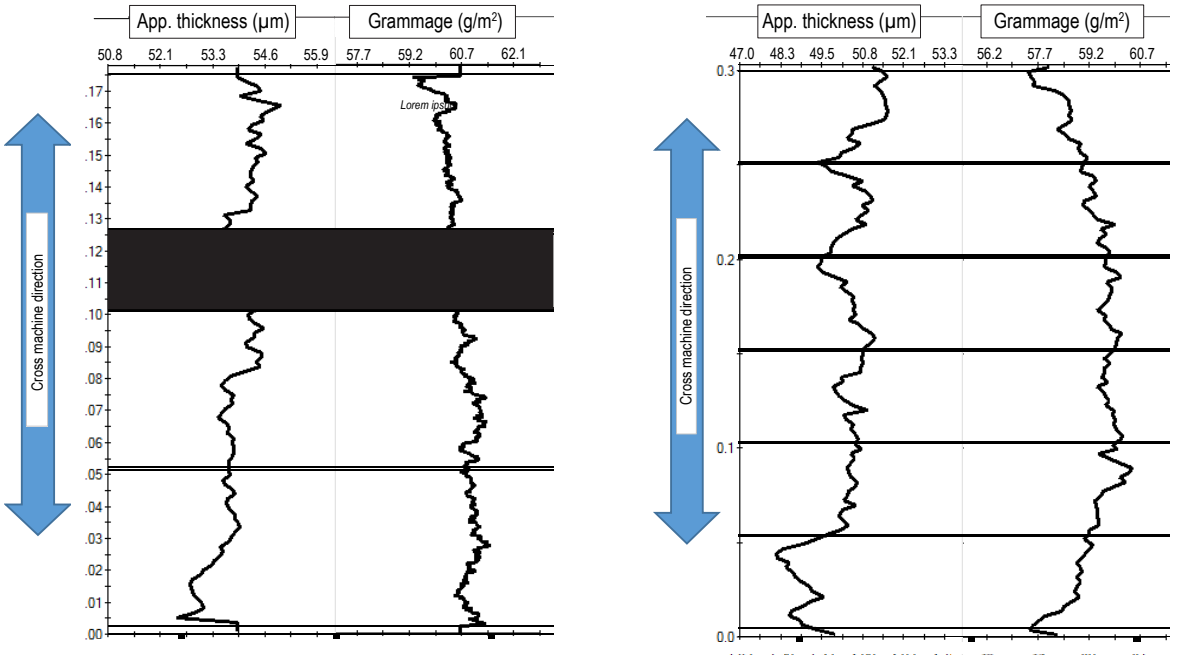

a) *b)*

Figure 5: Apparent thickness (µm), and grammage (g/m²) cross direction profiles (a) for the target paper machine, and (b) for a competitive paper machine, adapted from Shields (2017)

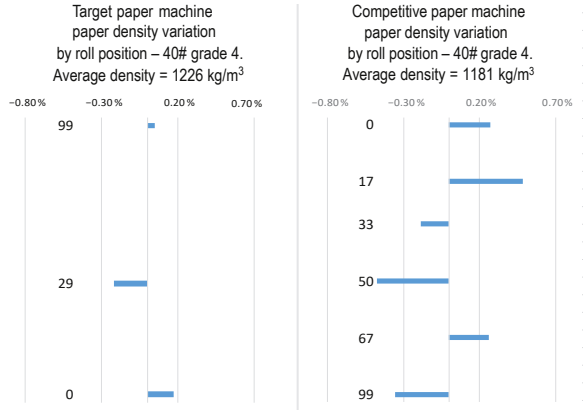

Figure 6: Paper density variation by roll position for the target and competitive paper machines (Shields, 2017)

The target paper machine experienced a higher level of lateral web shift than the competitive machine for both normal printing and blanket wash conditions. In normal printing conditions the target paper machine sheet was slightly off center at 92.07 mm ($3\,^{5}/_{8}$") while the competitive sheet was almost exactly centered at 98.42 mm ($3\,^{7}/_{8}$"). See Figure 7 for an explanation of the measurements. In the four unit blanket wash condition (all eight printing blankets washed simultaneously), the ink and fountain solution feed were stopped and the water based blanket wash sprayed on the blankets with the printing nips closed and the press operating at normal speed. The maximum guide position column in Table 2 shows the extent to which the web guide had to move during blanket wash to keep the web centered on the slitters. The two digits in the maximum guide position result represent a percentage of the maximum travel of the web guide, for instance 60 %. The letter in the third position of the maximum guide position result represents the direction the web guide was acting to correct the lateral shift. The O represents "operating side", G represents "gear side". Therefore, 60 O indicates that the web guide was at 60 % of its' maximum travel and correcting the sheet to the operator side of the press. This is typical of the lateral web shift. Air flow in the dryers is from the operator side to the gear side of the press, and the web moves towards the gear side. The web guide must correct the web back towards the operator side to center the sheet on the slitters.

The competitive paper machine had a similar response regardless of the pulp used to manufacture the paper, and was very nearly centered for all conditions, including blanket wash. Conclusions were that the lateral web position during normal printing is a predictor for blanket wash response. In a second portion of the trial, the web response to changes in the amount of applied fountain solution at constant ink supply rate was checked. Under normal printing conditions the web position was recorded. Fountain solution feed rate was increased until the printed surface was noticeably washed out indicating too much water was present in the image areas. The water amount setting, 5.3 mm (an increase of 15 % feed rate of fountain water), was

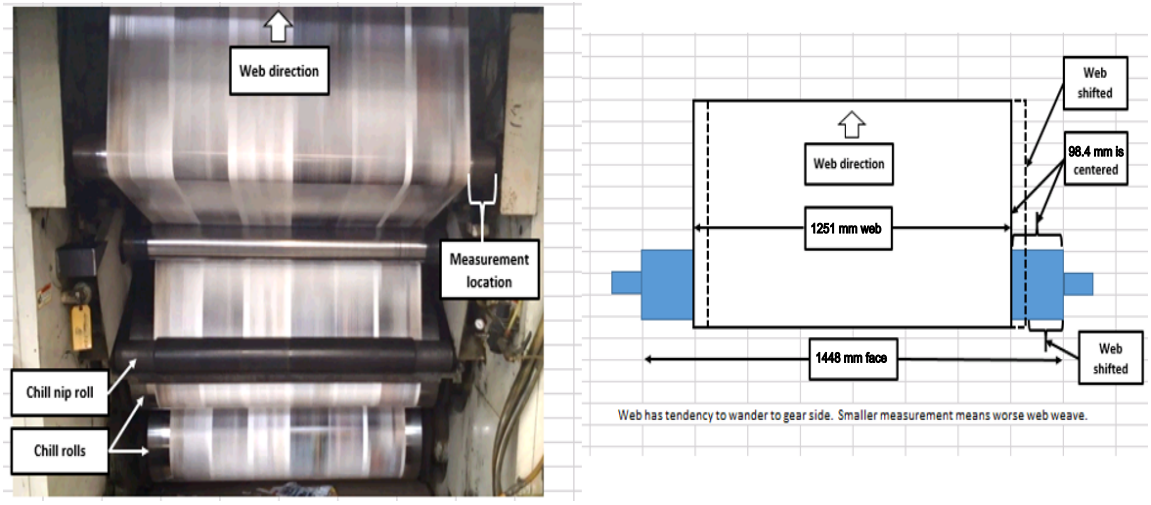

a) *b)*

Figure 7: Target printing press chill section exit; (a) actual measurement location; (b) schematic of measurement area (Shields, 2017)

recorded and web position noted before returning the fountain solution feed rate to standard. As each successive trial sheet was run, the dampening water feed rate was returned to the same setting as noted above. The results of this trial are shown in Table 2.

Increasing the fountain solution feed rate caused lateral shift on both the target and competitive sheets. The target paper machine sheets were affected to a larger degree than the competitive sheets. The slitter guide column in Table 2 shows the extent to which the web guide had to move to correct the web position back to centered on the slitters. The target PM was off center at the chill exit under normal printing conditions and moved a further 25.4 mm (1") laterally with increased fountain solution feed. The softwood PGW / increased SBK trial point started more centered under normal printing conditions and shifted less with increased fountain solution feed than the softwood PGW / normal SBK condition. Neither target PM condition was as stable as the competitive sheet, which was very close to centered at the chill exit under normal printing conditions (with very little web guide correction needed) and only 6.3 mm (¼") of lateral movement with increased fountain solution feed rate.

Finally, the target paper machine web response to decreased fountain solution feed rate was noted for one of the pulp conditions. The fountain solution feed rate was reduced until scumming was visible in the non-image areas, indicating not enough water was present on the printing plate. The web position was noted as shown on the lower portion of Table 2. Reducing the fountain solution feed rate to the printing plate caused the web to move closer to center at the chill exit, and the web guide had to make less correction to center the web on the slit-

Table 2: Response of dampening solution on lateral web position for two paper machines

Mill trial point	**Trial point description**	**Normal printing** Web running poition (mm)	Slitter guide position	**Changed water feed** Web running poition (mm)	Slitter guide position	**Result** Difference in web position (mm)
	Fountain solution feed increased by 5.3 mm Flat/print/loss of density on signatures					
2	Target PM all softwood mech. pulp	82.5	60 O	57.1	80 O	25.4
3	Target PM all softwood plus increased kraft	92.1	25 O	76.2	35 O	15.9
6	Competitive PM standard	98.4	O	90.5	25 O	7.9
8	Competitive PM high HW mech. pulp	98.4	O	90.3	30 O	6.3
	Fountain solution feed decreased by 3.5 mm Scummings visible on signatures					
2	Target PM all softwood mech. pulp	82.5	60 O	88.9	30 O	–6.3

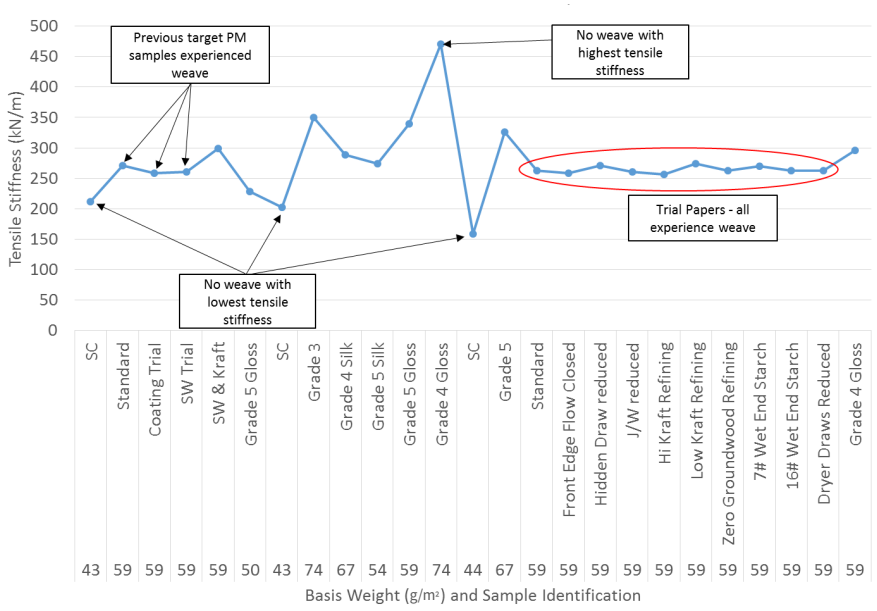

Figure 8: Tensile stiffness at printed moisture content for tested paper samples (Shields, 2017)

ters. For sheets from both paper machines the amount of water applied affects the chill section exit tension and lateral web position. The effect is greater on sheets from the target paper machine with one of the conditions showing a full 25.4 mm (1") of movement from normal to increased dampening water amount. The conclusions from this set of trials were that the paper machine rather than the pulp type was responsible for the effect of water on the lateral web position, and, the effect of additional fountain solution is similar (although not as severe) to the effect of blanket washing on lateral web position. This second fact indicates that the water amount taken on by the web during normal printing or blanket wash conditions is the most important printing press factor determining later web position.

The tensile stiffness at printed moisture content is shown for each of the samples tested in Figure 8. Papers with higher and lower tensile stiffness at printed moisture amounts are included in the sample set. None of the competitive papers experience lateral web movement during blanket wash, including the samples with lower tensile stiffness. Also obvious is the fact that all of the trial papers from the competitive paper machine have similar tensile stiffness at printed moisture content. None of the trial conditions had a measurable effect on tensile stiffness. It is apparent that the difference in lateral web position cannot be explained by the tensile stiffness at printed moisture.

3.2 Air permeability

Gurley air permeability of the samples was measured and the average results are plotted in Figure 9. Higher permeability (lower Gurley test results) should represent faster penetration time (Kettle, et al., 1997) and therefore more contact with fibers leading to lower web tension. The lowest Gurley permeability sheets are the SC sheets. These are the lightest basis weight papers and therefore have the lowest resistance to air flow. The SC sheets are typically made with a high proportion of mechanical pulp, which is stiffer than chemical pulp. The resulting sheets are therefore stiffer and bulkier. These two factors are likely reasons for the low Gurley permeability results. The papers with the highest results are those of the target paper machine. These papers contain a high proportion of coat weight and are heavily calendered forming a dense sheet. While the proportion of mechanical pulp is still significant for these papers, the coating and supercalendering are dominating factors. Most other samples range in the 1 000–3 000 s per 100 ml range. These papers range from heavier weight high kraft containing sheets with high levels of calcium carbonate in the coating to grade 5 papers with high proportions of mechanical pulp. It is unclear exactly how these papers are made, however they come mainly from mills with integrated SBK mills and it is possible that the base paper portion of the sheet is quite open due to low fines content or lower sheet consolidation during paper formation or calendering. While there are differences in air permeability, the papers showing highest air permeability (lowest Gurley permeability results) do not experience web movement. These are the SC sheets. In fact, the papers with the lowest permeability are those from the target PM. Two competitive sheets show the values in the same permeability range as the target PM and they do not experience lateral web movement on press. It appears that lateral web movement on the samples from target PM cannot be predicted by Gurley permeability. It is

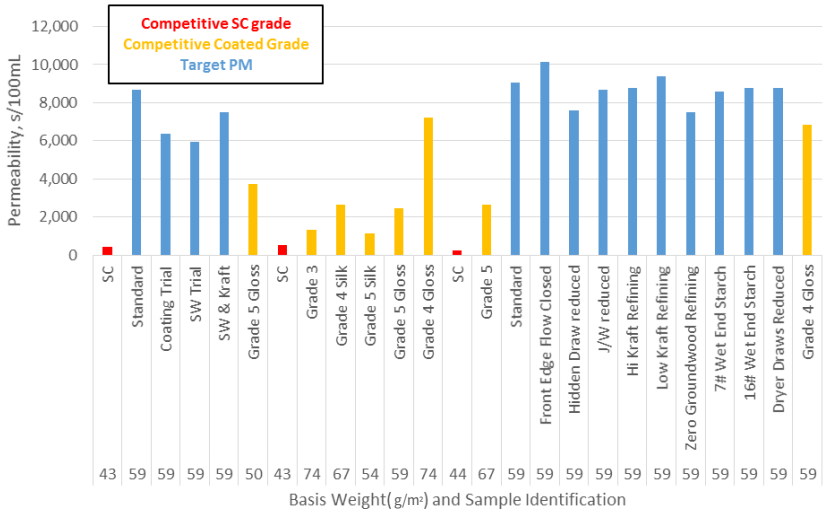

Figure 9: Gurley permeability results (Shields, 2017)

also apparent that the air permeability results do not correspond with the Emtec (Ultrasound Penetration Dynamics Analyzer) results (Shields, 2018). While the SC sheets have the lowest Gurley permeability results and the fastest absorption rate, the target PM has the second fastest absorption rate according to Emtec but the highest Gurley porosity results.

3.3 Creep and hygroexpansion

Three samples were selected representing the target PM, a competitive PM at the same basis weight, and a light weight SC paper. The competitive PM and SC sheets are known to have no lateral movement on press. These samples represent a spread of basis weights as well as a comparison between coated and uncoated papers. The results of the creep and hygroexpansion testing is plotted in Figure 10. For the 50 % RH tests, no discernable creep occurred after the initial loading of the samples. Over 30 s, all three samples were stable at the reference length. Upon heating, all three samples contracted, with the target PM contracting most. Upon cooling and regaining moisture from the ambient conditions, all three samples recovered their original length while still under load. These results indicate that no plastic deformation is occurring over the test duration at 50 % RH, i.e. no creep occurs. The samples contract upon heating as the fibers give up moisture and shrink. The difference in the magnitude of shrinkage can be explained by the fiber

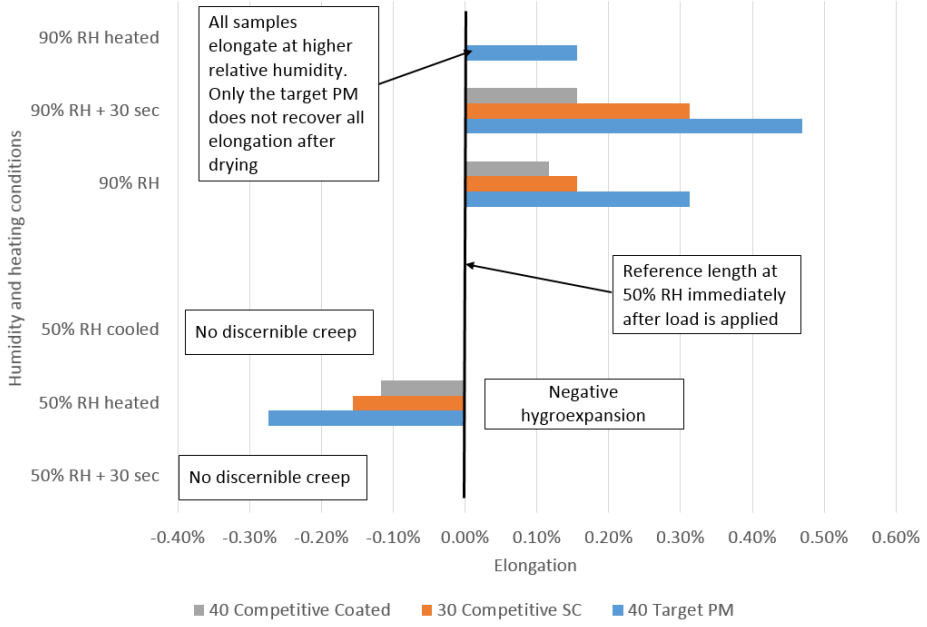

Figure 10: Creep and hygroexpansion test results for three paper samples (Shields, 2017)

orientation. Fibers shrink laterally. Papers that have higher fiber orientation in the measured direction will shrink less than papers with lower fiber orientation. The competitive coated sheet and the SC sheet have similar MD/CD tensile ratio results at 3.7 and 3.5 versus 2.4 for the target PM. For the 90 % RH testing, all samples measured longer after initial application of load than they were at 50 % RH. All samples also increased length after remaining under tension for 30 seconds. The competitive coated PM and light weight SC sheet regained their original 90 % RH length on heating while the target PM did not. The hygroscopic nature of wood fiber means that paper will absorb water. From 50 % RH to 90 % RH, the samples rise in moisture content approximately equal to that gained from printing 3 g/m^2 of water (Trollsås, 1995; Kela and von Hertzen, 2007). In fact, the SC sheet gains more than the printed water amount. The increased moisture of the samples at 90 % RH swells the fibers and increases the sample lengths. Analogous to the drying shrinkage, papers with higher fiber orientation in the measured direction will grow less than less oriented papers. The higher fiber orientation of the competitive coated and SC sheets results in less growth due to hygroexpansion.

When the samples are heated at 90 % RH the competitive samples regain their original fiber length at 50 % RH, however they do not shrink to the level they did when heating from 50 % RH. This seems consistent with the concept of creep. The samples have gained moisture in the amorphous regions of the fiber wall and grown in dimension, due to both hygroexpansion and softening of the amorphous matrix, which allows some movement of the microfibrils. In the case of the two competitive sheets with high fiber orientation, the creep seems to be quite small; just the difference between 0.1 % and 0.15 % respectively for the competitive coated and SC sheets.

For the target PM sheets, the elongation remaining after heating from 90 % RH is significantly higher than that for the competitive sheets. The target PM sample has less fibrillar reinforcement in the applied load direction than the competitive sheets, due to the lower fiber orientation. The amorphous matrix will soften a similar amount as the competitive sheets, however more movement of fiber walls should be possible due to the lower microfibrillar reinforcement. It seems most likely that the mechanism allowing the extra creep on the target PM is the lower fiber orientation yielding lower reinforcement in the loading direction, while the amorphous components are soft. The additional creep is estimated at 0.4 %, the difference between the strain at 90 % RH heated and 50 % RH heated results.

3.4 Ultrasonic measurement

Samples for which cross machine direction strips were available were measured for fiber orientation properties using ultrasonic measurement techniques. This included the 11 target paper machine trial samples plus one competitive sheet. Figure 12 shows the comparison of the target PM standard front edge roll and competitive coated sheet for TSI ratio, TSI MD and MD angle. The black boxes on the TSI ratio charts indicate the locations of the rolls used for the trials. As with the MD/CD tensile strength ratio, the TSI ratio of the competitive sheet is substantially higher than the target PM. The TSI MD values are slightly higher for the target PM than the competitive PM indicating that at equivalent basis weight the target PM would have a slightly higher tensile stiffness than the competitive sheet. It was found earlier in this section that tensile stiffness is not an indicator of lateral web movement performance.

The chart of MD angle shows that across the paper machine, there is less variation in the target paper machine than on the competitive PM. An increase in MD angle has the effect of changing the fiber orientation and therefore the tensile ratio. The higher deviation near the edges on the competitive PM TSI ratio illustrates this point. The summary of all rolls is displayed in Table 4. The TSI ratio is lower than for the competitive paper machine for all target PM trial points except one. For the reduced groundwood refining test the chart of TSI MD shows quite a bit of variability in the CD. This trial point was made in succession with the other conditions that did not have this variation or magnitude. This measurement result is considered invalid.

Table 4: Summary of ultrasonic measurements for target PM conditions and one competitive paper (Shields, 2017)

TSI parameter	Compet. paper	Standard paper	Edge flow closed	Increased strain at 20 % solids	Reduced drying restraint	Reduced J/W ratio	Higher kraft refining	Lower kraft refining	Reduced grounwood refining	Increased wet end starch	Reduced wet end starch
TSI MD (mNm)	12.8	12.3	11.8	12.0	11.8	11.8	12.4	12.1	11.7	12.2	11.8
Std. dev.	0.4	0.4	0.5	0.4	0.4	0.6	0.5	0.5	0.6	0.4	0.5
TSI ratio	5.2	3.8	3.9	4.2	3.8	3.6	4.1	4.1	5.0	3.8	4.0
Std. dev.	0.4	0.2	0.3	0.5	0.4	0.3	0.4	0.4	1.7	0.5	0.4

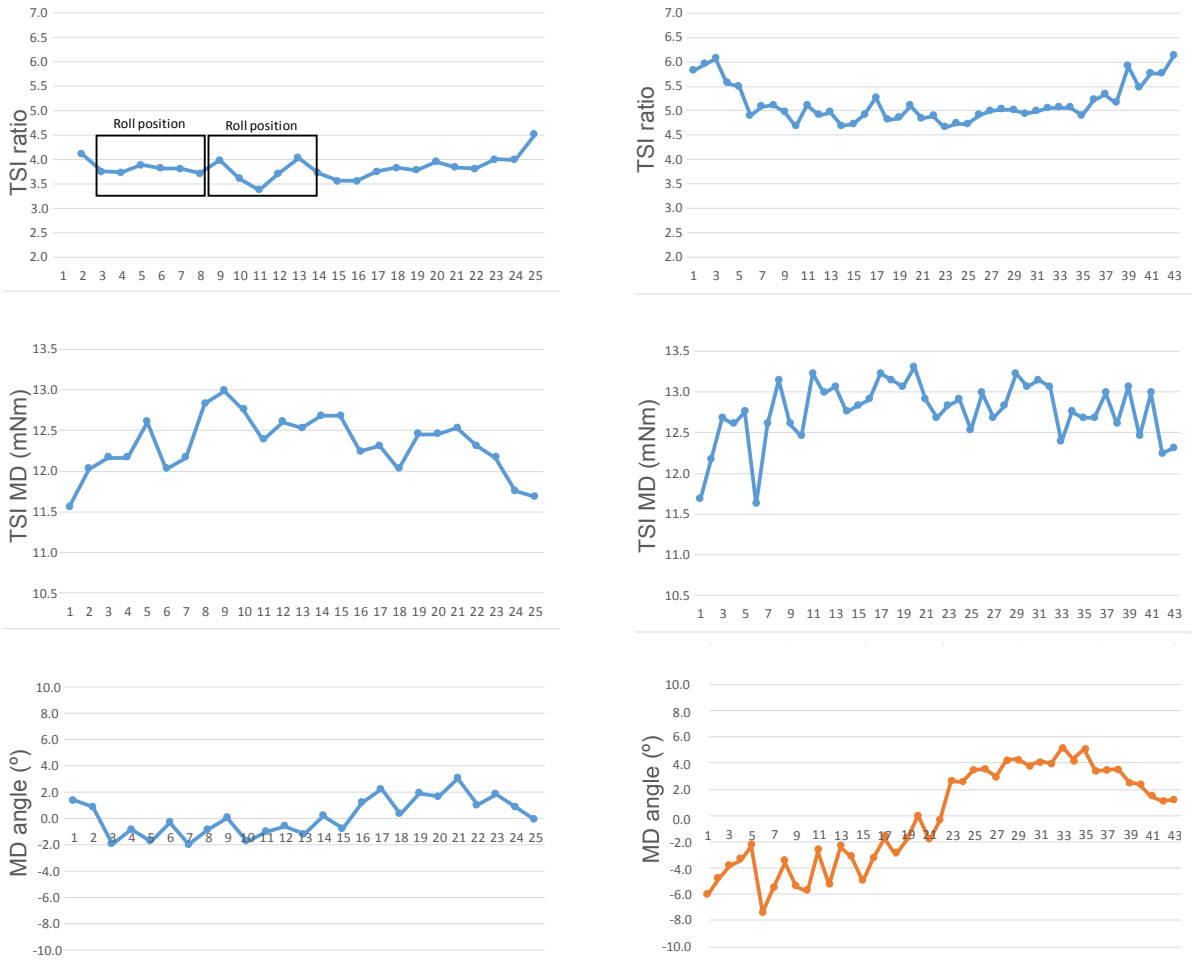

Figure 11: Ultrasonic tensile properties test results for 25 and 43 roll positions, respectively, for sheets taken from (a) target PM standard front edge roll, and (b) competitive coated paper roll; tensile ratios for the two sheets were 3.8 vs. 4.8 (Shields, 2017)

From the print testing results, the reduced J/W ratio performed poorly. In Table 4 the measurement for TSI ratio is the lowest at 3.6 of any sample tested. The two samples that tested highest for the target PM were the Increased strain at 20 % solids and the Edge flow closed sample.

The average results for the CD strip do not show the reason for the improved printing result. The tensile ratio of the area that the roll was cut from does show a possible tendency towards higher TSI ratio. In both cases the area of the roll tended towards a ratio of 4.5. The only item of interest from these results with respect to the lateral movement performance appears to be TSI ratio, which although the magnitude of the result is higher, is similar to that found using the ratio of MD to CD tensile strength (Shields, 2018). Tensile ratio appears to be of significance in determining reasons for weave on the target PM.

4. Conclusions

The purpose of this work was to determine the paper-making reasons for lateral shift of the moving paper web, made on a particular paper machine, on a specific printing press during heat set web offset printing. While there are differences in air permeability of all tested 25 papers, the papers showing highest air permeability (lowest Gurley permeability results) did not experience web movement, and they were the SC sheets. In fact, the papers with the lowest permeability were made at the target PM. Two competitive sheets tested in the same permeability range as the target paper machine did not experience lateral web movement on press. Thus, it appears that lateral web movement cannot be predicted by Gurley permeability. Creep is a good indicator of lateral movement on the press. Most likely, the mechanism allowing the extra lateral movement on the target PM is the lower fiber orientation of the sheet yielding lower

reinforcement in the loading direction. The reason for lower web tension in the target paper machine web is most likely due to lower fiber orientation. Fibers oriented in the direction of stress have reinforcement from the cellulose microfibrils. During printing, the matrix softens to some degree due to the addition of water. The stiff microfibrils serve to reinforce the matrix and prevent movement. Fibers oriented in the cross direction do not have this reinforcement. Therefore, a less oriented sheet has less reinforcement from the microfibrils and is more susceptible to movement of the matrix. Thus, of all tests executed, tensile ratio appears to be the only factor of significance in determining reasons for weave on the target PM.

List of abbreviations and glossary

Hydroexpansion	Expansion caused by penetration of liquid water into the pores of fiber wall.
Hygroexpansion	Expansion caused by penetration of water vapor into the pores of fiber wall.
J/W	Ratio of headbox jet velocity to forming fabric velocity
LWC	Light weight coated paper
MD	Machine direction
CD	Cross machine direction
PGW	Pressurized groundwood
PM	Paper machine
RH	Relative humidity
SBK	Softwood bleached kraft
SC	Supercalendered
TAPPI	Technical Association of the Pulp and Paper Industry
TSI	Tensile Stiffness Index

References

Brezinski, J.P., 1956. The creep properties of paper. *Tappi Journal*, 39(2), pp. 116–128.

Kajonto, I. and Niskanen, K., 1998. Dimensional stability. In: K. Niskanen, ed. *Paper Physics*. Helsinki, Finland: Fapet Oy, p.p. 222–259.

Kipphan, H., 2001. Offset Printing. In: H. Kipphan, ed. *Handbook of print media.* Berlin, Heidelberg, Germany: Springer-Verlag, p.p. 206–359.

Kela, L., and von Hertzen, L. (2007) *Printing Press Runnability.* KCL 0526370.

Kettle, J., Matthews, P., Ridgway, C. and Wågberg, L., 1997. Investigation of the pore structure of paper by novel porosimetric techniques: application to super and soft-nip finishing. In: C.F. Baker, ed. *The Fundamentals of Papermaking Materials*: *Transactions of the XIth Fundamental Research Symposium.* Cambridge, UK, September 1997. Letterhead, Surrey, UK: PIRA International, p.p. 1355–1393.

Lindblad, G. and Furst, T., 2001. *The ultrasonic measuring technology on paper and board: a handbook.* Kista, Sweden: Lorentzen & Wettre.

Niskanen, K., and Kärenlampi, P., 1998. In-plane tensile properties. In: K. Niskanen, ed. *Paper Physics*, Helsinki: Fapet Oy, p.p. 138–191.

Shields, G.W., 2017. *Papermaking factors affecting lateral web position during commercial heat set web offset printing*. Master Thesis. Western Michigan University.

Shields, G., Pekarovicova, A., Fleming, P.D., Pekarovic, J., 2018. Papermaking factors affecting lateral web position during commercial heat set web offset printing. *International Circular of Graphic Education and Research*, 11, p.p. 14–23.

TAPPI, 2011. *TAPPI T 460 om-11 Air resistance of paper (Gurley method)*. Atlanta, USA: TAPPI.

TAPPI, 2013. *TAPPI T 402 sp-13 Standard conditioning and testing atmosphere for paper, board, pulp handsheets and related products*. Atlanta, USA: TAPPI.

Trollsås, P.-O., 1995. Water uptake in newsprint during offset printing. *TAPPI Journal,* 78(1), p.p. 155–160.

Professional communication

JPMTR 2001
DOI 10.14622/JPMTR-2001
UDC 621.798-024.25|66-91:678.7

Professional communication
Received: 2020-01-24
Accepted: 2020-07-23

Influence of properties of materials for solventless lamination on the bonding strength of multilayer packaging

Vyacheslav Repeta, Yurii Kukura, Volodymyr Shibanov, Ihor Myklushka and Valentyna Kukura

Faculty of Publishing and Printing Information Technology,
Ukrainian Academy of Printing, 19, Pidholosko St., Lviv, 79020, Ukraine

vreneta@yandex.ua
yurii.lviv@gmail.com

Abstract

The article presents the study of the bonding strength of multilayer polymeric packaging films, the use of which is one of the directions of development of the flexible packaging technology to ensure high barrier properties and strength of packaging. The dependence of the viscosity of two-component polyurethane adhesive on temperature and time has been studied. During the research, polymer films of the different chemical structures have been selected: polyethylene terephthalate, polypropylene, including the metalized one, and polyethylene. The wetting of the selected polymer film surface with polyurethane adhesive has been studied, the value of their surface energy has been determined, and multilayer systems (laminates) have been formed in production conditions. It has been found that the value of surface energy has a great influence on the formation of laminates with high bonding strength. The surface energy components have been identified according to the Owens–Wendt method to study the nature of the intermolecular interaction in the adhesive bonding. The correlation dependence between the surface energy and its components has shown that the adhesive bonding strength increases as the polar component increases. In general, it has been found that all the systems under study have provided the sufficient strength for laminates (multilayer packaging).

Keywords: film, adhesive, viscosity, packaging strength, surface energy

1. Introduction

High requirements for food safety and quality, in turn, place high demands on the packaging quality. Various analytical forecasts show that more than 75 % of the world's flexible packaging materials are consumed in food packaging. In particular, in the countries of Central and Eastern Europe, their annual utilization is 1960 thousand tons, and the annual increase is 3.5 %; in Ukraine, the volume of production and consumption of flexible polymer packaging is approximately 140 thousand tons per year with an annual growth of 2 % (Alexandrov, 2017). The worldwide market for lamination adhesives for flexible packaging is expected to grow at a compound annual growth rate of roughly 0.9 % over the next five years, reaching 3 000 million US$ in 2024, from 2 850 million US$ in 2019, according to a new study (360marketupdates, 2019).

One of the priority areas for the development of flexible packaging technology is the use of multilayer polymeric materials – laminates. Among the wide range of manufacturing technologies, the most popular is solventless lamination technology, which provides a number of significant technological and economic benefits (NIIR Board, 2010). Thorough studies of the processes and materials of solventless lamination make it possible to understand the essence of the physicochemical processes underlying the technology and thus to influence their efficiency and quality of the finished packaging.

2. Literature review

The studies in which the authors examine the features of a particular lamination technology, their advantages and disadvantages, and particularities of their application in detail are of considerable practical interest. Such studies

(Wolf, 2010; Schetschok and Kupsch, 2011; Anjani and Annu, 2015) may serve as a guideline when selecting the lamination technology for a particular packaging segment.

The properties of the basic materials used in the technological process, in particular the properties of polymer films and adhesives, have a decisive influence on the operating characteristics of the finished laminate. The knowledge about the range of adhesives (Petrie, n.d.), their composition (Ardman, 2014), as well as the specifics of systems for their application (Ling, Wencai and Guangshen, 2010) is an important basis for further improvement of the technology and the study of immediate practical properties (Singh, 2017).

The adhesive bonding of objects occurs mainly under the influence of intermolecular interaction forces in the boundary layer between the substrate and the adhesive, and its strength depends on the nature and the number of functional groups, the structure of materials, and the interphase surface energy. It is appropriate to mention that a functional group (e.g., carboxyl –COOH, hydroxyl –OH, aldehyde –CHO, amino $-NH_2$, nitrile $-C\equiv N$, thio –SH, etc.) is a fragment of an organic molecule that determines its physical and chemical properties and it is a criterion for assigning this molecule to a certain class of organic substances – acids, alcohols, phenols, aldehydes, etc., respectively (Shibanov, 2016). Due to the wide variety of properties of adhesives, one can create materials that have brand new, often unexpected, but sometimes predictable functional parameters and characteristics.

In the bonding process, as a rule, there is a change in the aggregate state of the adhesive from a liquid (which provides better contact between the adhesive and the substrate) to solid. This greatly increases the viscosity (physical viscous state) and the melting point of the adhesive. Obviously, the hardening mechanism of adhesives that contain and do not contain solvents will be different. In the first case, the solid phase in the adhesive layer appears due to the evaporation of the solvent or dispersion medium (often water) and an increase in the concentration of the main component – a film-forming agent. In the other case, the adhesive hardening is due to chemical reactions leading to a multiple increase in the molecular weight of the main component of the adhesive composition in the chemical process, in its polymerization, polycondensation, polyaddition, three-dimensional crosslinking.

During hardening, the cohesive strength of the adhesive increases significantly. Cohesion is known to express the bonding power between molecules (atoms, ions) inside the object within a single phase and it characterizes the body strength. The destruction of the adhesive bonding under the action of external forces can occur either at the boundary between the adhesive and the substrate (there is adhesive destruction then), or on the adhesive seam or the substrate itself (cohesive destruction). The adhesive must have such adhesion to the substrate that the mechanical action on the adhesive bonding can cause cohesive destruction.

Previous works (Cheruvathur, 2009) have shown that the type, thickness, and surface properties of polymer films and the adhesive type and conditions of its application (its viscosity, and temperature) play an important role in determining the durability parameters, such as the bonding strength of laminates. The thickness and characteristics of the ink layer applied to the laminated films also have a significant effect on the bonding strength (Izdebska, Żołek-Tryznowska and Wirtek, 2015).

Studies of the properties of basic materials and solvent-free lamination modes provide not only additional information for improving the efficiency of the technological process, but also create a certain theoretical basis for further deeper analysis of the quality factors of the processes of forming flexible multilayer materials.

3. Methods

One of the important factors that significantly affect the lamination process is the properties of the two-component adhesive composition. It is known that in addition to the surface energy ratios of the substrates, the viscosity plays an important role in the liquid spreading over the material surface. The process of solventless lamination occurs at a raised temperature; the adhesive components are mixed in the laminator head just before being applied to the opening. The multilayer laminates were formed on solventless laminator Laminastar 2 (DCM); the amount of adhesive applied was 2 g/m^2. Mor-Free L75-300/C79 (Dow) adhesive was used in the process of solventless lamination. It is a two-component solventless polyurethane adhesive system for high speed operation (up to 400 m/min).

Polymer films with different chemical structures and different storage times from the date of manufacture were selected for this study. Their characteristics are shown in Table 1. Table 2 shows the characteristics of solvent-based

flexographic inks, which were used to print polymer films before the lamination operation. When studying the effect of the ink layer on the adhesive bonding strength of the films, the relative dot area of the CMYK image was 95 %. The apparent viscosities of printing inks were determined by measuring of efflux time with 4 mm DIN cup (Deutsche Institut für Normung, 1987). The viscosity of the adhesive was determined with the Brookfield RVT viscometer, rotor No 5.

The surface energy of the polymer films was determined according to ASTM D 5946–09 standard (American Society for Testing and Materials, 2009) by the contact angle of their surface with a drop of distilled water. The contact angles of the substrate by liquid were determined according to the methodology described in Repeta (2013), by digital registration of drop profiles. Small droplets of test liquid and ink 7.5 ± 0.5 µl were placed on the substrate with a micropipette. The drop images were captured with a CCD camera (1280 × 720 px) attached to the microscope, and then recorded by a computer. The spreading of liquids was evaluated 1 min after application on the substrate at temperature of 20 ± 0.5 °C and 82 % relative humidity.

Table 1: Characteristics of polymer films

Film name	SHD	SVD	MLD	CMVV.M	FBW	F-CHE-0.12
Producer	Treofan	Treofan	Treofan	Biaxplen	Technologia JSC	Flex P.Films
Type	Polypropylene	Polypropylene	Polypropylene	Metallized polypropylene	Polyethylene	Polyethylene terephthalate
Thickness [µm]	28	28	20	30	50	12
Orienting type	monoaxial	monoaxial	biaxial	/	/	/
Surface activation	physical	physical	physical	physical	physical	chemical
Roll width [mm]	520	520	540	540	820	600
Grammage [g/m^2]	21.5	21.0	18.2	27.3	50.0	16.8

Table 2: Characteristics of printing inks

Ink	Ink name	Producer	Apparent viscosity (DIN 4 cup), s
Yellow	Polistar Process Yellow	FlexoRes	40
Magenta	Polistar Process Magenta	FlexoRes	32
Cyan	Polistar Process Cyan	FlexoRes	34
Black	Polistar Process Black	FlexoRes	34

The polar and dispersive components of the surface energy are determined by Owens–Wendt method for contact angle of test liquids (Owens and Wendt, 1969):

$$0.5\,\gamma\,(1+\cos\theta)\,/\,(\gamma_d)^{0.5} = (\gamma_d^s)^{0.5} + (\gamma_p^s)^{0.5}\,(\gamma_p\,/\,\gamma_d)^{0.5} \quad [1]$$

where γ is a surface tension of the liquid; and γ_d and γ_p are dispersive and polar components of the surface energy that characterize solid body marked by index S, or liquid (no index).

For the calculation of the results of Equation [1], which lies in the intersection of the coordinates $0.5\,\gamma\,(1+\cos\theta)\,/\,(\gamma_d)^{0.5}$ and $(\gamma_p\,/\,\gamma_d)^{0.5}$ represented as a straight line with a slope of $(\gamma_p^s)^{0.5}$, and the point of intersection of this line with the axis value of ordinates $(\gamma_d^s)^{0.5}$, the developed program was used, which interface is shown in Figure 1. Liquids with known surface tension and polar and dispersive components such as distilled water and ethylene glycol have been used for testing.

Adherent interaction of the adhesive with the surface of the polymer films and the ink layer is of particular importance both for the printing and the lamination quality. Accordingly, the value of the surface energy of the selected films has been studied and the value of the contact angles of their surface with the adhesive has been determined.

The resultant indicator of the lamination quality of multilayer polymer materials is the bonding strength of the laminated materials. The preparation of samples and the determination of adhesive strength were carried out in

accordance with ASTM F904-16 (American Society for Testing and Materials, 2016) and DIN EN 868-5:2019 standards (Deutsches Institut für Normung, 2019). At the beginning of preparation before measuring, strips in dimension of 25 mm × 310 mm were cut from the finished laminate in the transverse direction and immersed in ethyl acetate (the immersion depth 70–80 mm) for 15 min to 20 min in a sealed container. Subsequently, the strips were removed, wiped, and stratified to form a T-shape. Tearing the laminates and testing the adhesive strength was carried out on the equipment shown in Figure 2.

The laminated material is considered to be of good quality according to the standard DIN EN 868-5:2019, if the bonding strength of the non-medical packaging is not less than 1.2 N (Deutsche Institut für Normung, 2019).

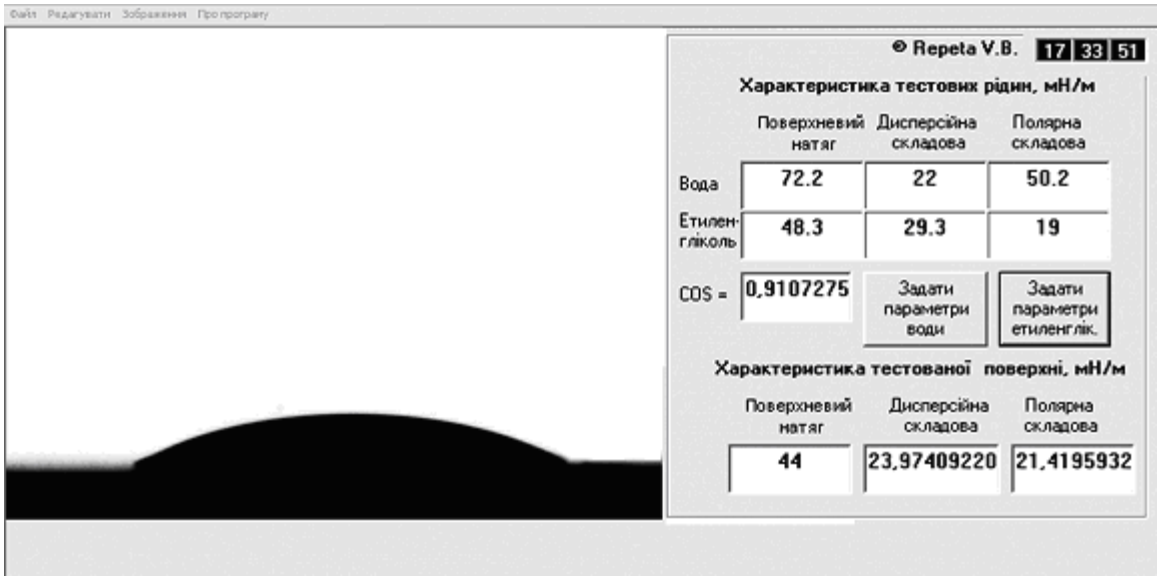

Figure 1: The program interface for determining the cosine of the wetting angle and the substrate surface characteristics

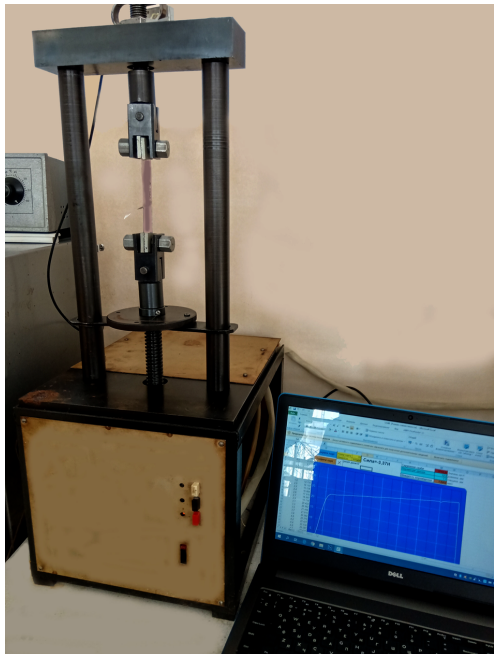

Figure 2: The equipment for testing the adhesive strength of laminates

4. Results and discussion

The process of chemical inter-component interaction begins immediately after mixing, so the open time of the adhesive is 20–30 min. During this time, the adhesive hardens; this is accompanied by the change in its viscosity, which is temperature dependent in its turn. Therefore, the dependence of the viscosity of the two-component adhesive on temperature (Figure 3) and time (Figure 4) has been analysed. The results obtained show that when the adhesive is heated to the temperature of 35–40 °C, its viscosity decreases very significantly – almost 10 times, which positively affects the parameters of its spreading and the ability to form a thin uniform film on the surface of the polymer film.

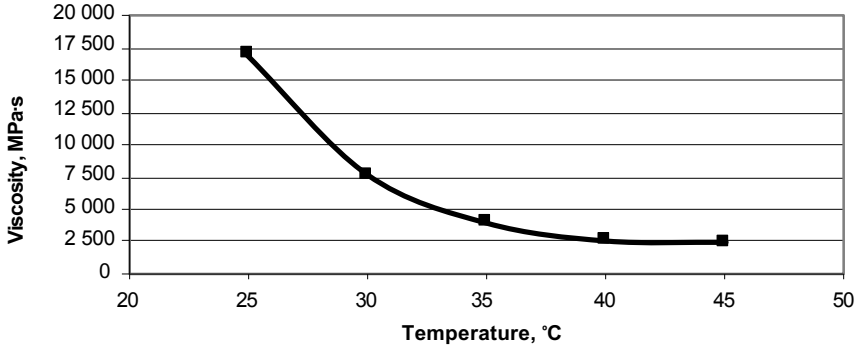

Figure 3: The dependence of the viscosity of Mor-Free L75-300/C79 adhesive on temperature (the viscosity is determined just after the heated components mixing)

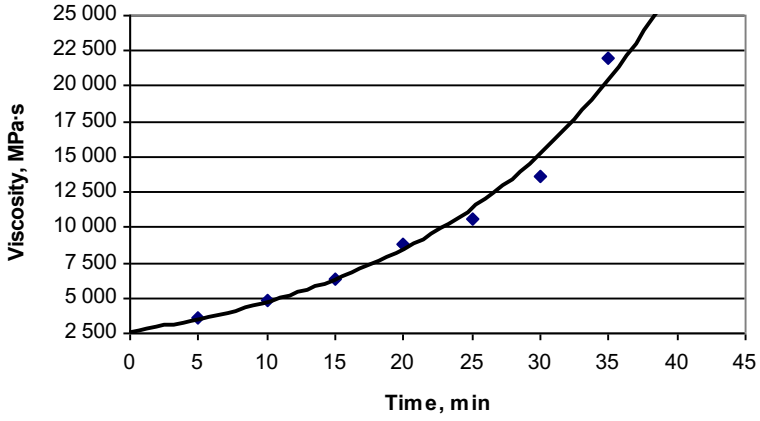

Figure 4: The dependence of the viscosity of Mor-Free L75-300/C79 adhesive on time after the component mixing

The results of the measurements of adhesive contact angles with polymer films, including four-color printed SVD marked as SVD+CMYK, used in this study are shown in Table 3.

Table 3: The surface energy of polymer films and the cosine of the wetting angle with the adhesive

Materials	Surface energy (ASTM D5946-09), mN/m	Surface energy (Ovens–Wendt), mN/m			Cosine of the adhesive wetting angle
		Dispersive component γ_d	Polar component γ_p	Total surface energy γ_s	
SVD	43	28.5	14.6	43.1	0.651
SHD	47	26.3	19.8	46.1	0.808
F-CHE-0.12	46	28.4	17.5	45.9	0.798
FBW	43	27.2	16.1	43.3	0.677
MLD	45	24.8	19.9	44.7	0.768
CMVV.M	42	27.7	15.5	43.2	0.632
SVD+CMYK	40	31.3	10.4	41.7	0.683

Over time, the adhesive viscosity (Figure 4) increases quite rapidly – in 10 min twice, and in 20 min almost four times. These data correlate with the recommendations received from the manufacturer, according to which the open time of the adhesive is 20–30 min. The data obtained give the additional information about the essence of the technological process and will allow to regulate it more precisely, which will provide a laminated product of appropriate quality. According to the results, in the study of the process of spreading the adhesive compositions, their application was carried out 10 min after the component mixing.

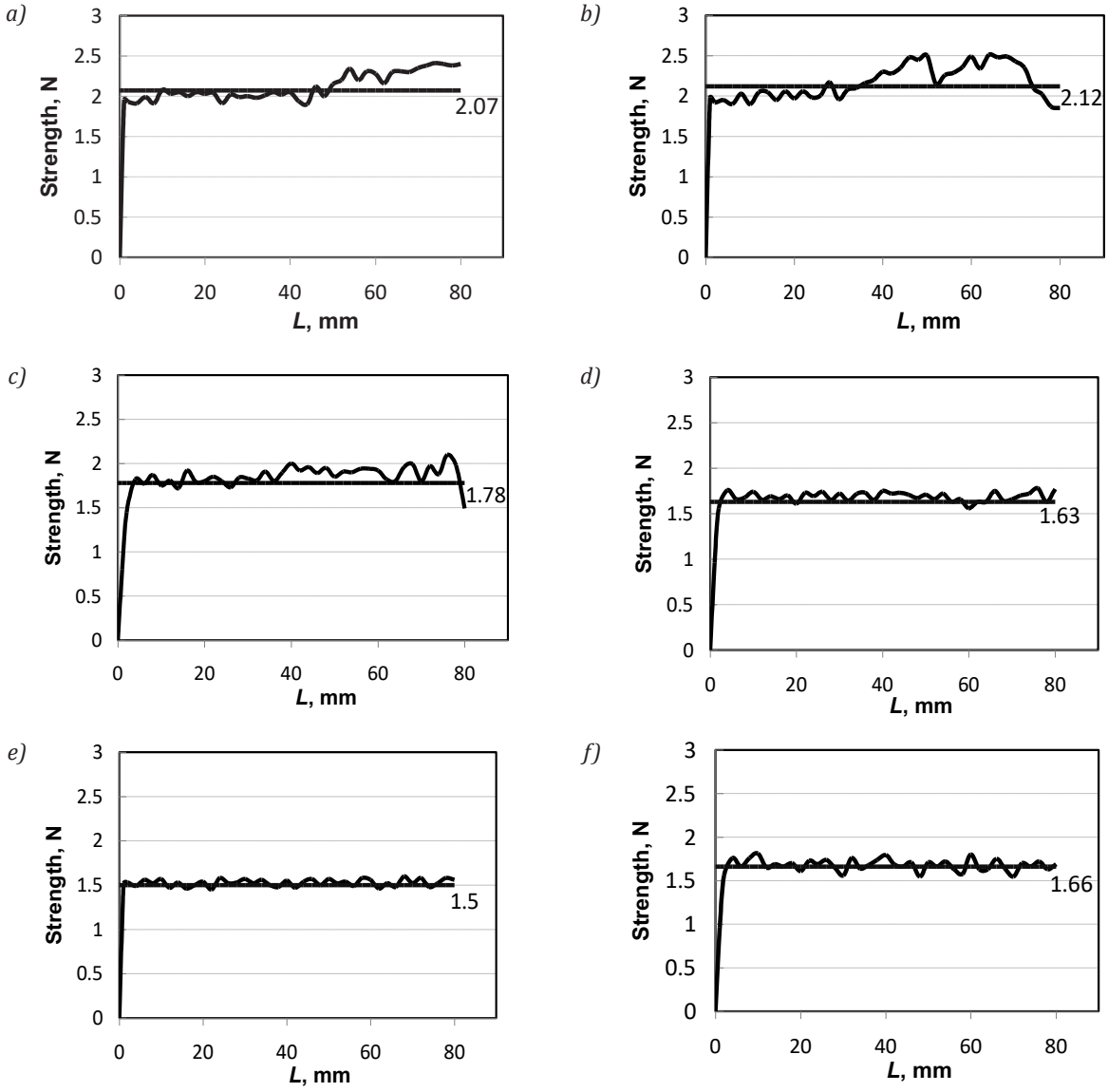

Figure 5: Bonding strength of the MLD film system with the film: (a) F-CHE-0.12; (b) SHD; (c) FBW; (d) SVD; (e) CMVV.M; (f) SVD+CMYK; L is the length of the measured sample

The bonding strength of various polymer films, including the printed surface, was determined on the bursting machine; the results are shown in Figure 5. MLD film was used for laminating in all cases. The results clearly show similar dependencies of the applied bursting force on the passed way. For SHD laminated polypropylene and F-CHE-0.12 polyethylene terephthalate, one can see some non-uniformity of the tensile force (Figure 5b), which can probably be caused by fluctuations in the distribution of the surface energy of the films. The analysis of the experimental dependencies obtained allowed one to determine the average bursting force for different types of laminates. The results indicate that MLD-F-CHE-0.12 and MLD-SHD films, have the highest strength (Figures 5a, and 5b), about 2.07 N and 2.12 N on average, respectively.

The bonding strength in MLD laminated on FBW systems, and MLD laminated on SVD+CMYK is somewhat lower, in the range of 1.66 N to 1.7 N. The lowest strength values of 1.5 N are for laminated material based on CMVV.M. It should be noted that all the studied laminates meet the requirements for laminated polymer films by the adhesive strength. The obtained values of the bonding strength of the films (Figure 5) correlate with the results obtained in the study of the surface properties of the polymers (Table 3). Higher surface energy films logically provide better orientation of the molecules when wetted with the adhesive and, accordingly, higher bonding strength of the laminate for multilayer packaging. It is clear that the surface characteristic of the MLD film is decisive for the bonding strength. An interesting pattern has been found for films with the highest surface energy, for which much larger variations of the sampling force data are observed (the difference between the maximum and minimum is 0.3 N on average). First of all, this indicates the heterogeneity of the distribution of active centers on the surface of the film formed in the modification process, which in general is not significant because of the high value of their surface energy. A similar situation is observed in the case of lamination of the printed film, which is explained by the unevenness of the ink layer.

The components of the surface energy of the substrates have been determined for a more detailed study of the nature of the intermolecular adhesion interaction (Table 3). The results have shown that the surface of all film samples has a high polar component, which lies in the range of 14.6 mN/m to 19.8 mN/m. We see a different situation for the ink layer, for which the polar component is the smallest and the dispersive component is high. Nevertheless, the ink layer surface provides high adhesive parameter of the bonding strength (1.66 N), which indicates a slightly different intermolecular interaction.

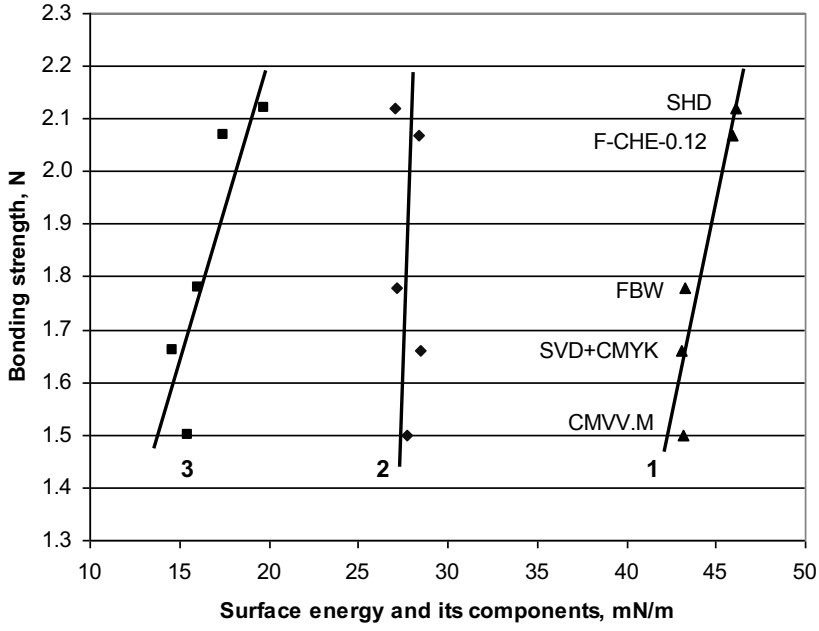

Figure 6: The relationship between bonding strength and surface energy with its components: 1 – total surface energy; 2 – dispersive component; 3 – polar component

Figure 6 shows the relationship between the bonding strength and the surface energy components. The analysis of the experimental data shows that the increase in the adhesive bonding strength is proportional to the increase of the polar component of the surface energy, which indicates that there are more functional polar groups on the surface involved in the intermolecular interaction.

5. Conclusions

In the paper, the compliance of the open time of the adhesive composition to the manufacturer's recommendations has been confirmed and the change in its viscosity with the temperature has been studied, which makes it possible to apply the adhesive in the lamination process and to form a thin layer. The results of the research have shown the influence of the surface energy of the substrates on the formation of adhesive bonding in the system of polymer

film–adhesive–polymer film, which determines the future operating parameters of such multilayer packaging. For films with the highest surface energy, larger differences between the maximum and minimum of the sampling force data are observed. This indicates, the heterogeneity of the distribution of active areas on the surface of the substrate.

The observed dependence between the surface energy and its components suggest that the increase in the adhesive bonding strength is due to the increase in the polar component of the surface energy. The ink layer of solvent-based inks of Polistar series (FlexoRes), applied on polymer films, does not cause the change in the bonding strength of the laminates.

References

360marketupdates, 2019. *Global lamination adhesives for flexible packaging market 2019 by manufacturers, region, type and application, forecast to 2024.* [online] Available at: <https://www.360marketupdates.com/global-lamination-adhesives-for-flexible-packaging-market-2019-by-manufacturers-regions-type-and-application-forecast-to-2024-13790615> [Accessed 21 January 2019].

Alexandrov, A., 2017. Klei dlya laminirovannykh plenok. *Upakovka*, 2–2017, pp. 20–22. (In English: Adhesive for laminating films).

American Society for Testing and Materials, 2009. *ASTM D5946-09, Standard test method for corona-treated polymer films using water contact angle measurements*. West Conshohocken, PA, USA: ASTM.

American Society for Testing and Materials, 2016. *ASTM F904-16, Standard test method for comparison of bond strength or ply adhesion of similar laminates made from flexible materials*. West Conshohocken, PA, USA: ASTM.

Anjani, B. and Annu, R., 2015. Lamination suitability for flexible packaging application. *International Journal of Engineering Research*, 4(5), pp. 228–230.

Ardman, C., 2014. *Solventless lamination benefits products as well as the environment*. [online] Available at: <https://www.lpsind.com/solventless-lamination-benefits-products-well-environment> [Accessed 21 November 2019].

Cheruvathur, R., 2009. *The effect of bond strength of flexible laminates on puncture resistance*. Master of Science thesis. Clemson University.

Deutsche Institut für Normung, 1987. *DIN 53211:1987-06 Paints, varnishes and similar coating materials; determination of the flow time using the DIN flow cup* (withdrawn). Berlin, Germany: DIN.

Deutsche Institut für Normung, 2019. *DIN EN 868-5:2019 Packaging for terminally sterilized medical devices – Part 5: Sealable pouches and reels of porous and plastic film construction – Requirements and test methods*. Berlin, Germany: DIN.

Izdebska, J., Żołek-Tryznowska, Z. and Wirtek, M., 2015. Study of the effects of the ink layer on selected properties of multilayer packaging films. *Journal of Print and Media Technology Res*earch, 4(1), pp. 27–32.

Ling, L., Wencai, X. and Guangshen, Z., 2010. Characteristics research about coating system of solventless laminator. In: T. Goedecke, ed. *Proceedings of the 17th IAPRI World Conference on Packaging*. Tianjin, China, 12–15 October 2010. USA: Scientific Research Publishing, pp. 63–67.

NIIR Board, 2010. *Handbook on modern packaging industries*. 2nd ed. New Delhi, India: Asia Pacific Business Press, p. 270.

Owens, D.K. and Wendt, R.C., 1969. Estimation of the surface free energy of polymers. *Journal of Applied Polymer Science*, 13, pp. 1741–1747.

Petrie, E.M., n.d. *Laminating adhesives for flexible packaging.* [online] Avaliable at: <http://www.academia.edu/9215453/Laminating_Adhesives_for_Flexible_Packaging> [Accessed 23 November 2019].

Repeta, V., 2013. Influence of surface energy of polymer films on spreading and adhesion of UV-flexo inks. *Acta graphica*, 24(3–4), pp. 79–84.

Schetschok, H.-G. and Kupsch, E.-M., 2011. Adhesive lamination vs. extrusion lamination trends & technology update. In: *Proceedings of the 13th European PLACE Conference 2011*. Bregenz, Austria, 30 May – 1 June 2011. TAPPI Press.

Singh, N., 2017. Impact of various adhesives used in solvent free lamination technique (a case study of Parle Biscuits Pvt. Ltd., Bahadurgarh). *International Journal of Engineering Sciences & Research Technology*, 6(7), pp. 741–743. https://www.doi.org/10.5281/zenodo.834477.

Shibanov, V., 2016. Khimiya kholodnykh kleyev. *Flexo Plus*, 4–2016, pp. 56–61. (In English: Chemistry of cold adhesives).

Wolf, R., 2010. A technology decision – adhesive lamination or extrusion coating/lamination? In: *TAPPI PLACE Conference 2010*. Albuquerque, NM, USA, 18–21 April 2010. TAPPI Press.

TOPICALITIES

Edited by Markéta Držková

CONTENTS

News & more

An overview of changes in ISO standards for graphic technology

The extent of changes in the standards and specifications under the direct responsibility of the ISO technical committee TC 130 Graphic technology since the regular summary published a year ago is the same as in the previous periods, despite the current limitations. Only the technical report ISO/TR 19300:2015 Graphic technology – Guidelines for the use of standards for print media production is withdrawn. The standards reconfirmed after a review include ISO 11084-2:2006 Graphic technology – Register systems for photographic materials, foils and paper – Part 2: Register pin systems for plate making, ISO 12642-2:2006 Graphic technology – Input data for characterization of 4-colour process printing – Part 2: Expanded data set, and two parts of ISO 15930 Graphic technology – Prepress digital data exchange using PDF – Part 4: Complete exchange of CMYK and spot colour printing data using PDF 1.4 (PDF/X-1a) and Part 6: Complete exchange of printing data suitable for colour-managed workflows using PDF 1.4 (PDF/X-3), both from 2003. Those confirmed for the first time are two parts of ISO 12647 Graphic technology – Process control for the production of half-tone colour separations, proof and production prints – Part 4: Publication gravure printing (from 2014) and Part 5: Screen printing (2015), ISO 15341:2014 Graphic technology – Method for radius determination of printing cylinders, and ISO 16760:2014 Graphic technology – Prepress data exchange – Preparation and visualization of RGB images to be used in RGB-based graphics arts workflows. New editions and brand new standards are presented below.

ISO 12641-2:2019
Graphic technology – Prepress digital data exchange
Part 2: Advanced colour targets for input scanner calibration

The previous ISO 12641 from 1997 changed to a multipart standard, where the new ISO 12641-2 published in December 2019 is intended for the calibration and characterisation of image capturing devices and specifies the requirements for advanced layouts and colorimetric values of targets, together with data reporting. It is based on the exchange format CxF/X-2. The framework can be used for ISO defined as well as custom targets, both reflective and transmissive; the self-emissive ones are covered only if designed to simulate the targets using transmission of light through an optical filter.

ISO 12647-6:2020
Graphic technology – Process control for the production of half-tone colour separations, proofs and production prints
Part 6: Flexographic printing

This version released in September 2020 cancels and replaces the second edition from 2012 and incorporates the amendment from 2015. While the focus of the previous editions was on the process control and specific printing condition aims were defined, the present document reflects the versatility of flexographic technology; therefore, it specifies the way of exchanging the colour characterisation data and other information necessary to define the printing characteristics of the desired product for four-colour flexographic printing of packaging and publication materials, including newsprint.

Trends in the publications on printing during the last 20 years

This brief overview is based on the Web of Science by Clarivate. When searching for records containing the word starting with “print” in the title and published from 2000 onwards, it returns almost 60 thousand results. Almost 60 % comprises articles and about 25 % proceedings papers. When considering the countries or regions, almost 25 % come from the USA and 15 % from China, followed by England, South Korea, Germany, Japan and others. Over 11 thousand are open-access publications, more than 75 % of which are articles and 10 % proceedings papers.

The yearly number of these records grows, from about 11 hundred to nearly 7.5 thousand in 2019, with a considerably higher rate approx. since the year 2015, when the average increase changed to about 900. When refining the records to those with open access, the change in slope is even more pronounced due to the average increase about 400 in recent years. Looking at the topics of publications, over 16 thousand deal with 3D (or 4D) printing, almost a quarter of which was published in the year 2019. The yearly number was increasing by about 700 in the last five years, thus representing the fastest growing area of research employing printing.

Among the ten publications most cited (all having over a thousand citations from the Web of Science Core Collection, the newest published in 2014), five deal with a particular application of printed electronics, namely the solar cells, transistors or supercapacitors, and three present the application of inkjet printing to material printing in general. From the open-access publications, the ten most cited ones have between approx. 500 and 800 citations each and mostly deal with 3D printing, which is focused on biomaterials in four cases.

Research at RIT's College of Art and Design

The Image Permanence Institute, a university-based research centre in the College of Art and Design at RIT (Rochester Institute of Technology), has recently received a National Leadership Grant award from the Institute of Museum and Library Services for its three-year research project that aims to identify the most cost-efficient and environmentally responsible methods of preparing paper-based collection objects for transit and display while maintaining preservation standards. The Image Permanence Institute also operates Graphics Atlas, a web-based resource that presents an object-based approach for the identification and characterisation of prints and photographs. The site features the timeline and detailed characteristics of a wide range of processes, not only photographic but also pre-photographic, photomechanical and digital ones, ranging from woodcut relief printing to inkjet or thermal printing. The tools let the user compare the selected print with another one, reproduced by a different process, captured using different lighting angles and magnifications, up to the level revealing substrate fibres, individual raster dots and other features. The key identifying features of each process are explained and documented, including the cross-section images showing the multi-layer structure, for example.

The RIT MAGIC (Media, Arts, Games, Interaction, and Creativity) Center, on the other hand, is dedicated to research and production of digital media, both within sponsored research and independent study projects. Other multidisciplinary collaborations and projects of RIT's College of Art and Design are facilitated thanks to partnerships with companies such as Autodesk and Nikon. Faculty and students also took part in the development of an algorithmic-based platform that can identify the image, audio, and video manipulation in a government-funded project on a topic that is gaining high importance.

ISO/TS 18621-11:2019
Image quality evaluation methods for printed matter
Part 11: Colour gamut analysis

This new specification from December 2019 defines procedures to measure and compare the colour gamuts of RGB and CMYK printing processes. Since this summer, its new version is under development.

ISO 19301:2020
Graphic technology – Guidelines for schema writers – Template for colour quality management

Published in March 2020, this new standard specifies the requirements for certification schemes to facilitate comparable attestations or certifications worldwide. It assumes the quality management based on ISO 9001, with the relevant print-specific ISO standard referenced in the certification scheme.

ISO/TS 19303-1:2020
Graphic technology – Guidelines for schema writers
Part 1: Packaging printing

This new specification available since September 2020 provides the guidelines for globally comparable technical and conformity assessment of colour reproduction capability in typical packaging printing workflow, either using CMYK, spot colours, their combination or multi-colour printing. It refers to the related best practices and international standards.

ISO 20616-2:2020
Graphic technology – File format for quality control and metadata
Part 2: Print quality eXchange (PQX)

This new standard from March 2020 defines an extensible file format for the exchange of print quality data and metadata for colour measurement (both spectral and non-spectral), process control, quality management, etc.

ISO/TS 23031:2020
Graphic technology – Assessment and validation of the performance of spectrocolorimeters and spectrodensitometers

This new specification released in August 2020 is intended for optical spectrometers capturing the spectral reflectance or radiance factor of printed areas comprised of non-fluorescent or fluorescent materials, respectively.

ISO 23498:2020
Graphic technology – Visual opacity of printed white ink

This brief new standard from September 2020 specifies a method of measuring the visual opacity of opaque white ink as printed, including the range of suitable substrates and standard conditions.

ISO/TS 23564:2020
Image technology colour management – Evaluating colour transform accuracy in ICC profiles

Available since January 2020, this new short specification defines the procedures for evaluation of the accuracy of colorimetric rendering intents in v4 ICC profiles conforming to ISO 15076-1.

Bookshelf

Handbook of Image Processing and Computer Vision
Volume 1: From Energy to Image
Volume 2: From Image to Pattern
Volume 3: From Pattern to Object

Three volumes of this new handbook in the field of artificial vision provide a systematic and comprehensive review of the individual steps from the formation of an image up to the 3D reconstruction of a scene while explaining the related concepts and processes.

Volume 1 begins with four chapters presenting the image formation process, radiometric model, colour and optical system. The authors provide the background on energy, electromagnetic waves, photons, light and light–matter interaction, the spectrum of electromagnetic radiation, light sources, the bidirectional reflectance distribution function, theory of colour perception, human visual system and visual phenomena, colour constancy, colorimetry and colour spaces, colour reproduction technologies, reflection and refraction of light on spherical elements, thin lens, optical magnification and optical aberrations. The fifth chapter describes the image acquisition systems, digitisation and display. The next four chapters outline the properties of the digital image, data organisation, structure and encoding, representation of objects and description of forms, and image enhancement techniques, such as histogram modifications and various filters.

Volume 2 first details the local operators and filtering techniques for the boundary extraction and the fundamental linear and geometric transformations, including various discrete and wavelet transforms, the transform based on the eigenvectors and eigenvalues, geometric operators, affine transformations, nonlinear geometric transformations, and different interpolation approaches. Further, it deals with the methods for the reconstruction of degraded images and image segmentation, as well as with the commonly used algorithms detecting the points of interest and describing the surrounding area in terms of radiometric spatial invariance attributes.

Volume 3 then presents a number of the object recognition methods and algorithms, introduces the significant types of neural networks – the radial basis function networks, self-organising map networks, Hopfield networks and deep neural networks – and the analysis of texture with statistical, syntactic, spatial, spectral, structural and model-based texture description methods. It also reviews the 3D vision, Marr's paradigm, stereo vision, the approaches to the reconstruction of a 3D scene from shading, texture, structured light, focus or defocus, as well as the motion analysis algorithms estimating the 3D motion from sequences of 2D images including the methods applied for motion in complex scenes. Finally, the last chapter deals with the calibration of the image acquisition system, which is important for detecting the size and pose of objects in the scene to enable the 3D reconstruction.

Authors: Arcangelo Distante, Cosimo Distante

Publisher: Springer, 1st ed., July 2020
ISBN: 978-3-030-38147-9 &
978-3-030-42373-5 & 978-3-030-42377-3
491 & 432 & 676 pages,
309 & 272 & 271 images
Hardcover
Available also as an eBook

Understanding Surface Scatter Phenomena A Linear Systems Formulation

Author: James E. Harvey

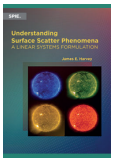

Publisher: SPIE Press
1st ed., July 2019
ISBN: 978-1510627871
252 pages
Softcover
Also as an eBook

This book presents the generalised Harvey–Shack surface scatter theory that integrates the radiometric principles with scalar diffraction theory and enables a detailed analysis of scattering behaviour of rough surfaces illuminated at arbitrary incident angles, which should help in solving the problems caused by scattered light, such as the image quality degradation.

Advanced Graphic Communication, Printing and Packaging Technology

Editors: Pengfei Zhao, Zhuangzhi Ye, Min Xu, Li Yang

Publisher: Springer
1st ed., April 2020
ISBN: 978-9811518638
883 pages, 571 images
Hardcover
Also as an eBook

The Proceedings of the 10th China Academic Conference on Printing and Packaging held in November 2019 in Xi'an include over a hundred papers dealing with the technology related to colour science, image processing, digital media, printing and packaging engineering, information engineering and artificial intelligence, printing materials, films and novel functional materials. The topics include, for example, the improved spectral reflectance reconstruction algorithm, applications of augmented reality, screen-printed electrochromic devices, capacitive flexible pressure sensors, digital watermarking technology, moisture-proof coating for corrugated boards and boxes, advanced ink formulations, and super-hydrophobic surfaces.

Colour and the Optical Properties of Materials

The updated and extended third edition of this textbook provides the essential background on the subject, explaining the fundamental principles, and also covers the modern applications such as fibre optics, flat lenses, special coatings, multilayer stacks, liquid crystals, photonic crystals, holograms, lasers, optical amplifiers, super-resolution imaging, light-emitting diodes, including the organic and quantum dot based ones, different types of colour displays, electrochromic films, photovoltaics and plasmonic crystals, among others. The new edition keeps the proven structure. Six chapters are dedicated to light and colour, refraction and dispersion, reflection, polarised light and crystals, scattering and diffraction. The next three chapters deal with the interaction of light with atoms, ions and molecules, including the mechanisms of luminescence. The last chapter is focused on colour in insulators, semiconductors and metals.

Besides the recommended literature, the text is complemented by quizzes, calculations and questions at the end of chapters, with the answers and solutions available at the instructor companion site. The appendices contain information on definitions, units, conversion factors, the colour of a thin film in white light, the formation of a hologram, atomic electron configurations and energy levels.

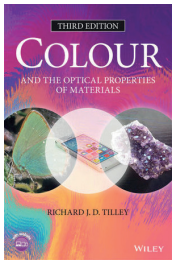

Author: Richard J. D. Tilley

Publisher: Wiley
3rd ed., March 2019
ISBN: 978-1-119-55469-1
608 pages
Hardcover
Available also as an eBook

Calculus for Computer Graphics

This concise book is intended to provide the understanding of calculus applied in computer graphics, games and animation to the readers who are already acquainted with algebra, trigonometry, vectors and determinants. The chapters go through functions, limits and derivatives, antiderivatives, higher and partial derivatives, integral calculus, the area under a graph, arc length and parameterisation of curves, surface area, volume, vector-valued functions, tangent and normal vectors, continuity and curvature; the last three, useful for shading algorithms, physically-based animation and Bézier curves, are new in the second edition, together with the part on curve parameterisation in the ninth chapter. The understanding of the topic is facilitated by numerous worked examples and illustrations.

Author: John Vince

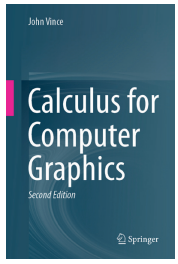

Publisher: Springer
2nd ed., March 2020
ISBN: 978-3-030-11375-9
303 pages, 179 images
Softcover
Available also as an eBook

A Social History of the Media

This overview of communication media, rather broad than detailed, helps to understand the present media industry and its fast changes. The authors focus on the context and impact of media communication, aiming to show the relevance of the past to the present. Just like not everyone today praises the social media, this was the case also with printing and every new mode of communication that came over time with the technological progress. The book also documents the mutual relationship between the development of the media and the politics, religion, economics and culture.

This new edition, appearing ten years after the third edition of the text originally published in 2002, is revised to make the book more reader-friendly, with a more clear structure, updated chronology and recommended further reading replacing the bibliography. Besides a thorough revision of the introduction, the last chapter by Asa Briggs, who has passed away, is newly written by Espen Ytreberg, covering the media developments in the 21st century.

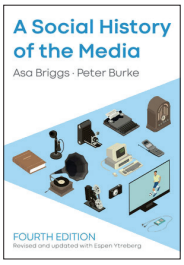

Authors: Asa Briggs, Peter Burke, Espen Ytreberg

Publisher: Polity
4th ed., June 2020
ISBN: 978-1-509-53371-8
360 pages
Hardcover
Available also as an eBook

Information Visualization
Perception for Design

The author of this book provides the relevant background on perception, based on the extensive research literature in the field, and derives the design principles helping to display information effectively, avoiding incomprehensibility and ambiguity. The text reviews the foundations, such as the perceptual data processing, types of data and differences between the approaches based on design and the science of perception, effects of the environment, optics, resolution and the display, concepts of lightness, brightness, contrast and constancy, the science of colour vision, the visual salience, patterns, both static and moving, the perception of space, the recognition and display of objects, the visual and verbal presentation, the interaction with visualisations, the visual thinking process, and the design of cognitively efficient visualisations. As in the case of previous editions, also the current one is revised and updated according to the recent findings – especially the one that the neural mechanisms for predicting the future and remembering the past are the same, reflected in the last three chapters.

Author: Colin Ware

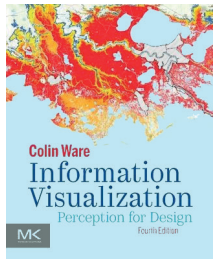

Publisher: Morgan Kaufmann
4th ed., March 2020
ISBN: 978-0-12-812875-6
560 pages
Softcover
Available also as an eBook

Practical Web Inclusion and Accessibility
A Comprehensive Guide to Access Needs

Author: Ashley Firth

Publisher: Apress
1st ed., May 2020
ISBN: 978-1484254516
470 pages, 128 images
Softcover
Also as an eBook

This guide on web accessibility is aimed at everyone involved, no matter the discipline and level of expertise, and provides numerous practical examples. After the introduction, the text in six chapters presents different disabilities and access needs, dealing with blindness, low vision and colour blindness, motor disabilities, deafness and hard of hearing, cognitive impairments, and mental health. The following part then discusses the ways how to improve the accessibility of images, videos and other graphic elements, as well as of the communication beyond a website. One chapter then presents the possibilities arising thanks to the emerging technologies. Finally, the author shows how to ensure that accessibility is considered during the whole development process, approaches to auditing an existing site, and tools for testing and improving a site.

Generative Design
Visualize, Program, and Create with JavaScript in p5.js

Authors: Benedikt Gross, Hartmut Bohnacker, Julia Laub, Claudius Lazzeroni

Publisher: Princeton Architectural Press
2nd ed., October 2018
ISBN: 978-1616897581
256 pages, 500 images
Softcover

This richly illustrated volume with step-by-step tutorials demonstrates the coding strategies to generate artwork, infographics, 3D models and animations using simple languages.

Low Temperature Chemical Nanofabrication
Recent Progress, Challenges and Emerging Technologies

Authors: Omer Nur, Magnus Willander

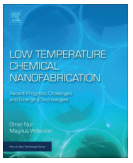

Publisher:
William Andrew
1st ed., January 2020
ISBN: 978-0128133453
252 pages, Softcover
Also as an eBook

The authors of this new book first provide the theoretical background to nanoscale phenomena and explain the differences between nanomaterials and the bulk, presenting the electronic band structure of nanomaterials, their optical properties, nanodielectric effects and other effects related to the nanostructure morphology. The following part deals with the nanofabrication methods, covering both the top-down and bottom-up processes. One chapter describes the conventional methods, another one the emerging ones, including the inkjet printing as a tool for nanofabrication, and the next one is focused on the low-temperature chemical nanofabrication methods. The last chapter covers the emerging applications in sensors, sustainable energy sources and photocatalysis.

The Effect of UV Light and Weather on Plastics and Elastomers

Author: Laurence McKeen

Publisher:
William Andrew
4th ed., March 2019
ISBN: 978-0128164570
464 pages, Hardcover
Also as an eBook

For individual polymer classes, this revised and expanded edition summarises the latest data on the effects of UV radiation and weathering, important for their use in outdoor applications; the book also covers the newly available materials, including the bio-based polymers and plastics for 3D printing.

Mechanically Responsive Materials for Soft Robotics

This volume brings a timely overview of the progress in the multidisciplinary field of soft robotics and the development of materials that mechanically respond to external stimuli. Part I reviews about a decade of basic research on the mechanically responsive crystals that exhibit a wide range of properties. Its six chapters describe photomechanical behaviour of photochromic crystals based on diarylethene, anthracene derivatives and other organic compounds, crystals with heat-induced mechanical motion, such as inchworm-like walking, fast-rolling locomotion or step-wise bending, crawling motion of crystals on solid surfaces by the photo-induced reversible crystal-to-melt phase transition, crystals that exhibit bending, jumping and self-healing, and shape memory molecular crystals showing superelasticity. Part II deals with the mechanically responsive polymers and composites together with their applications. It presents mechanical polymeric materials based on cyclodextrins as artificial muscles, cross-linked liquid-crystalline polymers as photomobile materials, photomechanical liquid crystal polymers and bioinspired soft actuators, organic–inorganic hybrid materials with photomechanical functions, multi-responsive polymer actuators by thermoreversible chemistry and their outlook in 3D printing, and mechanochromic polymers as stress-sensing soft materials. Part III then presents soft microrobots based on photoresponsive materials, 4D printing as an enabling technology for soft robotics, the self-growing adaptable soft robots, and the biohybrid robot powered by muscle tissues.

Editor: Hideko Koshima

Publisher: Wiley-VCH
1st ed., February 2020
ISBN: 978-3-527-34620-2
448 pages
Hardcover
Available also as an eBook

Solution Processed Metal Oxide Thin Films for Electronic Applications

This volume is a part of the series on metal oxides. After a brief outline of the solution-processed electronics and metal oxides in solution, it presents the metal-oxide conductors, semiconductors and dielectrics relevant for various electronic applications. Next, it deals with the sol–gel precursor inks and films and inks based on nanoparticles, along with their processing by coating or printing and thermal annealing. Finally, the text presents the selected applications of metal oxides in photovoltaics and electroluminescence devices, namely in organic and quantum dot light-emitting diodes.

Editor: Zheng Cui

Publisher: Elsevier
1st ed., June 2020
ISBN: 978-0-12-814930-0
180 pages
Softcover
Available also as an eBook

Bookshelf

Academic dissertations

A Robotic Multiaxis Additive Manufacturing System for Nonplanar and Dynamic Orientation Printing

Doctoral thesis – Summary

Author:
Nicholas Richard Fry

Speciality field:
Engineering Systems and Design

Supervisors:
Robert Richardson
Jordan Boyle

Degree conferral:
11 June 2018, University of Leeds,
School of Mechanical Engineering
Leeds, United Kingdom

Contact:
N.Fry@leeds.ac.uk

With a vision of a future automatic robot fabrication system producing small, customised and fully integrated robots for specific tasks, this thesis addresses the limitations of the current additive manufacturing systems in terms of anisotropic mechanical properties, the stepwise approximation of curves, need for support structures and embedding of components. The approach is based on varying build orientation allowed by the use of industrial robot arms. The dissertation reviews the literature on direct digital manufacturing, integrated robot fabrication and multiaxis additive manufacturing and presents the steps taken to develop a system capable of printing curved and non-parallel layers along with embedding pre-existing components. First, it details the design and development of the additive robot manufacturing system and its key aspects – four robotic arms (for the camera, gripper, extruder and build plate) with six axes each, materials and equipment for fused filament fabrication, software for the design and processing of 3D models and system control, as well as the kinematic model for the system with 12 degrees of freedom enabling to position the nozzle relative to the build plate. System validation involved visual inspection of conventionally 3D-printed items and testing of their tensile strength, dimensional accuracy and surface roughness. The resulting quality was at least comparable with other fused filament fabrication machines. Further experiments proved that printer orientations other than vertical have no adverse effects to the surfaces and that overhangs of arbitrary size and angle can be printed without any support structures thanks to dynamic build orientation during additive manufacturing. The possibility to increase strength was verified by printing the arch with nonplanar layers onto a smooth support structure. Finally, a model plane with an embedded DC motor was printed to demonstrate the ability to automatically embed functional components.

Copper Nanocrystals-Based Conductive Inks for Printed Electronics

Doctoral thesis – Summary

Author:
Arnau Oliva Puigdomènech

Speciality field:
Chemistry

Supervisors:
Zeger Hens
Christophe Detavernier

Defended:
10 January 2020,
Ghent University, Faculty of Sciences,
Department of Chemistry
Ghent, Belgium

Contact:
arnauolivapuigdomenech@gmail.com

This thesis contributes to the research on nanoparticle-based copper inks as a cost-efficient alternative to conductive inks containing silver. After introducing the background and outline of the thesis, the work reviews the known methods for copper nanoparticles synthesis. These comprise the methods employing the chemical and biological bottom-up processes and the physical methods, typically based on a top-down approach. The methods are assessed in terms of their cost, productivity and environmental impact, and also the ability to control the size of particles. Because copper has the inherent oxidation tendency and the oxidation rate is accelerated to a great extent in the case of nanoscale particles, the review also presents the strategies to preserve the electrical properties of the nanoparticles, i.e. to prevent oxidation. The colloids can be protected by a shell based on carbon, noble metal or silica; also, long-chain organic ligands and polymer stabilisers improve the oxidation resistance of colloids. When comparing these approaches, a drawback is the increased resistivity of the printed patterns in the case of the carbon or silica shells and high cost in the case of the noble metal shells; therefore, the ligand or polymer-capped nanoparticles

together with the appropriate sintering conditions are seen as a cost-effective solution to obtain highly conductive films. The experimental work building on this basis is described in four chapters. The first one presents the synthesis of metallic copper nanocrystals based on the low-temperature decomposition of copper formate, with oleylamine used as the surfactant. It was demonstrated that a self-cleaning effect suppressing oxidation is achieved with high precursor concentration. This economic approach does not need an additional reducing agent nor a protective atmosphere while producing a high amount of nanoparticles per volume of reaction. Moreover, by adjusting precursor and ligand concentrations and ratio, the size of the nanoparticles can be tuned from 10 nm to 200 nm. Next, the comprehensive study of the surface chemistry of copper nanocrystals helped to understand how amines and carboxylic acids bind and pack on the surface, creating a tightly-bound ligand shell. The further work was focused on the sintering of copper nanocrystals capped with different carboxylic acid ligands; also, the influence of particle sizes, atmosphere and temperature was studied. It was proved that oxidation can be reversed by thermal annealing in an N_2 atmosphere. Finally, the dissertation presents the upscaled synthesis and formulation of a copper-nanocrystal-based conductive ink with optimised adhesion and resistivity. The resulting screen-printing ink was used to produce conductive RFID antennas.

Doctoral thesis – Summary

Author:
Eli Nadia Abdul Latip

Speciality field:
Microfluidics and Microengineering

Supervisors:
Loic Coudron
Mark Tracey

Degree conferral:
5 February 2020,
University of Hertfordshire, School of Engineering and Technology
Hertfordshire, United Kingdom

Contact:
elinadia@uitm.edu.my

Development of a Digital Microfluidic Toolkit: Alternative Fabrication Technologies for Chemical and Biological Assay Platforms

The aim of this thesis was to use more affordable fabrication methods and materials to produce low-cost digital microfluidics and to increase the robustness of the device with respect to surface contamination by biomolecules. The work provides the background on actuating mechanisms in digital microfluidics with the focus on electrowetting-on-dielectric, the most commonly applied one, and reviews the requirements on the dielectric layer and actuating surface in the device, as well as the methods for its fabrication. The experiments first tested the possibility of electrode patterning by inkjet printing using a suitable combination of conductive ink and substrate. It was found that the most reliable droplet actuation performance of the device is achieved using poly(3,4-ethylenedioxythiophene) poly(styrene-sulfonate) (PEDOT:PSS) ink and polyethylene terephthalate substrate, with a velocity comparable to the standard chrome-on-glass device. Comparing a low-cost HP Deskjet 1000 J110 and a specialised Fujifilm Dimatix DMP-2850 printers, the desktop inkjet printer produced satisfactory electrode spacing and track width resolutions, but the printing reliability had to be improved by plasma treatment of the substrate, ink additives, filtering, and immediate cleaning of the cartridge. The inkjet printing using the laboratory printer proved to be a robust and reliable process with the potential to be widely applied in the fabrication of the electrowetting-on-dielectric devices. According to the preliminary testing of the off-the-shelf products in the search for alternative materials, the polyurethane finish from Rust-Oleum for the dielectric layer and the superhydrophobic top coating from NeverWet for the actuating surface performed the best in terms of electrowetting reversibility and the latter also in droplet actuation. Utilising the findings, three types of more complex electrowetting-on-dielectric devices were fabricated – the 3D 4 × 4 electrode array device allowing for future construction of multi-level digital microfluidic devices with the large functional area, a magnetic microimmunoassay device (both inkjet-printed with conventional dielectric and hydrophobic materials) and a superhydrophobic anti-biofouling device with the NeverWet top coating and chrome-on-glass electrodes.

Events

Virtual Fall Conference 2020

https://www.flexography.org
5–7 October 2020

The 2020 edition of the Flexographic Technical Association's Fall Conference is designed for an online environment and complemented by the Virtual Exhibit with new package printing and converting technologies, open since 5 October for ten days. Among six conference sessions, the first one presents a systematic approach to producing flexographic printing plates and covers calibration and optimisation, process and quality control, solving the common plate-related problems, and approaches to implementing new technologies while reducing the risk. The next one shows how to face the ongoing pandemic with the help of virtual interviews, web-based training, and remote press approvals. The second day is dedicated to proper file preparation for both flexographic and digital presses to produce matching products and colour management for spot as well as process colours, discussing also practical application of the ISO 12647-6 standard, the concept of neutral print density curves, G7 acceptance criteria, and spectral data. Finally, the last two sessions explore the print quality scoring and the process of package development.

Printing for Fabrication 2020

https://www.imaging.org
19–21 October 2020

The main programme of this online event is preceded by a week of live short courses starting on 12 October, with online discussions after each class and the recordings available for later or repeated viewing by the participants until 15 February 2021. Four courses focus on inkjet fluid dynamics and fundamentals, inkjet ink manufacturing and its practical characterisation. Another topic is adhesion and its optimising by improved surface properties, formulation or process. Two courses deal with textile printing. The last four courses present the fundamentals of digital fabrication along with two specific applications, namely direct-to-object printing and on-skin electronics by printing.

The topics of the 2020 keynotes include the hybrid supply chain models where 3D printing could be used to complement injection moulding (presented by Edward D. Davis), multi-disciplinary research undertaken at the Centre for Fine Print Research at UWE Bristol (by Carinna Parraman), and fundamental fluid dynamics challenges in inkjet printing (by Herman Wijshoff). The focal talks deal with the fabrication of magnetic polymer nanocomposites, the effect of the amount of filament on readability when recording the rewritable information by 3D printing inside an object, dynamic imaging by Kodak, 3D surface structures and 3D halftoning, probabilistic motion inference for fused filament fabrication, and aqueous inks for printed electronics based on two-dimensional materials, namely MXenes.

Further events cancelled for 2020 due to pandemic

While many events still take place online due to the ongoing pandemic, some are fully cancelled for this year.

The 52nd Annual Conference of the International Circle of Educational Institutes for Graphic Arts Technology and Management should take place in September 2021 in Athens, Greece as a joint event with the 47th International iarigai Conference. The 6th edition of CIDAG, the biannual International Conference in Design and Graphic Arts, has been postponed to 20–22 October 2021. The new date for the 7th European edition of The Inkjet Conference, TheIJC, is set to November 2021. Similarly, the ERA Packaging & Decorative Conference is rescheduled to November 2021.

Among the trade shows, the Latin American exhibition FuturePrint has been postponed again, now planned to 21–24 July 2021. The IDTechEx Show! 2020 in Santa Clara, California, USA and the 3rd International Exhibition of Print Technology for Industrial Manufacturing in Italy, InPrint Milan 2020, also have been cancelled, with new dates yet to be announced. InPrint Munich takes place on 9–11 March 2021. The next edition of PACK EXPO International that should take place this year in Chicago, Illinois, USA has been rescheduled to 23–26 October 2022. In 2021, the American edition of PACK EXPO takes place in Las Vegas, Nevada (27–29 September). A virtual event PACK EXPO Connects, with hundreds of exhibitors and over 2 600 live demonstrations, is held in a week of 9–13 November 2020, including a panel discussion on digital printing and finishing of packaging materials. Likewise, while the physical event SEMICON Europa 2020 has been cancelled and the next edition is planned to 16–19 November 2021, a differentiated digital forum is being prepared.

WAN-IFRA Events

The calendar of events for the end of the year includes the 2020 virtual editions of Digital Media for three regions – Asia (13–15 October), Europe (10–12 November) and Latin America (17–19 November); this last one with the 2020 LATAM Digital Media Awards on the first day. Other 2020 events are also virtual. The Newsroom Summit (20–21 October) this year explores e.g. how to lead and manage a remote team. The topics of the World Printers Summit (27–29 October) include newsprint procurement, the global campaign "I love Paper", optimisation of the paper supply chain and plate production, sustainable approaches, distribution of newspapers during the pandemic, new possibilities for layout and page assembly with artificial intelligence, and more. The 2020 Print Innovation Awards take place on the last day. Practical utilisation of artificial intelligence also belongs to the topics of the Middle Eastern Media Leaders eSummit (3–5 November). The Global Summit with a theme of 'Science in the Newsroom' (23–24 November) is focused on journalism in the age of global health emergencies, showcasing best practice journalism that has emerged in 2020.

In October 2020 also starts the online Cultural Change Ignition Program for Latin American News Publishers organised jointly with The Facebook Journalism Project. It is running until January 2021, with eight sessions aimed at rising media leaders in the region. The online training programme 'Managing Revenue Growth in Pandemic Times' is offered on 26–27 October.

AIPIA Smart Packaging Virtual Exhibition

https://www.aipia.info
7 October 2020

This event of the Active & Intelligent Packaging Industry Association can be attended online for free.

Ink Week 2020

This event dedicated to the developments in ink technology for graphic arts and printing is organised by the National Association of Printing Ink Manufacturers (NAPIM), along with the Ink World and Printed Electronics Now magazines. Ink Week features two online conferences with one registration fee providing access to both, including the recordings of all sessions shared after the event.

NAPIM Fall Technical Conference 2020

https://www.napim.org
12–14 October 2020

With a topic for this edition defined as 'Formulating for a Circular Economy', the agenda includes a lecture discussing the concept of circularity and its practical applicability to the printing industry, along with a panel discussion of raw material suppliers, ink manufacturers and printers to learn about their view on the current status and possible developments in graphic arts sustainability. There are also contributions dealing with the current Sustainability Report of the American Coatings Association, sustainability in the chemical supply chain, the presence of polychlorinated biphenyls, in particular PCB 11, in pigments, printing inks and environment, and compostability testing for packaging. Further, the schedule offers a lecture on the challenges and opportunities of supplier partnerships, the NAPIM State of the Industry report, the National Printing Ink Research Institute lecture, and several regulatory updates relevant to the ink industry, such as the stormwater monitoring requirements, regulation of printing inks in food packaging in Europe, policy activity on per- and polyfluoroalkyl substances, and amendments to the Toxic Substances Control Act.

Electronic and Conductive Ink Conference 2020

http://www.printedelectronicink.com
15–16 October 2020

The topics announced for the 3rd edition of this conference cover the developments in conductive inks, such as the particle-free silver inks with low sintering temperature, inks based on silver nanowires and metal gel compositions, processes for their application, including the direct-to-fabric printing, their utilisation in the production of various sensors and other electronic devices, as well as the characterisation and testing methods for printed and flexible electronics.

PRINTING United Digital Experience

https://www.printingunited.com
26 October – 12 November 2020

This year's digital edition of the PRINTING United event is scheduled for three weeks combining exhibitor showcases, product launches, educational sessions, equipment demonstrations, and more. The PRINTING United Insight Days encompass different market sectors and printing technologies. These include the hardware, consumables, finishing and workflow solutions

for wide-format sign and graphic printing, apparel decoration, including direct-to-garment printing and colour management in the digital textile segment, adoption of high-speed and cut-sheet production inkjet printing for commercial printing production, the possible combination of electrophotography and inkjet technology in this sector, as well as the advanced automation in offset commercial printing. Two days track the trends and opportunities in individual packaging sectors, i.e. labels, flexible packaging, folding carton and corrugated packaging, including digital printing, sustainability, e-commerce, and luxury brands. The workflow efficiency and innovative applications with wide-format printing in the in-plant segment, the current trends in industrial printing and direct mail, workflow automation systems and other software solutions are also included in the programme.

CIC28 – 28th Color and Imaging Conference

https://www.imaging.org
16–18 November 2020

As in the case of other traditional events sponsored by IS&T, the Society for Imaging Science and Technology, and transformed into the online mode, the live short courses lasting for 2–8 hours each are scheduled before the technical sessions of the conference, starting on 4 November). The day after, 19 November, is reserved for a workshop programme, which has not been specified yet. To further facilitate remote participation, the recordings of individual courses and technical presentations, including the online discussions, can be accessed later and as often as needed until 15 March 2021.

The short courses on colour theory and modelling range from the 4-hour introductory course on advanced colorimetry and colour appearance, to fundamentals of psychophysics and surface appearance characterisation on the intermediate level, up to the advanced course on individual differences in colour matching and appearance. The group of courses dealing with colour imaging consists of two introductory courses – the 8-hour course presenting the basic concepts of colour and imaging and the course on fundamentals of spectral measurements for colour science, together with three intermediate courses on the evolution of high dynamic range imaging, colour imaging challenges with compact camera optics, and colour-related aspects of the camera imaging pipeline. Two courses are focused on colour display – the introductory one presenting high dynamic range display concepts and technologies and the intermediate one providing colour essentials in LED lighting systems. The last group of courses is aimed at colour processing at the intermediate level. These include the 4-hour one on theory and practice of camera colour characterisation, using the iccMAX architecture for colour management and its practical applications, solving colour problems using vector space arithmetic, and spatial colour perception and image processing.

From the three days of the rich technical programme, Monday is focused on colour vision and perception, with the keynote on 'Colour appearance and spatio-chromatic vision' by Sophie Wuerger. Tuesday topic is computational colour, opened with the keynote by Derya Akkaynak asking 'Why are there colors in the ocean?'. Colour applications sessions on Wednesday begin with the keynote 'Rethinking Color Measurement' by Ayan Chakrabarti. Each day, the schedule offers both oral and poster presentations, in part within the interactive sessions.

ESMA Events

The European Association of Specialist Printing Manufacturers offers two ESMA Academy courses. Digital Printing on Textiles in Denkendorf, Germany (6–9 October 2020) is intended for participants from companies considering or preparing the implementation of a digital inkjet printing process in the production of textiles. The second one, Industrieller Digitaldruck for the German-speaking participants interested in industrial digital printing, takes place in Stuttgart, Germany on 16–19 November 2020.

Decorative Surfaces Conference 2020

Vienna, Austria
19–21 October 2020

This event held by TCM (Technical Conference Management) originally should take place in March. It combines two days of the conference with digital printing solutions among the topics and a workshop on the third day, Inkjet Technology for Décor Printing, presented in cooperation with IMI Europe.

Paper & Plastics Recycling Conference International

http://www.recyclingtodayevents.com
20–22 October 2020

For this year, the American and European editions of this established conference had to merge into a global broadcast and online networking event.

Inkjet Age of Materials Conference 2020–2021

The sessions of this new bi-monthly digital online conference designed by IMI to address the current and needed developments in inkjet materials start on 18 November 2020, with the last one scheduled for 15 September 2021.

Smithers Events for Printing and Packaging

The events organised by Smithers also had to be postponed or transformed into the virtual format. Those to be held at the end of this year include the 2020 editions of Digital Print for Packaging, the US conference on 12–14 October and the European one on 7–8 December. The American event is directly followed by Digital Textile Printing US on 15–16 October. The annual WEAR Conference for the smart fabrics, e-textiles, and wearable technology markets takes place the same week, 13–15 October 2020. The following weeks offer Specialty Papers Europe 2020 (19–21 October) and three packaging conferences, namely SmartPack US 2020 focused on collaboration and innovation to accelerate the commercial adoption of intelligent packaging on 26 October, the 3rd US edition of E-PACK for the e-commerce packaging supply chain on 27–28 October 2020, and Sustainability in Packaging Europe 2020 on 2–5 November.

GRID 2020
10th International Symposium on Graphic Engineering and Design

Novi Sad, Serbia
12–14 November 2020

For its 10th edition, this bi-annual event hosted by the University of Novi Sad and organised by the Department of Graphic Engineering and Design becomes either a hybrid or fully online event, depending on the situation on the symposium days.

The Holography Conference

https://holographyconference.com
8–9 December 2020

This traditional event held since 1990 is also going online, with a minimum of four sessions planned for two days of the conference.

Awayzgoose Conference

https://woodtype.org
5–8 November 2020

The Hamilton Wood Type & Printing Museum presents the 12th volume of its annual Wayzgoose Conference for type, design and letterpress printing as the 2020 Awayzgoose, an online event in partnership with the American Printing History Association. All workshops and presentations are thus this year easily accessible to designers, printers, typographers and educators from across the globe.

The online pre-conference workshops start on 26 October. The participants of the one-day workshops can learn how to design letterpress compositions for both digital and analogue output using the Adobe Creative Cloud software, try reduction block printing and calligraphy with Koch's textura, and take part in the Modus type project. The following four-day workshop covers all steps of wood engraving.

Besides the presentations, panel discussions, networking opportunities and demonstration of wood type cutting, the conference schedule features four keynotes – with Paula Scher on her new book about 25 years of working for the Public Theater in New York, Susan Skarsgard with presentation details yet to come, Erik Spiekermann, discussing the 21st-century methods of letterpress using tools from the 18th and 19th century, and Richard Kegler interviewing Bruce Licher about his career as a designer and printer, now documented in the extensive monograph on work of Independent Project Records & Press.

ICC DevCon 2020

http://www.color.org
November 2020 and January 2021

The upcoming International Color Consortium Developers Conference is held online with the theme 'The future of colour management'. The webinars scheduled to Mondays in the second half of November explore three topical areas. On 16 November, the focus is on the emerging needs in colour management of colorimetric and spectral data, with presentations contrasting the situation in graphic and other industries and discussing how to incorporate spectral reproduction workflows into colour management. On 23 November, the papers deal with colour and material appearance, presenting the selected new developments in colour appearance modelling, fabrication of objects with spatially varying colour and translucency using multi-material 3D printing, implementation of bidirectional reflectance distribution function in an ICC profile, and total appearance capture and reproduction. Finally, on 30 November, the lectures cover colour management for display and print, with one discussing colour on the web and broadcast, while the other two deal with practical aspects of n-colour reproduction. Another three webinars planned to January 2021 comprise an extended hands-on workshop on using iccMAX, from the introduction of iccMAX features and example implementation to working with RefIccMAX, using iccXML and calculator element programming, up to the Interoperability Conformance Specifications and their use.

Journal of Print and Media Technology Research
A PEER-REVIEWED QUARTERLY

ISSN 2414-6250 (Online)
ISSN 2223-8905 (Print)
CODEN JPMTBI
UDC 665

Call for papers

The Journal of Print and Media Technology Research is a peer-reviewed periodical, published quarterly by iarigai, the International Association of Research Organizations for the Information, Media and Graphic Arts Industries.

JPMTR is listed in Emerging Sources Citation Index, Scopus, Index Copernicus International, PiraBase (by Smithers Pira), Paperbase (by Innventia and Centre Technique du Papier), NSD – Norwegian Register for Scientific Journals, Series and Publishers.

Authors are invited to prepare and submit complete, previously unpublished and original works, which are not under review in any other journals and/or conferences.

The journal will consider for publication papers on fundamental and applied aspects of at least, but not limited to, the following topics:

- **Printing technology and related processes**
  Conventional and special printing; Packaging; Fuel cells, batteries, sensors and other printed functionality; Printing on biomaterials; Textile and fabric printing; Printed decorations; 3D printing; Material science; Process control
- **Premedia technology and processes**
  Colour reproduction and colour management; Image and reproduction quality; Image carriers (physical and virtual); Workflow and management
- **Emerging media and future trends**
  Media industry developments; Developing media communications value systems; Online and mobile media development; Cross-media publishing
- **Social impact**
  Environmental issues and sustainability; Consumer perception and media use; Social trends and their impact on media

Submissions for the journal are accepted at any time. If meeting the general criteria and ethic standards of scientific publishing, they will be rapidly forwarded to peer-review by experts of relevant scientific competence, carefully evaluated, selected and edited. Once accepted and edited, the papers will be published as soon as possible.

There is no entry or publishing fee for authors. Authors of accepted contributions will be asked to sign a copyright transfer agreement.

Authors are asked to strictly follow the guidelines for preparation of a paper (see the abbreviated version on inside back cover of the journal).

Complete guidelines can be downloaded from: <http://www.iarigai.org/publications/journals/>
Papers not complying with the guidelines will be returned to authors for revision.

Submissions and queries should be directed to: journal@iarigai.org

Journal of Print and Media Technology Research
A PEER-REVIEWED QUARTERLY

Vol. 9, 2020
Prices and subscriptions

Since 2016, the journal is published in digital form; current and archive issues are available at: <https://iarigai.com/publications/journals/>.

Since 2020, the journal will be published as "open access" publication, available free of charge for iarigai members, subscribers, authors, contributors and all other interested public users.

A print version is available on-demand. Please, find below the prices charged for the printed Journal, for four issues per year as well as for a single issue

Regular prices

Four issues, print JPMTR (on-demand)	400 EUR
Single issue, print JPMTR (on-demand)	100 EUR

Subscription prices

Annual subscription, four issues, print JPMTR (on-demand)	400 EUR

Prices for iarigai members

Four issues, print JPMTR (on-demand)	400 EUR
Single issue, print JPMTR (on-demand)	100 EUR

Place your order online at: <http://www.iarigai.org/publications/subscriptions-orders/>
Or send an e-mail order to: office@iarigai.org

Guidelines for authors

Authors are encouraged to submit complete, original and previously unpublished scientific or technical research works, which are not under reviews in any other journals and/or conferences. Significantly expanded and updated versions of conference presentations may also be considered for publication. In addition, the Journal will publish reviews as well as opinions and reflections in a special section.

Submissions for the journal are accepted at any time. If meeting the general criteria and ethical standards of the scientific publication, they will be rapidly forwarded to peer-review by experts of high scientific competence, carefully evaluated, and considered for selection. Once accepted by the Editorial Board, the papers will be edited and published as soon as possible.

When preparing a manuscript for JPMTR, please strictly comply with the journal guidelines. The Editorial Board retains the right to reject without comment or explanation manuscripts that are not prepared in accordance with these guidelines and/or if the appropriate level required for scientific publishing cannot be attained.

A – General

The text should be cohesive, logically organized, and thus easy to follow by someone with common knowledge in the field. Do not include information that is not relevant to your research question(s) stated in the introduction.

Only contributions submitted in English will be considered for publication. If English is not your native language, please arrange for the text to be reviewed by a technical editor with skills in English and scientific communications. Maintain a consistent style with regard to spelling (either UK or US English, but never both), punctuation, nomenclature, symbols etc. Make sure that you are using proper English scientific terms. Literal translations are often wrong. Terms that do not have a commonly known English translation should be explicitly defined in the manuscript. Acronyms and abbreviations used must also be explicitly defined. Generally, sentences should not be very long and their structure should be relatively simple, with the subject located close to its verb. Do not overuse passive constructions.

Do not copy substantial parts of your previous publications and do not submit the same manuscript to more than one journal at a time. Clearly distinguish your original results and ideas from those of other authors and from your earlier publications – provide citations whenever relevant.

For more details on ethics in scientific publication consult Guidelines, published by the Committee on Publication Ethics (COPE):
<https://publicationethics.org/resources/guidelines>

If it is necessary to use an illustration, diagram, etc. from an earlier publication, it is the author's responsibility to ensure that permission to reproduce such an illustration, diagram, etc. is obtained from the copyright holder. If a figure is copied, adapted or redrawn, the original source must be acknowledged.

Submitting the contribution to JPMTR, the author(s) confirm that it has not been published previously, that it is not under consideration for publication elsewhere and – once accepted and published – it will not be published under the same title and in the same form, in English or in any other language. The published paper may, however, be republished as part of an academic thesis to be defended by the author. The publisher retains the right to publish the printed paper online in the electronic form and to distribute and market the Journal containing the respective paper without any limitations.

B – Structure of the manuscript

Preliminary

Title: Should be concise and unambiguous, and must reflect the contents of the article. Information given in the title does not need to be repeated in the abstract (as they are always published jointly), although some overlap is unavoidable.

List of authors: I.e. all persons who contributed substantially to study planning, experimental work, data collection or interpretation of results and wrote or critically revised the manuscript and approved its final version. Enter full names (first and last), followed by the present address, as well as the E-mail addresses. Separately enter complete details of the corresponding author – full mailing address, telephone number, and E-mail. Editors will communicate only with the corresponding author.

Abstract: Should not exceed 500 words. Briefly explain why you conducted the research (background), what question(s) you answer (objectives), how you performed the research (methods), what you found (results: major data, relationships), and your interpretation and main consequences of your findings (discussion, conclusions). The abstract must reflect the content of the article, including all keywords, as for most readers it will be the major source of information about your research. Make sure that all the information given in the abstract also appears in the main body of the article.

Keywords: Include three to five relevant scientific terms that are not mentioned in the title. Keep the keywords specific. Avoid more general and/or descriptive terms, unless your research has strong interdisciplinary significance.

Scientific content

Introduction and background: Explain why it was necessary to carry out the research and the specific research question(s) you will answer. Start from more general issues and gradually focus on your research question(s). Describe relevant earlier research in the area and how your work is related to this.

Methods: Describe in detail how the research was carried out (e.g. study area, data collection, criteria, origin of analyzed material, sample size, number of measurements, equipment, data analysis, statistical methods and software used). All factors that could have affected the results need to be considered. Make sure that you comply with the ethical standards, with respect to the environmental protection, other authors and their published works, etc.

Results: Present the new results of your research (previously published data should not be included in this section). All tables and figures must be mentioned in the main body of the article, in the order in which they appear. Make sure that the statistical analysis is appropriate. Do not fabricate or distort any data, and do not exclude any important data; similarly, do not manipulate images to make a false impression on readers.

Discussion: Answer your research questions (stated at the end of the introduction) and compare your new results with published data, as objectively as possible. Discuss their limitations and highlight your main findings. At the end of Discussion or in a separate section, emphasize your major conclusions, pointing out scientific contribution and the practical significance of your study.

Conclusions: The main conclusions emerging from the study should be briefly presented or listed in this section, with the reference to the aims of the research and/or questions mentioned in the Introduction and elaborated in the Discussion.

Note: Some papers might require different structure of the scientific content. In such cases, however, it is necessary to clearly name and mark the appropriate sections, or to consult the editors. Sections from Introduction until the end of Conclusions must be numbered. Number the section titles consecutively as 1., 2., 3., ... while subsections should be hierarchically numbered as 2.1, 2.3, 3.4 etc. Only Arabic numerals will be accepted.

Acknowledgments: Place any acknowledgements at the end of your manuscript, after conclusions and before the list of literature references.

References: The list of sources referred to in the text should be collected in alphabetical order on at the end of the paper. Make sure that you have provided sources for all important information extracted from other publications. References should be given only to documents which any reader can reasonably be expected to be able to find in the open literature or on the web, and the reference should be complete, so that it is possible for the reader to locate the source without difficulty. The number of cited works should not be excessive - do not give many similar examples.

Responsibility for the accuracy of bibliographic citations lies entirely with the authors. Please use exclusively the Harvard Referencing System. For more information consult the Guide to Harvard style of Referencing, 6th edition, 2019, used with consent of Anglia Ruskin University, available at:
<https://libweb.anglia.ac.uk/referencing/files/Harvard_referencing_201718.pdf>

C – Technical requirements for text processing

For technical requirement related to your submission, i.e. page layout, formatting of the text, as well of graphic objects (images, charts, tables etc.) please see detailed instructions at:
<http://www.iarigai.org/publications/journals/>

D – Submission of the paper and further procedure

Before sending your paper, check once again that it corresponds to the requirements explicated above, with special regard to the ethical issues, structure of the paper as well as formatting.

Once completed, send your paper as an attachment to:
journal@iarigai.org

If necessary, compress the file before sending it. You will be acknowledged on the receipt within 48 hours, along with the code under which your submission will be processed.

The editors will check the manuscript and inform you whether it has to be updated regarding the structure and formatting. The corrected manuscript is expected within 15 days.

Your paper will be forwarded for anonymous evaluation by two experts of international reputation in your specific field. Their comments and remarks will be in due time disclosed to the author(s), with the request for changes, explanations or corrections (if any) as demanded by the referees.

After the updated version is approved by the reviewers, the Editorial Board will decide on the publishing of the paper. However, the Board retains the right to ask for a third independent opinion, or to definitely reject the contribution.

Printing and publishing of papers, once accepted by the Editorial Board, will be carried out at the earliest possible convenience.

3-2020

Journal of Print and Media Technology Research

A PEER-REVIEWED QUARTERLY

The journal is publishing contributions in the following fields of research

- Printing technology and related processes
- Premedia technology and processes
- Emerging media and future trends
- Social impacts

For details see the Mission statement inside

JPMTR is listed in

- Emerging Sources Citation Index
- Scopus
- Index Copernicus International
- PiraBase (by Smithers Pira)
- Paperbase (by Innventia and Centre Technique du Papier)
- NSD – Norwegian Register for Scientific Journals, Series and Publishers

Submissions and inquiries

journal@iarigai.org

Subscriptions

office@iarigai.org

More information at

www.iarigai.org/publications/journal

Publisher

The International Association of Research Organizations
for the Information, Media and Graphic Arts Industries
Magdalenenstrasse 2
D-64288 Darmstadt
Germany